A MULTIPLEX COMPARATIVE PROTEOMIC ANALYSIS OF HYPOXIA INFLUENCE IN THE PRESENCE AND ABSENCE OF p53 IN HCT116 CELLS

TAN WEE WEE
(MSc.), NUS

A THESIS SUBMITTED FOR THE DEGREE OF MASTER OF SCIENCE

DEPARTMENT OF BIOLOGICAL SCIENCES

NATIONAL UNIVERSITY OF SINGAPORE

2008

ACKNOWLEDGEMENTS

This thesis is dedicated to all who make it possible. Without them, this thesis would not be available today. Therefore, I would like to sincerely thank both my supervisors, Professor Hew Choy Leong and Dr. Liou Yih-Cherng, for giving me this invaluable opportunity to work on this project and their constant guidance. I would like to thank Dr. Liou for his confidence in me as well. I would like to thank Dr. Lin Qingsong for sharing his knowledge, time, and encouragements during my MSc. project. Furthermore, I would like to thank the members of Dr. Liou's laboratory and the staffs of Protein and Proteomic Centre for their assistance and friendship. Last, but not the least, I would like to thank my parents and my girlfriend, Weng Ruifen, for the tolerance and understanding during my course of study. For others whom I have failed to mention, please accept my apologies and my gratitude for the contributions that you have given to me.

~ Tan W W, August 2007~

TABLE OF CONTENTS

SUMMARY

Cells are constantly maintained and renewed in our body under a stringent homeostatic regulation. In the event when cellular damages are beyond repairs, these cells will be destroyed via the programmed cell death (PCD) pathway. In cancer, the PCD pathway becomes dysfunctional due to genetic mutations. Consequently, cells proliferate uncontrollably and lead to disruption of the vascular network. This results in the formation of hypoxic microenvironments within the tumor due to insufficient oxygen supply to the cells and the presence of hypoxic regions has been shown to correlate with poor prognosis and therapeutic resistance. Cellular activities of cancer cells undergo changes to cope with the oxygen-deprived (hypoxia) condition and these changes are achieved mainly by the action of hypoxia-inducible factor-1 (HIF-1), a transcription factor. In the presence of hypoxia, apoptotic-resistant tumor cells are selected, such as through the attenuation of p53 apoptotic response. However, attempts to confirm the relationship between p53 and hypoxia/HIF-1 have met with conflicting results. In this study, we investigate the differential gene expression in cultured human colorectal cancer cells, HCT116, subjected to hypoxic condition using isobaric tags (iTRAQ) and mass spectrometry. Using p53 knockout (KO) cells, we also examine the elusive relationship between hypoxia and p53 by analyzing their protein profiles. At 95% C.I., a total of 217 proteins were identified in our iTRAQ experiments and of which, the expression levels of 54 proteins were found significantly altered with at least 30% fold change in terms of protein abundance. Among the significantly affected proteins, 14 were potentially regulated by hypoxia and this includes the known hypoxia affected proteins, PGK1, LDHA, and FAS. Fifteen proteins were found potentially regulated by p53 and the remaining 25

proteins were affected by both hypoxia treatment and the presence of p53. An ontology analysis of these 54 proteins revealed that they were mainly involved in the regulation of cellular growth and proliferation. Downstream validation analysis using RT-PCR and immunoblotting assays further confirmed the observations in our iTRAQ results. Both RT-PCR and immunoblotting results strongly indicate that ANXA2 and PCBD1 may be novel interacting targets of p53 while the regulation of EFHD2 and CKS2 may be influenced by hypoxia (1% O_2) treatment. Therefore, we proposed that these distinct differentially expressed proteins may be used as potential biomarkers and/or therapeutic targets in colorectal cancer.

LIST OF FIGURES

LIST OF TABLES

LIST OF ABBREVIATIONS

WT-N	Wildtype treated under normoxia
WT-H	Wildtype treated under hypoxia
KO-N	p53 knockout treated under normoxia
KO-H	p53 knockout treated under hypoxia
SDS-PAGE	Sodium dodecyl sulphate polyacrylamide gel electrophoresis
iTRAQ	Isobaric Tags for Relative and Absolute Quantification
MS	Mass spectrometry
MS/MS	Tandem mass spectrometry
LC	Liquid chromatography
RP	Reverse phase
TOF	Time of flight
MALDI	Matrix-assisted laser desorption/ionization
RPA	Relative peak area
m/z	mass to charge ratio
RT-PCR	Real-time polymerase chain reaction
PCD	Programmed Cell Death
PTM	Post-translational modification
PMSF	Phenylmethylsulfonyl fluoride
DEPC	DiethylenePyrocarbonate

CHAPTER 1 – INTRODUCTION

Cells are constantly kept in a dynamic equilibrium of proliferation and cell death. At any given time point in their life spans, the number of cells in each organism is kept relatively constant, with each individual cell being highly regulated by transcription factors that control the expression of genes to synthesize the necessary proteins for carrying out all cellular functions in order to maintain this homeostatic condition and viability in response to extracellular biological (e.g. hormones and neurotransmitters) and non-biological (e.g. temperature and oxygen fluctuations) signals. In the presence of cellular dysfunction, genes regulating cell cycle (e.g. p16, $p21^{WAF1/CIP1}$, p53, cyclins, and CDKs) will be activated to arrest the cell for repair (Brugarolas et al., 1995; Gartel and Radhakrishnan, 2005; Zhang et al., 1994). If the damage is extensive and beyond repair, the dysfunction cells will be directed for programmed cell death (PCD) by activation of pro-apoptotic genes such as p53, BID, BAX and caspases. Hence, a constant homeostatic condition is maintained in the body.

In cancer, this dynamic equilibrium does not exist or is being disrupted. Thus, cells proliferate uncontrollably and are more resilient to cell death. This phenomenon is mainly due to multiple genetic alterations or mutations in the genome that impaired the cell's ability to regulate its cellular activities normally (Calabretta et al., 1985; Renan, 1993). As a result, in the presence of cellular dysfunction, the cell is not arrested and bypasses PCD, leading to tumor formation and cancer development. Therefore, tumors are characterized by cells which have the ability to escape the natural cell death program that maintain cellular homeostasis. Newly developed tumor can be benign initially and are non-cancerous. However, they can develop, gain

malignancy and become capable of invading into surrounding tissues or metastasize – a key characteristic of cancer cells (Hanahan and Weinberg, 2000). Other hallmarks of cancer include the ability to evade apoptosis, self-sufficiency in growth signals, insensitive to anti-growth signals, sustained angiogenesis and unlimited replicative potential.

Cancer develops as a result of a series of genetic mutations, which gives rise to the 6 key characteristics of cancer. Among the many genes that are affected, the gene that encodes for a transcription factor known as p53 is frequently found mutated in cancer. The p53 protein is also a well known tumor suppressor protein that plays important roles in cell cycle arrest and apoptosis in the event of cellular dysfunctions (Yu et al., 1999). However, these functions of p53 can be abolished when mutations occur in the p53 gene or its upstream/downstream regulating genes. This results in cellular dysfunction and cells containing genetic defects get propagated, leading to the development of cancer.

In cancer, the microenvironment plays an important part in affecting cancer progression as well as cancer treatment. The presence of hypoxic microenvironment is a common phenomenon observed in many cancer tumors. Rapid cell growth during cancer development results in the disruption of vascular network within the cancerous tissue/tumor. As a consequence, the supply of oxygen and nutrients supplied to the cells becomes inadequate and certain regions in the tumor become hypoxic (Semenza, 2000b). Hypoxic cells in tumors undergo a series of biological changes in order to survive since hypoxia is an unfavorable condition for cell growth. These biological changes are controlled by a major transcription factor, called hypoxia inducible

factor-1 (HIF-1), that acts as a chief regulator of oxygen homeostasis. The activation of HIF-1 downstream target genes promotes the survival of hypoxic cells as well as selection of apoptosis-resistant cells in the tumor and hence, promoting a more malignant cancer phenotype (Giaccia et al., 2004).

Interestingly, although hypoxia positively correlates with tumor malignancy, several contrasting reports have indicated that hypoxia can cause accumulation of p53 in a HIF-1 dependent manner as well as inducing cell death via the p53-dependent pathway (An et al., 1998; Graeber et al., 1994; Yao et al., 1995). These conflicting findings question the intriguing, yet elusive, relationship between hypoxia, HIF-1 and p53. Thus, it is critical to elucidate this complex relationship to better understand the hypoxic effects in cancer progression.

In the following chapters, I aim to review the intertwining relationship shared between cancer, p53 and HIF-1 under hypoxic condition. This chapter may also provide the updated background of my thesis studies.

1.1 CANCER

1.1.1 Cancer Development

Cancer is a disease of genes and it involves dynamic genetic alterations or mutations in the genome that produce over-active oncogenes (gain-of-function) and inactivated/attenuated tumor suppressor genes (loss-of-function) (Bishop and Weinberg, 1996). The former promotes the abnormal rapid proliferation and survival of cells under unfavorable condition while the latter allows cells to evade cell cycle arrest/checkpoints and thus, apoptosis too. Although most types of cancers have been

reported to be sporadic, some are recognized as hereditary due to the inheritance of a mutated allele, often a tumor suppressor. A classic example is familial adenomatous polyposis (FAP) which is an autosomal dominant inherited colorectal cancer syndrome. The cause of this disorder has been attributed to germline mutations in the adenomatous polyposis coli (*APC*) gene inherited from the parents (Lamlum et al., 2000; Miyoshi et al., 1992). *APC* gene is a tumor suppressor gene that promotes apoptosis in colonic cells and is also involved in the sequestration of β-catenin, which leads to an inhibitory effect on the β-catenin's stimulatory effects on the cells (Neufeld et al., 2000). Mutations in the *APC* gene result in a truncated/non-functional protein that does not trigger apoptosis and instead allows β-catenin to accumulate in the cell, promoting abnormal cell proliferation. Thus, FAP patients are characterized by multiple non-cancerous polyps growing in the colon and the number of polyps will increase with age. If these benign polyps are not removed, they will eventually become malignant and develop into colorectal cancer.

On the other hand, patients with sporadic cancers do not inherit cancer-causing mutated alleles/genes from their parents. Instead, the spontaneous mutations are usually the results of DNA damage that can be caused by exposures to carcinogens and/or mutagens. Carcinogens are cancer-causing agents (e.g. asbestos, cigarette smokes, acrylamide, etc.) and typically, mutagens are carcinogenic as multiple mutations will lead to development of cancers. Mutagens are any substance that causes genetic mutations; for example, ethidium bromide (EtBr), nitrous acid (HNO_2), sodium azide (NaN_3) and radiations (ultraviolet and gamma). Some carcinogens do not cause mutations but affect the level of transcriptions of certain genes that are critical to cell regulation instead. Furthermore, not all genetic mutations are caused by

mutagens. Some are due to errors in DNA replication (e.g. base pair substitution, frame-shifts), repair (e.g. mismatch repair) and recombination of DNA sequences. Normally, these genetic errors would be repaired or the cells would be destroyed if the genetic damage is irreparable; but due to the multiple mutations, the genetic defects get retained and are propagated to future generations which can lead to cancer development. Typically, highly proliferating tissues such as liver and bone marrow, which divide more frequently, will have a higher risk of developing cancer.

Cancer can occur in any person, regardless of races, genders and ages. Generally, the risk increases with age too (Jemal et al., 2006) and there are many types of cancers (e.g. breast, colorectal, skin, prostate, cervical, etc.), with occurrences reported in most, if not all, tissues in human. Currently, it is reported that there are more than 11 million people diagnosed with cancer each year and the number of new cases reported will soar to a predictive number of 16 million every year by 2020 (Cho, 2007). Cancer is also one of the leading causes of death in the world, accounting for 7.6 million (13%) of the global mortality in 2005 alone (Cho, 2007). In Singapore, death by cancer is the 2nd highest mortality rate listed (Figure 1.1) according to a report released by National Cancer Center Singapore (NCCS), with colorectal cancer (CRC) as the commonest cancer diagnosed – with 1 in 4 cancer patients detected (Seow et al., 2004). The average 1- and 5-year survival rates[1] for CRC are 83% and 62% respectively (Kauh and Umbreit, 2004). However, if CRC is detected at an early stage (modified Dukes' stage A and B), the 5-year survival percentage has been shown to be higher compared to detection at a later stage (modified Dukes' stage C and D) (Table 1.1). Yet, only a low percentage of CRC patients are typically detected

[1] Cancer survival rates or survival statistics indicates the percentage of people who survive a certain type of cancer for a specific amount of time and they are based on research that comes from information gathered on a big population of cancer patients.

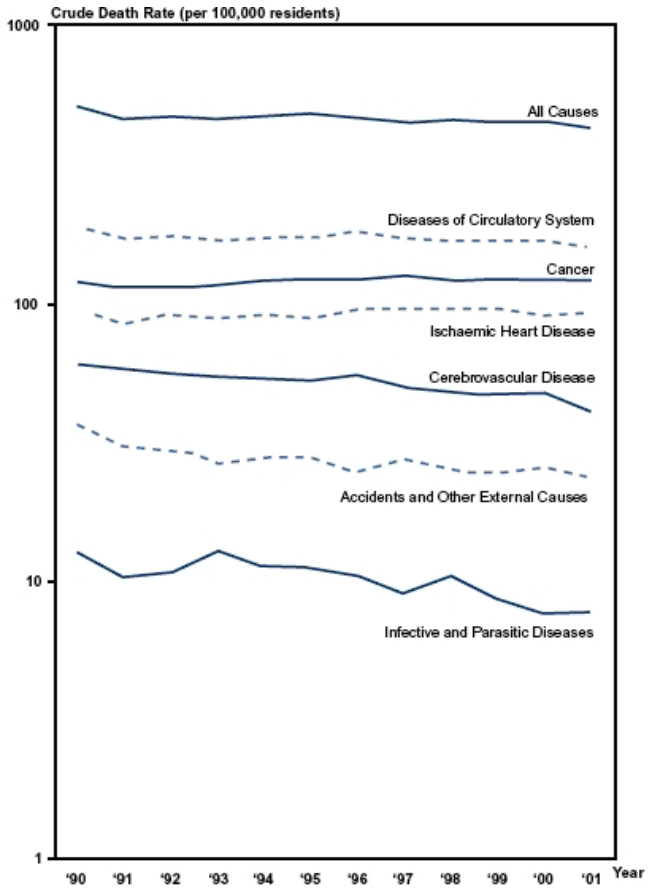

Figure 1.1: Singapore mortality rates for all causes from 1990 to 2001. Death caused by cancer was maintained constantly at 2nd place with no sign of decrease. Extracted from NCCS Singapore Cancer Registry report volume 6, pp 9 (Seow et al., 2004).

Table 1.1: Colorectal cancer staging, stage distribution, and survival. Data obtained is just a representation as actual percentage might vary among different surveys. (Extracted from Melville et al., 1998)

Dukes' stage (modified)	*Definition*	*Approximate frequency at diagnosis (%)*	*Five year survival (%)*
A	Cancer localised within the bowel wall	11	83
B	Cancer which penetrates the bowel wall	35	64
C	Cancer spread to lymph nodes	26	38
D	Cancer with distant metastases (most often in the liver)	29	3

at the early stages (Kauh and Umbreit, 2004; Melville et al., 1998). Therefore, it is critical to have more sensitive and accurate cancer diagnostic methods such that patients suffering from cancer can be diagnosed at an earlier stage. This leads to a strong urgency and requirement for the development of key biomarkers.

1.1.2 Colorectal Cancer

Colorectal cancer refers to the cancer of the colon and rectum. The colon is the longest portion of the large intestine, measuring about 5 to 6 feet in length. The main function is to convert liquid stool into solid stool by absorbing excess water into the body. This process can take several hours to several days. On the other hand, the rectum, which is located at the end of the colon, is about 5 inches in length and is usually empty except prior to excretion of stool. CRC normally develops initially in the colon and spread to the rectum in most cases, thus leading to the commonly use of the combined name. It may be hereditary or spontaneous. However, only about 5~10% of CRC are linked to inherited genes, e.g. APC, MYH. There are many causes that have been proposed to influence CRC development and some examples are family history, diet, environment, gender, lifestyle, and the number of existing polyps.

1.1.3 Diagnosis & Treatment

Diagnosis of cancer is an attempt to accurately identify the origin and malignancy of the disease, as well as the type of cells involved. The effectiveness of treatment and prospects for survival depend critically on early detection of cancer. Currently, diagnostic methods in practice include the use of ultrasound equipment to detect lumps, blood tests, computed tomography (CT) scan, and tumor biopsy. An example of cancer markers is carcinoembryonic antigen (CEA) used for detecting

several types of cancer (such as gastrointestinal, lung and breast cancers). However, the sensitivity and specificity of these diagnostic methods are often insufficient and inaccurate. Moreover, early detection of cancer is made more difficult due to the lack of specific symptoms in the early stage (before invasion – Dukes' stage A) as well as limited understanding of etiology and oncogenesis. For example, the use of CA 15-3, a blood tumor marker for breast cancer, is useless for early detection as it has low sensitivity (41.9%) (Lumachi et al., 2000). Thus, there is a critical need for an expedited development of biomarkers with greater specificity and accuracy and the use of proteomic technique is a common approach used for identification of novel potential biomarkers that can be used for cancer diagnosis and even cancer therapies.

Conventionally, cancer patients undergo a combination series of therapeutic treatments involving surgery (excision of tumors), radiotherapy, and chemotherapy to control and eradicate the cancer cells from their bodies. Radiotherapy involves the use of ionizing radiations, usually X-rays, to damage DNA and kill the cancer cells while chemotherapy utilizes chemical substances, called anticancer chemo-drugs, to treat cancer. Adriamycin®, Platinol® (cisplatin), 5-fluorouracil and hydroxyurea are some common examples of chemo-drugs used in chemotherapy to slow and hopefully halt the growth and spread of a cancer. These chemodrugs are developed to (i) damage DNA in cells (induce apoptosis), (ii) inhibit new DNA strands synthesis (inhibits repair), and/or (iii) stop mitosis/cytokinesis (inhibits cell multiplications). Nonetheless, like radiotherapy, a majority of these drugs are not specific, i.e. they target normal cells too, and often many common side effects (e.g. hair loss, weight loss, edema, etc.) arise when used in cancer therapy. Furthermore, the administration of cancer treatments and their efficiencies are often influenced or hindered by various biological

and non-biological factors, including tumors' location(s), the stage of cancer development, presence of drug resistance transporters, altered drug metabolism, altered DNA repair, over-expression of anti-apoptotic genes, inactivity of pro-apoptotic genes, and non-autonomous features of tumor growth in *vivo*, such as the presence of hypoxic microenvironments in solid tumors (Albiero and Pozzi, 1994).

1.1.4 Hypoxic Effects on Diagnosis, Treatments and Prognosis

The effects of oxygen are of interest in cancer treatment because high levels of hypoxia in tumors have been shown positively to be correlated with treatment failure or relapse for many cancers, independently of treatment (Brizel et al., 1997; Fyles et al., 1998; Sundfor et al., 2000). Solid tumors are often in a low-oxygen state known as hypoxia due to the existence of limited arteriolar supply and arteriolar deoxygenation (Dewhirst et al., 1996), low vascular density and disrupted vascular architecture (Secomb et al., 1993), insufficient oxygen supply (Secomb et al., 1995), and an unstable blood supply to the tumor cells (Kimura et al., 1996). Although angiogenesis and neovascularisation do occur in these tumors, the newly formed blood vessels are often inadequate, disorganized and prone to collapse (Helmlinger et al., 1997). Together, these physiological factors contribute to the formation of hypoxic microenvironments/regions heterogeneously distributed within the solid tumors (Padhani et al., 2007; Semenza, 2003).

The presence of hypoxic regions poses a huge obstacle for effective cancer therapies as cells in hypoxic regions are less sensitive to the effects of radiotherapy and chemotherapeutic drugs than their normal counterparts (Erler et al., 2004; Teicher, 1994; Vaupel, 2004). In radiotherapy, oxygen are essential to make DNA damage

permanent and it is known that DNA damage can be chemically restored in hypoxia (Alper and Howard-Flanders, 1956; Harrison et al., 2002). According to the oxygen fixation hypothesis (OFH), developed based on the works of Alexander and Charlesby on polymer chemistry in the 1950s, oxygen is a radiation sensitizer. DNA radicals produced by radiation will react with oxygen to form organic peroxides that in turn "protects" radiation-damaged DNA from restoring to an undamaged state. Stable DNA damage accumulates and leads to an increased lethality from a given dose of radiation in cells, inducing apoptosis eventually. Therefore, in a hypoxic condition, DNA damage is not accumulated as much as under normal condition and tumors become more resistant to the effects of radiation. The solid mass of tumor also makes it difficult for radiation to penetrate into the tumor core. It has been reported that for a similar biological effect in hypoxic tissues as in normoxic tissues, a higher therapeutic dose of 2.5- to 3-fold of radiation (e.g. x-rays and gamma rays) is required (Teicher, 1995; Wachsberger et al., 2003) or only about one third lethal DNA lesions reported in hypoxic cells compared with aerobic cells when subjected to the same amount of irradiation (Koch, 1982). Much research has been done to improve radiotherapy efficiency on solid tumors and one such promising method is the use of metal-based small molecules, such as ^{64}Cu-ATSM, as agents for higher effective cancer radiotherapy (Lewis et al., 2001; Obata et al., 2005).

The disordered tumor cell profusion and constricted blood vessels that contributes to hypoxia also leads to an inefficient delivery of some chemotherapeutic drugs to the site of action as the delivery relies on the tumor vasculature. Studies on solid tumor cells have also further suggested that through induction of apoptosis by cytotoxic chemotherapeutic drugs, hypoxia may select for cells with defective

apoptotic regulators such as p53 and thus, gaining a more malignant phenotype in the end (Graeber et al., 1996). Furthermore, the presence of multiple hypoxic regions within a tumor may confer tumor inhomogeneity, resulting variations towards treatment sensitivities (Vaupel et al., 2002). Inevitably, this may contribute to relapses even after years of remission as not all cancer cells were eradicated by the treatment.

In cancer treatment, the level of hypoxia in a tumor may also be used to help predict the response of the tumor to the treatment. The poor prognosis association with tumor hypoxia has stimulated the development of equipment for measuring oxygen concentrations of tumors *in vivo*. Such tools can be used to evaluate patient-specific distributions of hypoxia within a tumor so that more effective treatment can be administered. An example is the use of polarographic electrodes, commonly known as the Eppendorf electrode, to measure partial pressure of oxygen (pO_2) of tumor in vivo (Fyles et al., 1998; Movsas et al., 2002; Parker et al., 2004). The downside is that this method is invasive and it is restricted to only superficial tumors. On the other hand, techniques such as positron emission tomography (PET) and the use of endogenous hypoxia-induced proteins can allow the potential for non-invasive assessment of a tumor's hypoxic condition. Hence, there is a paramount importance for a deeper understanding of the biological mechanism behind hypoxia in tumors in order for the discovery of endogenous protein markers as well as the development of more effective and sensitive cancer treatments.

1.2 HYPOXIA

1.2.1 The Nature of Hypoxia

Hypoxia is a condition in which the level of oxygen supplied to the body/tissue becomes inadequate, i.e. much lesser than the norm. It is also a hallmark characteristic of most tumors and tumor hypoxia results from an imbalance between the cellular oxygen consumption rate and the oxygen supply to the cells (Semenza, 2003; Vaupel and Harrison, 2004). During tumor expansion, growing cells rapidly outstrip the supply of oxygen and nutrients while the growing cell mass also limits the availability of oxygen and nutrients to each individual cell by existing blood vessels. Formation of new blood microvessels within the tumor (i.e. tumor neovascularisation) would be required for growth beyond 2 mm in order to supply adequate oxygen and nutrients to the cells. Although many factors can contribute to tumor hypoxia, they can be classified generally into 3 types – perfusion-, diffusion-, or anemia-related (Hockel and Vaupel, 2001; Padhani et al., 2007; Vaupel et al., 2002). Perfusion-related hypoxia is an acute type of hypoxia and it is often temporary. It arises as a result of inadequate blood flow (ischemic) in the tissues due to severe structural and functional abnormalities of tumor neovascularisation, such as disorganized vascular network, dilations, lack of functional receptors, incomplete endothelial lining, absence of flow regulation, and an elongated tortuous shape. Diffusion-related hypoxia, on the other hand, is a chronic type of hypoxia that results as a consequence of tumor expansion which increases the oxygen diffusion distance. Tumor cells that are distant (greater than 70 μm) from the microvessels receive inadequate oxygen supply. Anaemic hypoxia results from reduced oxygen-carrying capacity of the blood which may be due to factors relating to treatments or tumor-associated. Furthermore, it has been shown experimentally that the combined effects of low blood perfusion rate to

tumors and low oxygen-carrying capacity of blood amplifies hypoxia due to lowered oxygen supply to the tumors (Figure 1.2) (Vaupel et al., 2001).

1.2.2 The Flipside of Hypoxia

Interestingly, despite conferring resistance to cancer treatment, hypoxia can also have a direct toxic effect as a form of stress on many cell types. Numerous reports have shown that hypoxia can induce necrosis and apoptosis in normal cells (Yamaguchi et al., 2001; Zhu et al., 2002) as well as in tumor cells with cell death observed most notably in the zones furthest from the tumor vasculature (Shimizu et al., 1995; Yao et al., 1995). Therefore, this illustrates hypoxia with two seemingly opposing effects on tumor biology – one protective and the other toxic. The toxic effect of hypoxia is exhibited by its ability to arrest cell at G_0/G_1 checkpoint and induce p53 accumulation, which can lead to p53-dependent PCD (Graeber et al., 1994). Although, p53 is known to be involved in cell cycle regulation, many reports indicated that hypoxia-induced p53 is transcriptionally inactive but serves more as a transcription repressor in tumor cells (Koumenis et al., 2001). Further evidences have also indicated that p53 accumulation induced by hypoxia did not induce $p21^{WAF1/CIP1}$, a well-established p53 downstream gene involved in cell cycle G_1 arrest (Gartel and Radhakrishnan, 2005; Koumenis et al., 2001). Therefore, the accumulation of p53 during hypoxia does not play a role in cell cycle arrest. Hypoxia has also been implicated with the development of a more malignant cancer phenotype and metastases through functioning as a selection pressure for p53-deficient tumor cells with reduced apoptotic potential to hypoxic areas within the tumors (Graeber et al., 1996). While it has been widely known that hypoxia can protect tumors by increasing their resistance to radiotherapy and chemotherapy, there is a possibility that these

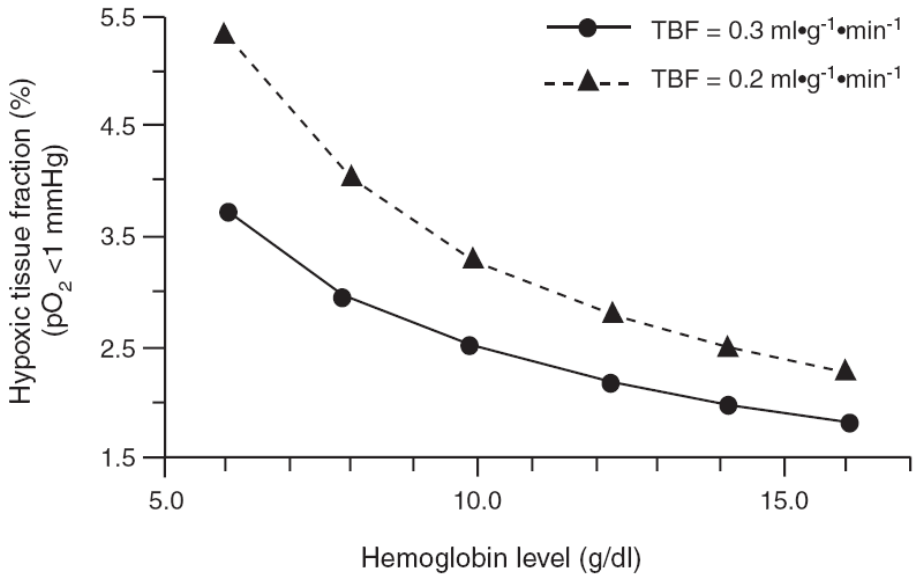

Figure 1.2: Effects of tumor blood flow and oxygen-carrying capacity of blood in tumor tissue. Low rate of tumor blood flow and low oxygen-carrying capacity can decrease pO2 further and aggravate hypoxic condition in tumor. (Extracted from Vaupel et al., 2001)

treatments may actually "assist" hypoxia and promote a more malignant phenotype by killing off cells containing wildtype p53 in conjunction with the toxic effect of hypoxia instead (Lechanteur et al., 2005). Therefore, regardless the existence of two opposing effects of hypoxia, hypoxia fundamentally leads to a more aggressive phenotype (Figure 1.3).

On the other hand, the ability of cancer cells to survive and further develop into a more aggressive phenotype under hypoxic condition appears to be paradoxical since hypoxia is a condition unfavorable for cell growth and may even stimulate cell death. Clearly, many biological changes must have occurred in the tumor cells for survival response to hypoxia and these changes promote anaerobic energy metabolism, metastasis, angiogenesis, and selection of cells with diminished apoptotic potential (Giaccia et al., 2004). Therefore, in order for hypoxia to stimulate these relevant changes, the tumor cells must first have the ability to detect fluctuations in oxygen level and respond accordingly to hypoxia. One way that the cells respond to hypoxia is through hypoxia inducible factor-1 (HIF-1) – the major transcription factor that is responsible for the resulting adoptive responses during hypoxia and acts as a global regulator of cellular and systemic oxygen homeostasis, facilitating oxygen delivery and adaptation to oxygen deprivation (Pouyssegur et al., 2006; Semenza, 1999; Wang and Semenza, 1995).

1.3 HYPOXIA-INDUCIBLE FACTOR-1

1.3.1 The Structure of HIF-1

HIF-1 is a heterodimer protein composed of two constitutively expressed subunits, namely HIF-1α and HIF-1β (Figure 1.4A). Both subunits contain two

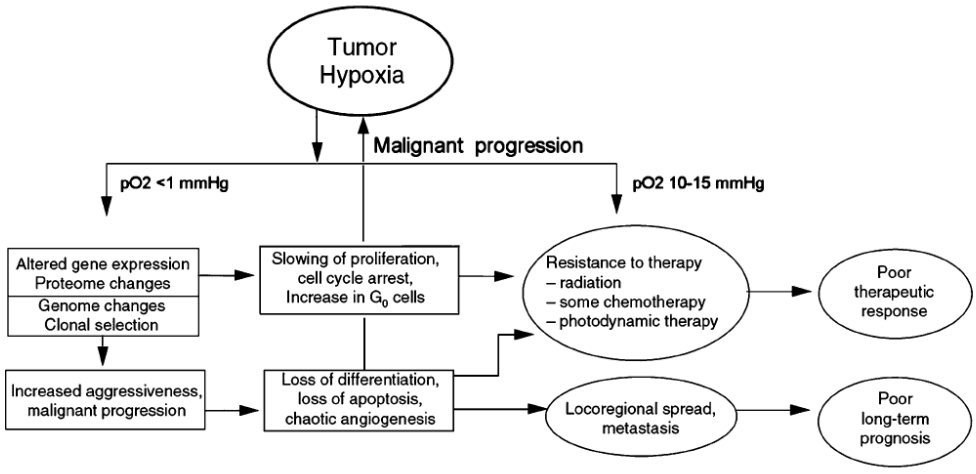

Figure 1.3: A flow diagram showing how hypoxia leads to therapy resistance and the development of a more aggressive tumor phenotype. (Extracted from Vaupel and Harrison, 2004)

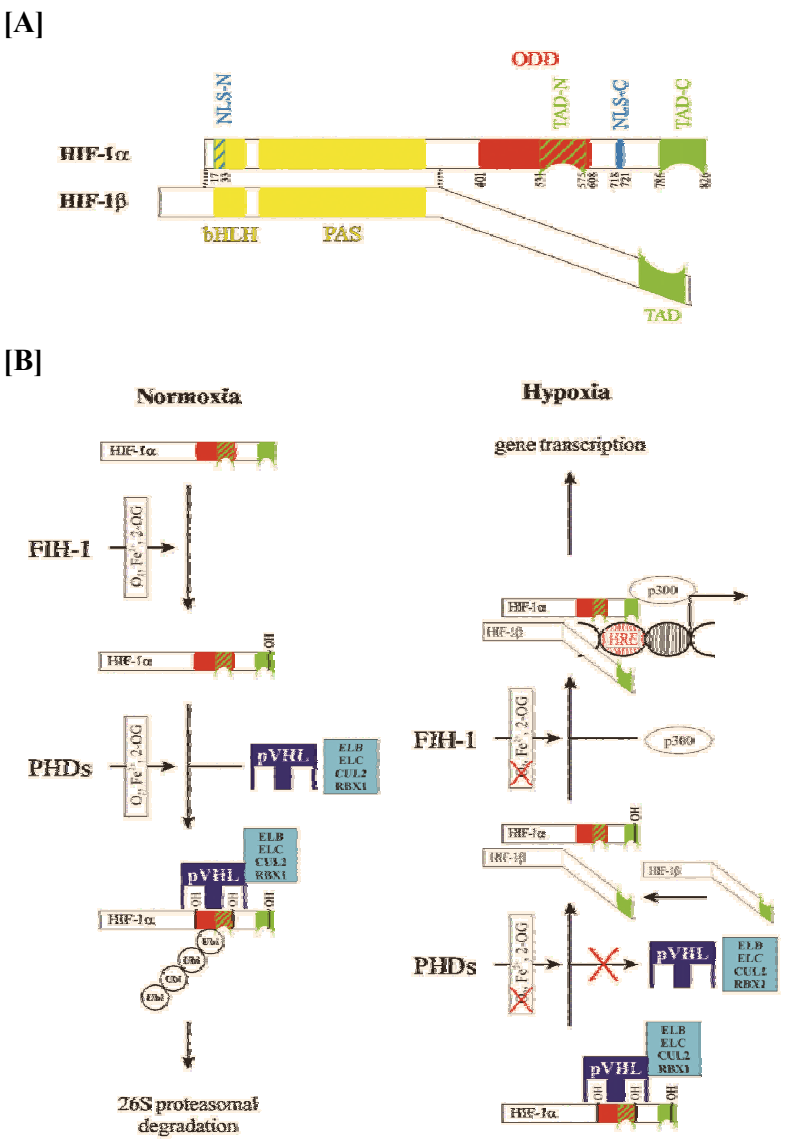

Figure 1.4: HIF-1 structure and its regulation. **[A]** The basic helix-loop-helix (bHLH) and the PER-ARNT-SIM (PAS) domains of HIF-1α and HIF-1β (yellow) are crucial for dimerization and DNA binding. In addition, HIF-1α contains an N- and C-terminal nuclear localization sequence (N-NLS and C-NLS respectively, blue) and an oxygen dependent degradation (ODD) domain (red) that regulates its stability. Transcriptional activity of HIF-1 is facilitated transactivation domains (TAD) in both subunits (green). **[B]** Under normoxia, O_2 and 2-OG (2-oxoglutarate) are available and hydroxylation *via* FIH-1 and PHDs proceeds. FIH-1 hydroxylates Asn803 in the C-TAD of HIF-1α. This modification causes CBP/p300 to dissociate from HIF-1α thus repressing HIF-1 transcriptional activity. PHDs hydroxylate Pro402 and Pro564 within the ODD domain (red) of HIF-1α thereby making it available for the binding of pVHL, which forms an E3-ubiquitin ligase complex with co-factor, leading to poly-ubiquitination of HIF-1α and thus degradation by the 26S proteasome. Under hypoxia, O_2 is limited and PHDs as well as FIH-1 are inactive. HIF-1α stabilizes and associates with β-subunit upon recruitment of the co-factor p300 to form a transcriptionally active HIF-1, activating genes that contain HIF-responsive elements (HRE) in their promoter regions. (Extracted from Schmid et al., 2004a)

characteristic domains: the basic helix-loop-helix (bHLH) domain and the PAS (Per-AHR-ARNT-Sim) domain. The bHLH domain is a common characteristic for many transcription factors that facilitates protein dimerization and DNA binding while the PAS domain is highly conserved throughout evolution, consisting of two internal homology units (A and B repeats) which are involved in protein-protein interactions (Wang et al., 1995a). The latter was termed as an acronym with respect to the first three proteins found in this motif, namely the Drosophila period (Per) and single-minded (Sim) proteins and the mammalian aryl hydrocarbon receptor (AHR) and aryl hydrocarbon receptor translocator (ARNT) proteins (Schmid et al., 2004a). Both domains are essential for HIF-1 heterodimerization and both intact domains must be present in order for the highest efficiency of heterodimerization to occur (Jiang et al., 1996). Other splice variants of HIF-1α and β subunits have also been reported and both contain multiple potential phosphorylation sites, indicating a high possibility for posttranslational modifications (PTMs) in both subunits (Wang et al., 1995b).

1.3.2 HIF-1α & β subunits

The HIF-1α subunit contains 826 amino acids (aa) and has a molecular weight (MW) of 120 kilodaltons (kDa) observed under reducing condition. The bHLH domain and the PAS domain with PAS-A and PAS-B repeats, are localized at the N-terminus of HIF-1α. At its C terminus, there are two transactivation domains (N-TAD and C-TAD) and an oxygen-dependent degradation domain (ODD), which is responsible for the degradation of HIF-1α during normoxic conditions, (Huang et al., 1998; Pugh et al., 1997). The ODD domain contains two PEST-like motifs, a commonly found motif in many proteins with a short half-life of less than 2 hrs (Rechsteiner and Rogers, 1996). These motifs are potential signals for rapid protein

degradation and the sequences are rich in proline, glutamic acid, serine, and threonine. In fact, under normoxic conditions, the half-life of HIF-1α has been reported to be less than 10 min and it has a very low steady-state level that is undetected by immunoblotting assays (Chun et al., 2002; Pan et al., 2007). In addition, HIF-1α contains N- and C-terminal nuclear localization signals (termed as N-NLS and C-NLS, respectively) and it has been reported that only the C-NLS is crucial for nuclear import of HIF-1α (Kallio et al., 1998). The detailed mechanism is not yet known.

HIF-1β, also commonly known as aryl hydrocarbon nuclear receptor translocator (ARNT), was first identified as a heterodimer with aryl hydrocarbon receptor (AHR) to form the functional dioxin receptor. Two isoforms have been identified (774 and 789 aa) and they differ only by the presence of the sequence encoded by a 45 basepairs (bp) alternative exon (Wang et al., 1995a). Little progress has been made for the β subunit but it is crucial as a dimering partner to produce a functional HIF-1 transcription factor as well as a dioxin receptor.

There are two other α subunits identified and they are HIF-2α (also known as endothelial PAS protein or HIF-related factor) and HIF-3α (also known as inhibitory PAS protein) These two isoforms were identified by homology screening for interaction partners with HIF-1β and both were implicated in hypoxia responses (Ema et al., 1997; Hogenesch et al., 1997). HIF-2α is very closely related with HIF-1α, sharing a 48% overall amino acid identity, and transactivates HRE-containing genes when dimerized with HIF-1β (Wenger, 2002). Interestingly, HIF-3α is only distantly related to HIF-1α and lacks a C-terminal transactivation domain. It is thought that transcription factors that contain the HIF-3α subunits are dominant negative

regulators of HIF transcriptional activities (Jang et al., 2005). Furthermore, knockout and knockdown studies have demonstrated that HIF-1α and HIF-2α give rise to different phenotype(s) and analysis of the expression profiles of the 3 α subunits indicates that HIF-2α and HIF-3α appears to be tissue-specific while HIF-1α is ubiquitously expressed (Wiesener et al., 2003). For example, HIF-2α has been identified only in certain cell types such as macrophages and endothelial cells and is found up-regulated only in certain cancers, such as non-Hodgkin lymphoma and bladder cancers (Semenza, 2000a). This observation suggests that HIF-1α, HIF-2α and HIF-3α each regulate a different set of distinct transcription targets.

1.3.3 The Regulation of HIF-1

The regulation of HIF-1 activity is a multistep process involving HIF-1α stabilization, nuclear translocation, hetero-dimerization, transcriptional activation and interaction with other proteins. Although several steps of this process are independently regulated by oxygen, the oxygen-dependent regulation of the proteasomal degradation of HIF-1α stability is the most important step in regulating HIF-1 transcriptional activity (Berra et al., 2006; Salceda and Caro, 1997). This is because the availability of HIF-1α will determine the activity of HIF-1. Therefore, the transcriptional activity of HIF-1 is primarily controlled through the stability of its α subunit – HIF-1α. Although both the α and β subunits are constitutively transcribe and translated, HIF-1α is rapidly ubiquitinated and degraded via the 26S proteasome pathway under normoxic conditions (Kallio et al., 1999). This rapid degradation of HIF-1α is facilitated by the direct interaction between the β domain of von Hippel-Lindau protein (pVHL), a substrate recognition component of an E3 ligase complex,

and the ODD domain of HIF-1α that must be preceded by the hydroxylation of proline residues (Pro402 and Pro564) within the ODD domain of HIF-1α by HIF-1 prolyl hydroxylases (HPHs/PHDs) (Figure 1.4B). Molecular oxygen and iron (Fe) are essential for prolyl hydroxylation to occur and therefore, interaction between pVHL and HIF-1α occur only during normoxia and not hypoxia (Maxwell et al., 1999). Hence, under hypoxic conditions, the latter is not degraded but accumulates since prolyl hydroxylation does not take place and proteasomal degradation decreases. In addition, hypoxia has been shown to not only block HPH activity but also results in a downregulation of HPH/PHD proteins via E3 ligase, Siah2, that is activated during hypoxia (Nakayama et al., 2004).

The DNA binding and transcriptional activity of HIF-1 is also oxygen-dependently regulated by the hydroxylation of a critical asparagine residue (Asn803) located within the C-TAD of HIF-1α. Under normoxia, this highly conserved asparagine residue is hydroxylated by an asparaginyl hydroxylase, identified as Factor Inhibiting HIF-1 (FIH-1) (Lando et al., 2002), and prevents interaction with transcriptional coactivator, p300/CBP. Similar to HPHs/PHDs, this hydroxylation activity of FIH-1 requires molecular oxygen and Fe to take place. Therefore, during hypoxia, the C-TAD of HIF-1α is not silenced and is possible to interact with p300/CBP, leading to the recruitment of transcriptional coactivator complex.

Beside hypoxia, stability of HIF-1α can be regulated by gene mutations, inhibitors of HPHs, hormones and cytokines, and other physiological stresses under normoxia too. For example, the inactivation of pVHL has been associated with the development of highly vascularised tumors with constitutive HIF-1 expression due to

HIF-1α accumulation (Ivan et al., 2001) while the mutated *Ras* gene can increase HIF-1α protein level and HIF-1 activity during normoxia . Increased temperature can also directly promote the stabilization of HIF-1α as reported by Wenger's group (Katschinski et al., 2002).

1.3.4 Target Genes of HIF-1

HIF-1 has been referred also as the "guardian" of oxygen homeostasis, inducing a vast array of gene products that regulate energy metabolism, neovascularization, survival, pH and cell migration, and a strong promoter of tumor growth (Pouyssegur et al., 2006; Semenza, 2003). There are more than sixty putative direct HIF-1 regulated genes reported (Figure 1.5) and the list still grow continuously (Semenza, 2003). These genes have been identified through various methods such as identification of a *cis*-acting hypoxia-response element (HRE) that contains a HIF-1 binding site (Semenza and Wang, 1992), overexpression of HIF-1α using von Hippel-Lindau (*VHL*)-null cells or HIF-1α transfected cells (Carmeliet et al., 1998; Krishnamachary et al., 2003), and knockout or knockdown expression of HIF-1α (Wykoff et al., 2000). The DNA consensus sequence for HIF-1 binding is identified as 5'-(A/G)CGTG -3' and it is common for many genes that are up-regulated in the presence of oxygen deprivation (Semenza et al., 1996).

These HIF-1 downstream target genes serve various functions and biological processes that are ultimately involved in the survival of the tumor cells during hypoxia. Furthermore, these genes have been categorized into four main groups according to their biological involvement (Table 1.2) (Zagorska and Dulak, 2004). The first group of genes (e.g. vascular endothelial growth factor (VEGF), VEGF

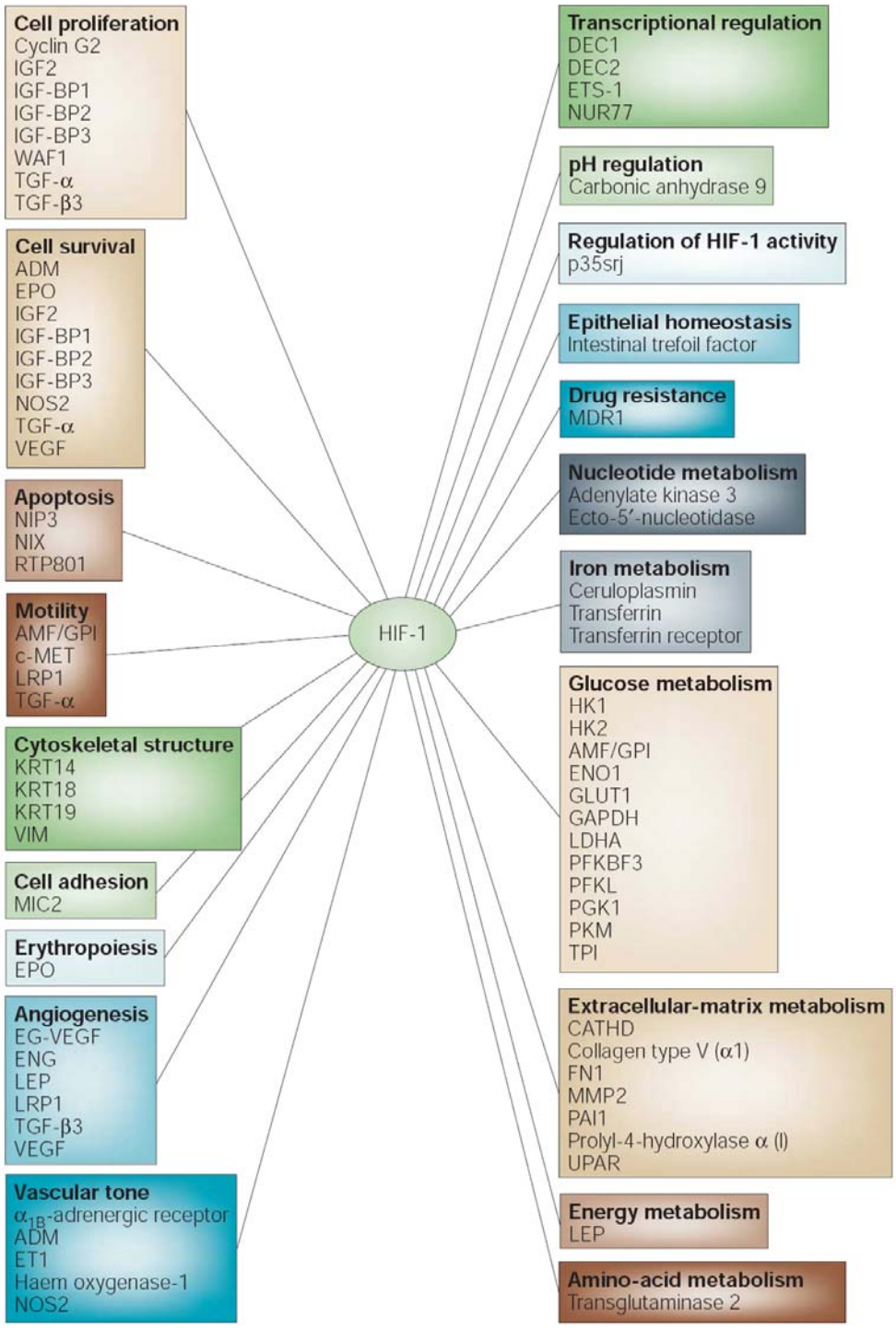

Figure 1.5: Genes that are transcriptionally activated by HIF-1. Over 60 putative HIF-1-regulated genes have been reported and these genes are separated into groups according to their functions (Extracted from Semenza, 2003).

Table 1.2: Genes upregulated by HIF-1 classified into four main categories based on their biological involvements (extracted from Zagorska and Dulak, 2004).

Process		Gene product	References
Control of vascular system	Angiogenesis	Vascular endothelial growth factor	Forsythe *et al.*, 1996
		VEGF receptor 1	Gerber *et al.*, 1997
		Plasminogen activator inhibitor 1	Kietzmann *et al.*, 1999
		Transforming growth factor β3	Caniggia *et al.*, 2000
	Vasomotor control	Nitric oxide synthase 2	Melillo *et al.*, 1995
		(inducible nitric oxide synthase)	Palmer *et al.*, 1998
		Endothelin-1	Hu *et al.*, 1998
		α_{1B}-adrenergic receptor	Eckhart *et al.*, 1997
		Adrenomedullin	Cormier-Regard *et al.*, 1998
		Heme oxygenase 1	Lee *et al.*, 1997
Maturation of red blood cells	Erythropoiesis	Erythropoietin	Jiang *et al.*, 1996
	Iron transport	Transferrin	Rolfs *et al.*, 1997
		Transferrin receptor	Lok & Ponka, 1999
			Tacchini *et al.*, 1999
		Ceruloplasmin	Mukhopadhyay *et al.*, 2000
Energy metabolism	Glycolysis	Lactate dehydrogenase A	Firth *et al.*, 1994
		Phosphoglycerate kinase 1	Semenza *et al.*, 1994, 1996
		Aldolase A and C	Iyer *et al.*, 1998
		Phosphofructokinase L	
		Pyruvate kinase M	
		Enolase 1	
		Hexokinase 1 and 2	
	Glucose transport	Glucose transporter 1	Gleadle & Ratcliffe, 1997
		Glucose transporter 3	O'Rourke *et al.*, 1996
			Iyer *et al.*, 1998
	Multifunctional enzyme	Glyceraldehyde-3-phosphate	Lu *et al.*, 2002
		dehydrogenase	Iyer *et al.*, 1998
Cell proliferation and viability	Arrest of cell cycle	p21	Carmeliet *et al.*, 1998
	Apoptosis	Bcl2/EIB 19kDa-interacting protein 3 (BNIP3)	Bruick, 2000
		Nip3-like protein X	Sowter *et al.*, 2001
	Growth factors	Insulin-like growth factor 2	Feldser *et al.*, 1999
		Insulin-like growth factor binding protein 1, 2 and 3	
Other	pH regulation	Carbonic anhydrase 9	Wykoff *et al.*, 2000
	Nucleotide metabolism	Adenylate kinase 3	O'Rourke *et al.*, 1996
	Matrix metabolism	Collagen prolyl-4-hydroxylase α1	Takahashi *et al.*, 2000
	Catecholamine synthesis	Tyrosine hydroxylase	Norris & Millhorn, 1995
	Feedback regulation	p35srj	Bhattacharya *et al.*, 1999

receptor 1, inducible nitric oxide synthase, and adrenomedullin) is involved in the control of vascular system through angiogenesis and regulation of vasculogenesis. The second group comprises of genes (e.g. erythropoietin and transferring) that induces red blood cell formation and maturation. The third group of genes (phosphoglycerate kinase 1, aldolase A and C, glucose transporters 1 and 3, and triosephosphate isomerase) mediates a switch in the main source of energy through a change in energy metabolism from aerobic metabolism to anaerobic glycolysis and an increased uptake of glucose. The fourth group includes genes (e.g. clusterin, $p21^{WAF1/CIP1}$, Nip3-like protein X, insulin-like growth factor 2) whose products are responsible for apoptosis and cell proliferation. Lastly, there are also other equally important HIF-1 target genes that are involved in other biological aspects other than these four main categories. They are grouped together in a separate category.

1.3.5 HIF-1α & Cancer

Immunohistochemical analyses for the presence and distribution of HIF-1α protein revealed that it is highly overexpressed in many cancers (Talks et al., 2000). In some cancers such as cancers of the brain, breast and cervix, strong positive correlation between HIF-1α overexpression and patient mortality has been reported for either all stages or specific stages of cancer development (Aebersold et al., 2001; Birner et al., 2000). Interestingly, in other cancers like head and neck cancer and non-small lung cancer, a decreased mortality was observed in patients with tumors overexpressing HIF-1α (Volm and Koomagi, 2000). Furthermore, studies have shown that the presence of functional or non-functional pro- and anti-apoptotic factors can affect the overall patient survival. One such example is the overexpression of HIF-1α and mutant p53 (non-functional) in ovarian cancers which significantly increase

mortality through lowered apoptosis (Birner et al., 2000). Therefore, the effect of HIF-1α overexpression is dependent on the type of cancer as well as the functional implications brought by other genetic alterations.

1.4 TP53: Tumor Protein 53

1.4.1 Tumor Suppressor p53

TP53 is a well known tumor suppressor gene and in human, it is located on chromosome 17p13.1. Perhaps this gene is more popularly known by its encoded protein – p53, a transcription factor that regulates the expression of many target genes (Vogelstein et al., 2000). It has been credited with titles like "guardian of the genome" (Lane, 1992), "death star" (Vousden, 2000) and "savior and slayer" (Bensaad and Vousden, 2005) over the years since its discovery in 1979. There are nearly 40,000 publications on p53 to date and it was voted as the "Molecule of the Year" in 1993 by *Science* journal. Originally, TP53 was thought to be an oncogene with immunocytochemical and immunohistochemical studies indicating accumulation of p53 protein observed only in the nucleus of transformed or tumor cells but not in normal cells. Furthermore, p53 level was found highly overexpressed in approximately half of the cancer cells tested. However, this notion was refuted when p53 gene of these tumors was found with mutations (Finlay et al., 1988; Hainaut and Hollstein, 2000). In addition, of those tumors not carrying mutated p53, majority was found with p53 inactivated at either the transcriptional or posttranscriptional level (Bykov and Wiman, 2003). Together, these arguably justify the importance of p53 in cell regulation and cancer biology even till today.

The fact that p53 function is impaired in the majority of human cancers has stimulated many efforts in deciphering the activation and function of this gene in cell at both normal and neoplastic states. Regulation of p53 level in cell is mainly under the control of Mdm2 while activation of p53 involves its dissociation from Mdm2 and this can be triggered in response to a wide variety of stimuli (Refer to Section 1.4.3). Many functions have been attributed to p53 and these include cell cycle regulation, apoptosis, angiogenesis, intracellular reactive oxygen species (ROS) removal, and genetic stability (Levine, 1997; Sablina et al., 2005; Yu et al., 1999). Figure 1.6 summarizes the different factors that activate (blue boxes) p53 and the many functions (pink boxes) performed by p53. Among the many publications on p53, the most well-studied biochemical function of p53 was its ability to bind specific genomic sequences and activate transcription of adjacent genes, which account for the variety of functions exhibited by p53. It was predicted that there could be as many as 300 genes under the control of p53 (el-Deiry, 1998).

Besides being a transcription factor and found predominantly as a nuclear protein, the cytoplasmic fraction of p53 is found translocated to the mitochondria and to perform a non-transcriptional function. It induces apoptosis by directly binding to pro-apopototic proteins like Bax and Bak (Leu et al., 2004; Mihara et al., 2003). The interaction will cause the inner mitrochondrial membrane to become permeable and this will allow cytochrome *c* and other pro-apoptogenic factors to be released into the cytosol, leading to apoptotic cell death. During genotoxic stress, cytoplasmic p53 is bound by Bcl-xL, an anti-apoptotic protein, and PUMA, a transcription target of p53, mediates the release of p53 so that it can interacts with pro-apoptotic proteins (Chipuk et al., 2005). Thus, two functions of p53 exist – One, as an important

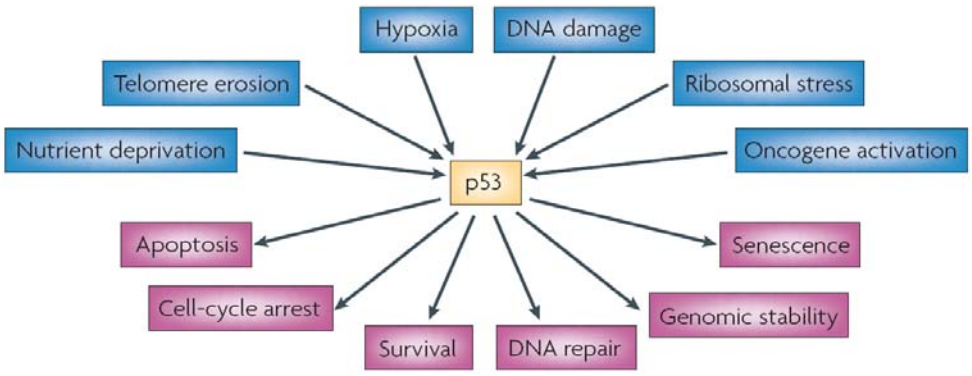

Figure 1.6: Activation and functions of p53. p53 has key roles in integrating cellular responses (pink boxes) to different types of stress (blue boxes). Activation of p53 can result in a number of cellular responses, and it is possible that different responses are induced by different stress signals. This is evidence that p53 can play a part in determining which response is induced through differential activation of target-gene expression. (Vousden and Lane, 2007)

transcription factor to regulate pro-apoptotic genes; two, directly interacts with pro-apoptotic proteins to initiate apoptosis.

1.4.2 The Structure of p53

The human p53 protein is made up of 393 aa and has a MW of 53 kDa under reducing condition. Although it has a complex domain structure, its structure can be simply broken down into 3 main regions – the N-terminal region, the core region, and the C-terminal region (Figure 1.7). The N-terminal region comprises of two transactivation domains (TDI aa 1-40 and TDII 40-60) and a proline-rich region (aa 40-94). The two transactivation domains, especially TDI, are important for interactions with other regulatory proteins, such as negative regulator MDM2 (Marine et al., 2006; Momand et al., 2000), components of transcription initiation complex (Lu and Levine, 1995), and coactivators (Gu et al., 1997). The proline-rich region is highly conserved and contains a SH3-domain binding motifs (PXXP). It is also responsible for the higher molecular weight observed on SDS-PAGE than the theoretical. The core region makes up the majority of the molecule, containing a DNA-binding domain (DBD, aa 94-292) that is responsible for the DNA-protein interactions. This core region is also the hotspot for most of p53 mutations found in human. In the C-terminal region, several nuclear localization sequences (NLS), a nuclear export signal (NES) and most importantly, an oligomerization domain can be found. The oligomerization domain is crucial for the formation of homotetramer of p53.

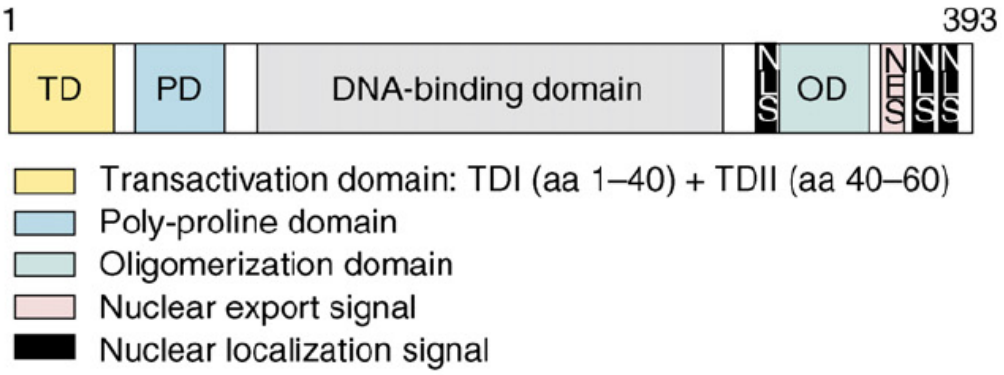

Figure 1.7: A schematic diagram illustrating the domains of p53. The transactivation domain (TD) is critical for the regulation of transcriptional activity of p53. (Fuster et al., 2007)

1.4.3 The Regulation of p53

Similar to the subunits of HIF-1, p53 is constitutively expressed and can be found in all tissues. However, at its steady state, p53 level is low and its activity is inhibited, mainly by the actions of its negative regulator Mdm2. This regulation is important as inappropriate activation of p53 can induce cell cycle arrest, premature senescence, or cell death. Mdm2 regulates p53 activity through at least 3 ways. First, Mdm2 can bind directly to the transactivation domain of p53 and block the recruitment of transcriptional co-activators to p53 (Vlatkovic et al., 2000) and C-terminal acetylation (Jin et al., 2002). Second, the binding of Mdm2 promotes nuclear export of p53 to the cytoplasm and this relocalization is shown to be dependent on the intact RING-finger domain of Mdm2 as well as the NES of p53 (Geyer et al., 2000). Third, Mdm2 acts as an E3-ubiquitin ligase, which is also the main form of inhibitory action exhibited. The association promotes p53 ubiquitination, followed by degradation via the proteasome pathway (Haupt et al., 1997; Honda et al., 1997). In a way, this can be akin to the relationship shared between HIF-1α and its negative regulator pVHL. Under normal conditions, the half-life of inactive p53 is only about 20-30 min (Prives and Hall, 1999). Interestingly, the expression of Mdm2 is positively regulated by p53 (Prives, 1998). Furthermore, it has been shown that there are other proteins cooperating with Mdm2 in the regulation of p53 stability. Mdm2-dependent p53 poly-ubiquitination and degradation can be enhanced by Yin Yang 1 (YY1) transcription factor, which can increase the interaction between Mdm2 and p53 (Gronroos et al., 2004).

In response to various stimuli, such as oncogene expression, DNA damage, nucleotide depletion, and hypoxia, the association between Mdm2 and p53 is

abrogated, resulting in rapid accumulation and activation of p53 protein (Levine, 1997; Prives and Hall, 1999). Two mechanisms have been proposed to explain the dissociation of Mdm2 from p53 under such stressed conditions. The first proposed mechanism is that $p19^{ARF}$ can antagonize the ubiquitin ligase activity of Mdm2 on p53 by binding to it directly (Michael and Oren, 2003; Pomerantz et al., 1998). Expression of $p19^{ARF}$ is stimulated in response to DNA damage. Moreover, in many cancers, mutations in the human homologue $p14^{ARF}$ gene are commonly found. The second mechanism that mediates the dissociation is the N-terminal phosphorylation of p53 induced by stress. In vitro binding affinity between Mdm2 and p53 peptides was prevented when Thr18 or Ser20 on p53 was phosphorylated (Craig et al., 1999).

The stabilization of p53 is highly mediated by phosphorylation and other forms of post-translational modifications (e.g. dephosphorylation, acetylation, methylation, ribosylation, *O*-GlcNAcylation, etc.) invoked by the stimuli (Sakaguchi et al., 1998; Unger et al., 1999; Yang et al., 2006). In fact, more than 18 phosphorylation sites have been reported for p53. Although some sites (e.g. Thr155, Ser389) are phosphorylated under normal conditions (Bech-Otschir et al., 2001), most sites are modified in response to DNA damage or various stresses (Higashimoto et al., 2000; Sakaguchi et al., 2000). One example is the product of ataxia telangiectasia (*ATM*) gene, a kinase that precedes p53 accumulation by phosphorylating multiple sites on p53 such as Ser15, Ser20, and Ser46 (Canman et al., 1998; Saito et al., 2002). In addition, Ser15 was identified as one of the major sites on p53 that is phosphorylated in response to cellular stress (Siliciano et al., 1997). Upon release from Mdm2, PTMs also promote tetramerization of p53 which is the most active DNA binding form. Other kinases, such as casein kinase I and II, protein kinase A,

CDK7, DNA-activated protein kinase, and Jun-NH_2 kinase (JNK), also mediate phosphorylation of p53 and play important roles in regulating p53 function.

1.4.4 Target Genes of p53

Wild-type p53 binds, as a homotetramer, to specific sites on the genome with a consensus binding sequence 5'-PuPuPuC(A/T)(T/A)GPyPyPy-3' and stimulates expression of downstream genes that are involved in various activities (el-Deiry et al., 1992). Depending on the conditions of cell growth, DNA damage, and the type/ duration of stress, p53 selectively activates a different group of target genes which are involved in reversible cell cycle arrest, DNA repair, angiogenesis, and/or apoptosis. One of the first identified transcriptional targets of p53 is cyclin dependent kinase (CDK) inhibitor p21 (el-Deiry et al., 1994). CDKs are important in regulating successful progression through the whole cell cycle and their activities can be inhibited by p21. This results in a p53-induced cell cycle arrest and allows DNA repairs to take place. Other p53-activated genes, such as GADD45, WIP1, MDM2, EGFR, PCNA, Cyclin D1, Cyclin G, TGFα and 14-3-3σ, are also involve in cell cycle regulation. In situations when cells are beyond repair, activated p53 will induce apoptosis by stimulating the extrinsic death-receptor pathway or the intrinsic mitochondrial pathway. Some examples of p53 transcriptional targets in this pro-apoptotic category include Puma, Noxa, and Bax. These proteins cause the inner mitochondrial membrane to become "leaky" and result in the release if cytochrome *c* and other apoptogenic factors, which eventually leads to apoptosis (Villunger et al., 2003; Yu et al., 2003). There are other pro-apoptotic genes (PIG11) activated by p53 that induce apoptosis via increasing intracellular ROS too (Liang et al., 2004). The

DNA damage results from an increased intracellular ROS by these genes can further activates p53, forming an amplification loop.

1.4.5 p53, Hypoxia and HIF-1α

The tripartite relationship between hypoxia, HIF-1α and p53 has always been a complex and debatable issue. Conflicting reports have led to questionable doubts whether and to what extent p53 accumulates under hypoxia. One group has shown that in transformed cells, p53 stabilization under hypoxia is HIF-1-dependent too (An et al., 1998). Furthermore, although this hypoxia-induced p53 was found transcriptionally inactive, the ability to induce apoptosis is retained (Koumenis et al., 2001) and this could be through the non-transcriptional function of p53 mentioned earlier (Section 1.4.1). On the other hand, this concept was challenged by other reports showing p53 did not accumulate under hypoxic conditions (Wenger et al., 1998). One reason for these differences may be the severity and extent of hypoxia used in different experiments. HIF-1α becomes stabilized when oxygen drops to 1~2% (mild to moderate hypoxia) but for p53 to stabilize, a more severe or prolonged hypoxia or anoxia (0.0~0.2%) is required. The presence of acidosis and nutrient deprivation in the tumor may have mediated the accumulation of p53 observed under hypoxia instead (Pan et al., 2004).

Furthermore, interactions between HIF-1α and p53, under mediations from Mdm2 and/or p300, have been reported and the transcriptional activity of p53 has been shown to result in the degradation of HIF-1α in several studies (An et al., 1998; Chen et al., 2003; Schmid et al., 2004b). This, in turn, will lead to a decrease in HIF-1 activity. Direct interaction was proposed to have occurred between the ODD domain

of HIF-1α, with two p53-binding sites were identified, and the DBD of p53 (Sanchez-Puig et al., 2005). In addition, HIF-1 activity can be attenuated by the accumulated p53 in another manner too and this is through competitive binding for a common transcriptional co-activator, p300. Thus, it can be further argued that the mechanism behind p53 accumulation under hypoxia is unlikely dependent on HIF-1. But it is important to note that a much higher level of p53 is required to induce HIF-1α degradation than for transactivation of p53 target genes (Blagosklonny et al., 1998). The accumulation pattern and role of p53 in regulating HIF-1α under various extents of hypoxic conditions is illustrated in a proposed model by Schmid et al. in figure 1.8. Further analysis is required for a more complete understanding of this tripartite relationship and therefore, in this project, we have adopted a proteomic approach to perform comparative analyses.

1.5 Proteomics

The word "proteomics" was only coined in the early 1990s by Marc Wilkins, PhD candidate, in the Macquarie University, Sydney, Australia, even though the first high resolution 2D gel electrophoresis was performed in 1975. However, back in those times, tools for protein identification were unavailable and reproducibility was difficult. It was only in the 1980s that reproducibility of 2D experiments improved with the introduction of immobilized pH gradients (IPG) strips and the introduction of mass spectrometry allowed protein identification at a large scale which eventually became the mainstream method for protein identification in the 1990s.

Proteomics can be defined simply as the study of proteins but to many, this will be considered as superficial. The best definition is probably given by Howard

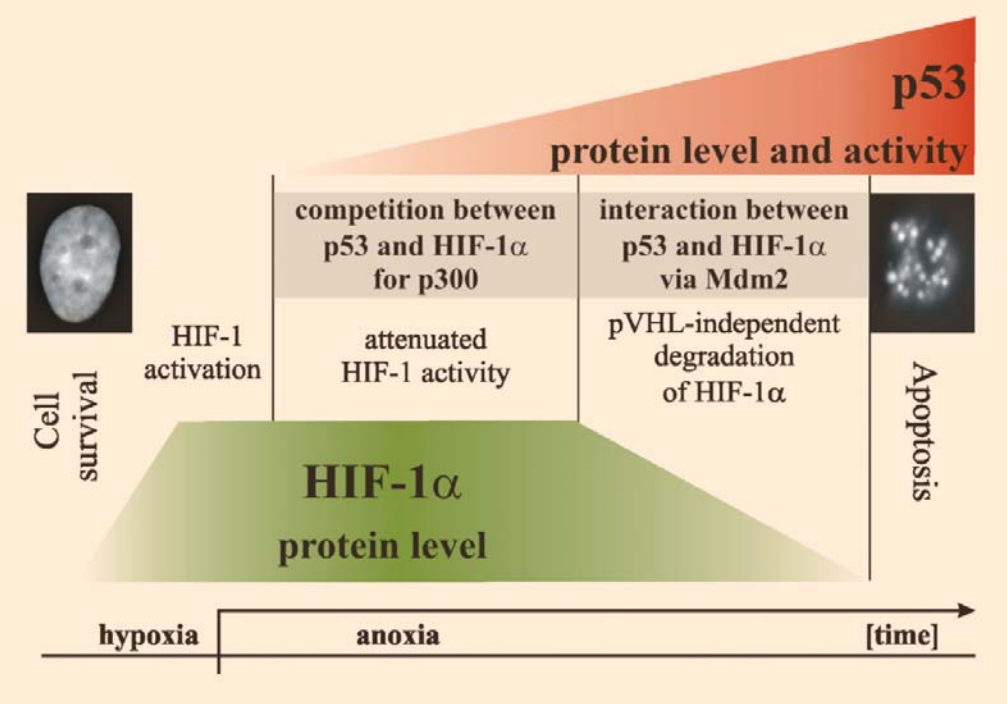

Figure 1.8: Proposed model showing different levels of HIF-1-p53 interactions in the presence of hypoxia and anoxia (Extracted from Schmid et al., 2004).

Hughes Medical Institute investigator, Professor Stanley Fields in *Science* who wrote "*Proteomics: the analysis of complete complements of proteins. Proteomics includes not only the identification and quantification of proteins, but also the determination of their localization, modifications, interactions, activities, and, ultimately, their function*" (Fields, 2001). Furthermore, this will include three-dimensional (3D) protein structure study at a large scale. Initially, proteomics study was restricted to only two-dimensional (2D) gel electrophoresis for protein separation and identification. Today, proteomics is referred to any methods used for the large scale characterization of proteins. There are currently many existing and emerging methods and approaches (e.g. 2D DIGE, shotgun proteomics, cleavable ICAT, iTRAQ, SILAC) available as technology for protein study becomes more sensitive and precise, resulting in a big influx of newly discovered proteins joining inline with already known proteins involved in known processes. Therefore, it is important that the new and old data are stringently curated.

1.5.1 Proteomics versus Genomics

Both proteomics and genomics studies contribute greatly and significantly to human health studies by allowing analysis of large scale of genes and proteins in a single experiment and thus, bypassing the traditional cumbersome and time-consuming protein characterization methods. Still, the shift in research from genome to proteome is a challenge for many scientists, mainly because the proteome, unlike the genome, is dynamic. If one is to liken genome to a blueprint of a house, the proteome will be the finished product that you see at the end of the day, with errors and changes made along the way or after it is finished (Fields, 2001). Likewise, proteins are subjected to many forms of PTMs such as phosphorylation, glycosylation,

acetylation, ubiquitination, farnesylation, and many others, to influence its cellular location, stability, binding affinity to other molecules, and activity. Furthermore, a gene can produce many different splice isoforms due to alternate splicing, or even a few different proteins due to varying translation start or stop sites, as well as frame shifts. The resulting protein products may have different or opposing functions and this can be exemplified in the case of p53 gene whereby several splice isoforms have been reported in human and mouse (Arai et al., 1986; Courtois et al., 2004; Courtois et al., 2002). These isoforms are either truncated at the N- or the C-terminal but all retain the characteristic core domain critical for DNA binding as well as function relating to apoptosis (Figure 1.9). Thus, all these possibilities can contribute to a more complicated proteome that is much bigger than the corresponding genome.

Through genomics, we can only understand that the gene exists and is activated by observing the synthesized mRNA level. On the other hand, the stability of mRNA is often short-lived and it has also been reported that mRNA levels are often not a true reflection of protein levels (Gygi et al., 1999). The direct measurement of protein will allow bypass of any mRNA inconsistencies that can arise and provides a more accurate level of gene activity. An example illustrating this is the expression of HIF-1α which is constitutively expressed but the protein level is nearly undetectable in all cell types under normoxic conditions (Kallio et al., 1999). Lastly, a protein can have several functions and may be involved in more than one process and likewise, similar functions may be carried by different proteins. A proteomic approach will allow the analysis of intact protein complexes from lysed cells and provide clues for their functions. Together, these reasons support the concept that

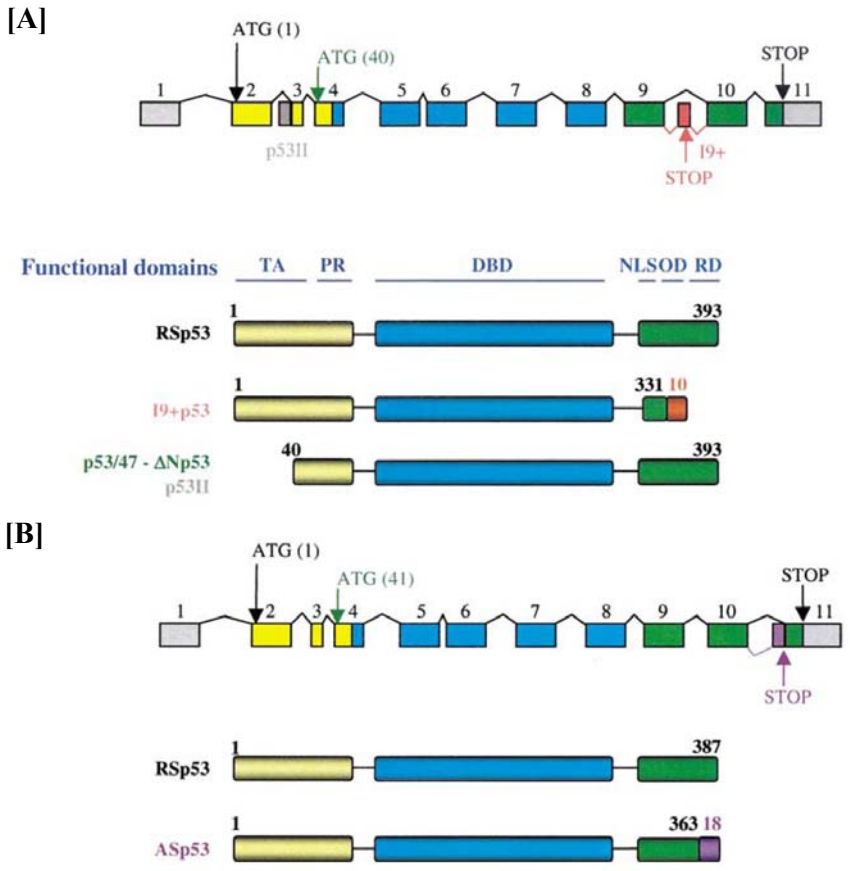

Figure 1.9: Different p53 isoforms and their mechanisms of production. **[A]** Human p53 isoforms. **[B]** Asp53, a mouse-specific isoform. Yellow: N-terminal domain; blue: DNA-binding domain; green: C-terminal domain; grey: noncoding exons of RSp53 and p53II; red: alternative exon identified in I9t p53; purple: alternative exon incorporated in ASp53. Major ATG and STOP codons are indicated in black. A second, alternative ATG at position 40 in DNp53 or in p53/47 is indicated in green. The corresponding ATG in the mouse is at codon 41. TA: transactivation domain; PR: proline-rich domain; DBD: DNA-binding domain; OD: oligomerization domain; RD: regulatory domain; NLS: nuclear localization signal. (Extracted from Courtois et al., 2004).

proteomics can allow a bigger and clearer picture of the actual cellular activities occurring in an organism.

1.5.2 Proteomic Techniques

Applications of proteomic approaches have been on the rise since the days of protein chemistry before the term "proteomics" was coined. This is evident by the exponential growth in the number of publications in proteomics compared to that in genomics as observed from 1995 to 2006 (Figure 1.10). The rapid development of better equipment and methods that can provide a quicker and more precise analysis might have promoted crucially to this trend. In this section, a brief introduction on a few currently popular methods used in proteomic study will be given.

1.5.2.1 Two-Dimensional Gel Electrophoresis & Two-Dimensional Difference Gel Electrophoresis

Two-dimensional gel electrophoresis (2D GE) is probably the oldest, yet popular, technique used today. This method is developed based on protein separation by their isoelectric points (pI) and molecular weights (MW), usually in a gel interface. The isoelectric point referred to as the pH at which a molecule carries no net electrical charge. The 2D GE is a two-step method – proteins are separated initially according to their pI (1^{st} dimension) in an IPG strip under the influence of an applied electric field, followed by MW separation (2^{nd} dimension) in a SDS-PAGE. Separated protein spots are visualized using various protein staining methods, such as silver staining. Typically, under reducing condition, an average of 2000~3000 protein spots can be visualized in a 20 by 20 cm high-resolution polyacrylamide gel. Comparative analysis is possible by loading equal amounts of proteins from test and control samples in

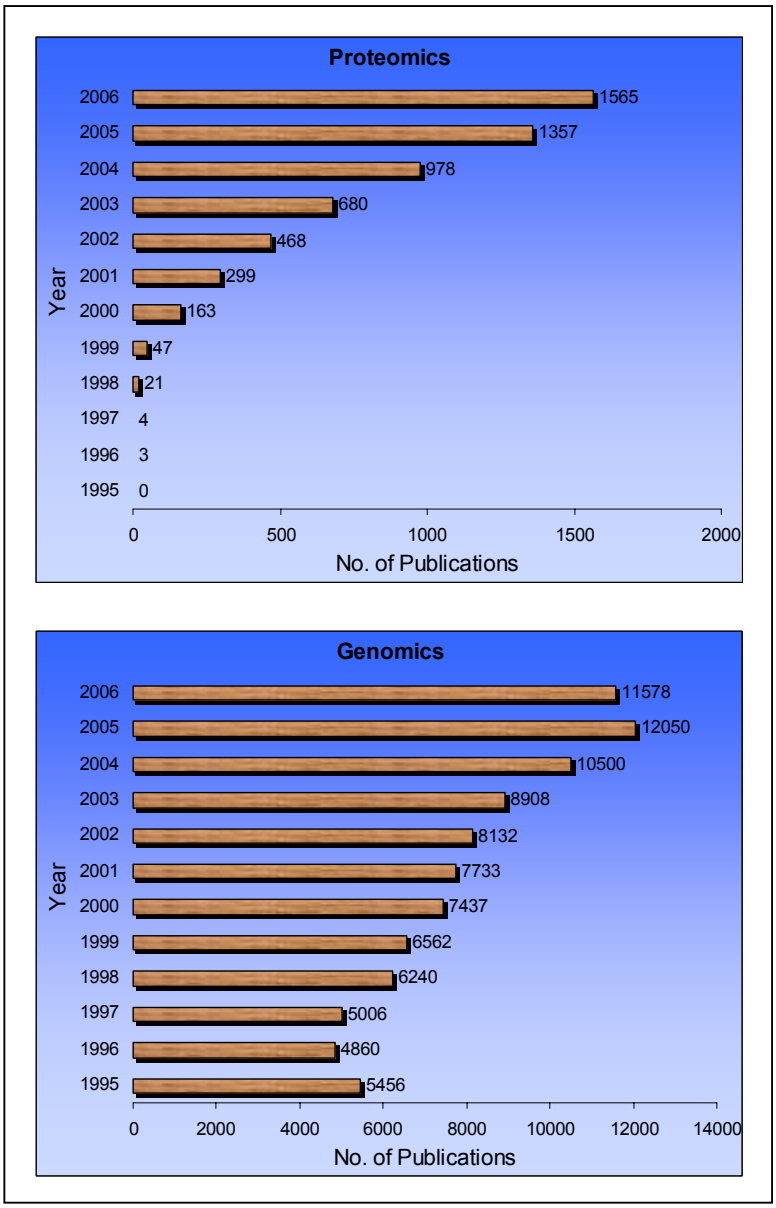

Figure 1.10: Numbers of publications in proteomics (top) and genomics (bottom) each year from 1995 to 2006 according to PubMed database. The search terms were the year and the words 'proteomics' or 'proteome' and 'genomics' or 'genome'. Search is limited to research/review articles or cited in PMC or manuscripts or open access articles or articles with supplementary material.

individual 2D GE under similar conditions. Several software (e.g. PDQuest, Melanie II, Genebio), some of which are free, have been developed for improving comparative analysis between two samples too. Protein spots can then be excised and sent for protein identification by mass spectrometry (MS). Two-dimensional difference gel electrophoresis (2D DIGE) is a similar technique but with some advantages over conventional 2D GE. It is a technique that incorporates protein fluorescent labeling with 2D GE and allows multiple protein samples that is labeled with different fluorescence dyes to be separated in the same IPG strip under identical experimental conditions. Comparative analysis is improved since the same protein from different samples will be located on the same spot. Although the total amount of protein is halved in 2D DIGE, it is claimed that the sensitivity is enhanced by the dyes. Differential expression profiles of each sample can also be visualized at each CyDye's excitation wavelengths under a fluorescence scanner. The disadvantage is that 2D DIGE is a lot more costly than conventional 2D GE.

The restricted pI and MW range used for protein separation is a limitation to this technique. Proteins with MW smaller than 10 kDa and greater than 200 kDa are usually hard to identify or resolve on PAGE gels. The presence of abundant proteins in protein samples can also prevent effective separation of proteins. However, this shortcoming can be overcome by removal of abundant proteins such as albumin using albumin depletion kit, or by fractionation of cellular proteins to selectively analyze the specific cellular fraction such as mitochondria.

1.5.2.2 Cleavable Isotope-Coded Affinity Tags & Isobaric Tags for Relative and Absolute Quantification

Cleavable isotope-coded affinity tags (cICAT) is a technique that utilizes cysteine-specific, light (^{12}C) and heavy (^{13}C), isotopic tags to label peptides (duplex labeling) for comparative proteomic analysis between two protein samples. On the other hand, a similar technique called isobaric tags for relative and absolute quantification (iTRAQ) can perform multiplex peptide labeling (currently up to four different samples) using four different amine-reactive isobaric tags with MW ranging from 114 to 117 Da instead. Both are able to provide a more complete protein identification and quantification data than with 2-D gels and are currently used popularly in many researches (Maurya et al., 2007; Tannu and Hemby, 2006). However, it is important to point out that in order to provide a more accurate analysis, relatively equal amounts of protein samples must be used for labeling. In addition, one critical downside is the limitation of information from databases which implies that not all detected peptides can be matched to known proteins.

1.5.2.3 Stable isotope labeling with amino acids in cell culture

Stable isotope labeling with amino acids in cell culture (SILAC) is a straightforward method that relies on *in vivo* metabolic incorporation of amino acids with substituted stable isotopes such as deuterium, ^{13}C, and ^{15}N. It shares a similar idea with cICAT and uses "light" and "heavy" forms of amino acids instead of tags. For example, in an experiment, two cell populations are grown in culture media that are identical except with one containing a 'light' and the other a 'heavy' form of a particular amino acid (e.g. ^{12}C and ^{13}C labeled L-lysine, respectively). In this way, the cells in both populations will uptake the amino acid from the media and incorporate

into all newly synthesized proteins. Therefore, labeling is possibly 100% and allows complete analysis of the whole cell proteome. The cells can then be lysed and the proteins can be pooled and processed (e.g. trypsin digestion, 2-dimensional liquid chromatography) before analysis by mass spectrometry. It is possible that SILAC is used as a multiplex technique like iTRAQ with different stable isotopes. Like any other techniques, SILAC has its own limitations and one limitation is that this technique is restricted to experiments involving cell culture.

CHAPTER 2 – OBJECTIVES

In this project, we adopt a quantitative proteomic approach using a recent method called iTRAQ and perform a multiplex comparative analysis on colorectal cancer cell line HCT116 that is either containing wildtype (WT) p53 or p53 knockout (KO), grown under normoxic or hypoxic conditions over a fixed period of time. The normoxic condition refers to the normal growing condition in cell culture, i.e. 5% CO_2; rest air, while hypoxic condition is set as 1% O_2; 5% CO_2; rest N_2.

In this study, we attempt to:

1. Identify novel targets regulated by p53 through comparative analysis between wild-type (WT) p53 cells and p53 knockout (KO) cells.
2. Identify novel targets regulate by hypoxia through comparative analysis between normoxic and hypoxic cells.
3. Elucidate possible relationships shared between proteins regulated by hypoxia and p53.
4. Construct the signaling pathways that are possibly regulated by hypoxia and p53.
5. Validate the potential markers regulated by p53 and hypoxia using RT-PCR and immunoblotting assays.

CHAPTER 3 – MATERIALS AND METHODS

3.1 Antibodies

Anti-p53 (DO-1), anti-Annexin II (3D5), anti-LDH-A (N-14) and anti-PGK1 (Y-12) were purchased from Santa Cruz Biotechnology (California, USA). Anti-HIF-1α and anti-EFHD2 were purchased from Becton Dickinson (BD) Biosciences (New Jersey, USA) and Novus Biologicals (Colorado, USA) respectively. Anti-PCBD1 was purchased from Abnova (Taipei City, Taiwan). Loading control anti-αtubulin (clone B-5-1-2) was purchased from Sigma-Aldrich (Missouri, USA). Secondary antibodies against mouse, rabbit and goat were also purchased from Santa Cruz Biotechnology. All antibodies were pre-diluted with 1X Tris-buffered saline Tween20 (TBST) (25 mM Tris-base, 150 mM NaCl, 0.05% (v/v) Tween-20, pH 7.4) before usage.

3.2 Primers

All primers were designed using ABI Primer Express® software (v3.0) (Applied Biosystems, California, USA) and purchased from 1st Base (Singapore), with the exception of GRIM19, ANXA2, PGK1, and MAPRE1, which were purchased from Research Biolabs (Singapore). Primers (Stock = 100 μM) used for conventional PCR were diluted individually to a working concentration of 10 μM while primer pairs used in quantitative RT-PCR were diluted to 5 μM per primer with RNase-free water.

3.3 Cell culture

Human colon carcinoma cell lines, HCT116 p53 knockout (KO) and its corresponding wild-type (WT), kindly provided by Dr. Yu Qiang (Genome Institute

of Singapore, Singapore), were cultured in Dulbecco's modified Eagles medium (DMEM), containing 4.5 g/L glucose, 4.0 mM L-glutamine, 10 % heat inactivated fetal bovine serum (FBS), 3.7 g/L sodium bicarbonate solution ($NaHCO_3$) and 100 units/mL penicillin-streptomycin (PS) solution. All were purchased from HyClone (Logan, Utah, USA). The cells were maintained under standard cell culture environment (5 % CO_2-containing humidified atmosphere) in a MCO-18AIC CO_2 incubator (Sanyo, Japan) at 37^{o}C.

3.4 Normoxia, hypoxia and hypoxia-mimetic drugs treatments

Both HCT116 p53 KO and HCT116 WT cells were initially seeded in 10 cm culture dishes (Nunc, Roskilde, Denmark) and cultured in DMEM, containing 4.5 g/L glucose, 4.0 mM L-glutamine, 10 % FBS, 1 % PS and 3.7 g/L $NaHCO_3$, under standard cell culture condition for 24 hours (hr) in the CO_2 incubator at 37 ^{o}C.

Subsequently, the cells were incubated under hypoxic (1 % O_2, 5 % CO_2, rest N_2) or normoxic (5 % CO_2, rest air) conditions for 18 hrs at 37 ^{o}C in fresh culture medium. In a separate experiment to stimulate hypoxic signaling pathways, we also treated cells with 100 μM cobalt chloride ($CoCl_2$) from Fluka (Sigma-Aldrich, Missouri, USA) for 18 hr at 37 ^{o}C in normoxic condition.

3.5 Protein extraction

Total cell extracts were prepared from HCT116 WT and HCT116 p53 KO immediately after 18 hr of hypoxic or normoxic or drug treatment. Each plate of cells was washed twice with ice-cold 1X phosphate-buffered saline (PBS; 3.2 mM Na_2HPO_4, 0.5 mM KH_2PO_4, 2.7 mM KCl, 135 mM NaCl, pH 7.4) briefly and the

cells were lysed in 400 μL radioimmunoprecipitation assay (RIPA) buffer (50 mM Tris-HCl pH 8.0, 150 mM NaCl, 1 mM EDTA, 1 % (v/v) NP-40, 0.5 % (w/v) sodium deoxycholate, and 0.1 % (w/v) SDS) prepared with some modifications to original recipe. Proteases inhibitors, containing 1 mM phenylmethylsulfonyl fluoride, 1 mM aprotinin, 1 mM pepstatin A, and 1 mM leupeptin were added into the RIPA buffer just before use. All protease inhibitors were purchased from Sigma-Aldrich (Missouri, USA). The cells lysates were then transferred into individual 1.5 mL microfuge tube (Axygen, California, USA) and incubated in ice for 15 minutes (min), vortexing for 1 min after every 5 min of incubation. The lysed samples were then centrifuged at 16,000 x g for 1 hr and clarified supernatants were collected in fresh 1.5 mL microfuge tubes for further experiments or stored at -80 ^{o}C. All steps were performed on ice or at 4 ^{o}C unless otherwise stated.

3.6 Protein Quantification

Protein concentrations of each sample collected were determined using a reducing agent compatible and detergent compatible (RC DC) Protein Assay Kit from Bio-Rad (California, USA) by following the instructions provided. A standard curve with 6 dilutions (0.2 to 1.5 mg/mL) of a protein standard (bovine serum albumin, provided by the kit) was also generated for each new assay. The samples were also diluted appropriately (between 2X to 25X dilutions) and prepared in duplicates each time. Absorbance values were read at wavelength 750 nm using Beckman DU®-65 photospectrometer (California, USA) and protein concentrations of each sample were calculated according to the protein concentration standard curve generated in each assay each time.

3.7 Sodium dodecyl sulphate polyacrylamide gel electrophoresis (SDS-PAGE)

Different percentages of SDS-PAGE gels, ranging from 8% to 15%, were prepared with Bio-Rad Mini-PROTEAN 3 (MP3) gel casting system (California, USA) as shown in table 3.1. Extracted protein lysates were mixed by vortexing with 6X SDS sample loading buffer (3 % (w/v) SDS, 40 % (v/v) glycerol, 600 mM β-mercaptoethanol, and 0.1 % (w/v) bromophenol blue in 150 mM Tris-HCl pH 6.8). Samples were then "cooked" at 95 ^{o}C for 10 min, following centrifugation at maximum speed for 1 min at room temperature to pellet down any residues before use. Gel electrophoresis was carried out in Tris-Glycine buffer (25 mM Tris-base, 192 mM Glycine, 0.1 % (w/v) SDS) at a constant current of 12 mA per gel at room temperature. Acrylamide/Bis solution (30 % stock; 29:1 ratio (3.3 % C)), ammonium persulfate (APS) and SDS powder were purchased from Bio-Rad. Tris-base and TEMED were purchased from 1st Base (Singapore) and Invitrogen (California, USA) respectively.

3.8 Staining and destaining of SDS-PAGE gels

The SDS-PAGE gels were stained in Coomassie Brilliant Blue staining solution (0.25 % (w/v) Coomassie Blue R-250 in 50 % (v/v) methanol and 10 % (v/v) glacial acetic acid), shaking for 30min at room temperature on an orbital shaker (Heidolph® unimax 2010, Germany). The gels were then destained with destaining buffer (30 % (v/v) methanol, 10 % (v/v) glacial acetic acid) to remove excess background.

3.9 Immunoblot Assay

Extracted protein lysates were mixed thoroughly with 6x SDS sample buffer and resolved on SDS-PAGE gels as described in the previous section 3.7. The

Table 3.1: Preparation for different percentages of SDS-PAGE gels. Measurement units are all in milliliter (mL) unless otherwise stated.

Reagents	**Resolving gel per 10mL**				**Stacking gel per 4mL**
	8%	**10%**	**12%**	**15%**	**5%**
30% Acrylamide/Bis	2.7	3.3	4.0	5.0	0.67
1.5M Tris-HCl, pH8.8	2.5	2.5	2.5	2.5	--
1.0M Tris-HCl, pH6.8	--	--	--	--	0.5
MilliQ Water	4.6	4.0	3.3	2.3	2.7
10% (v/v) SDS	0.1	0.1	0.1	0.1	0.04
10% (v/v) APS	0.1	0.1	0.1	0.1	0.04
TEMED	6µL	4µL	4µL	4µL	4µL

proteins were then electroblotted to BioTrace™ polyvinylidene fluoride (PVDF) transfer membranes (0.45 μm) (PALL, Florida, USA). The membranes were then blocked with 2 % bovine serum albumin (BSA) prepared in 1X TBST and incubated for 1h. Subsequently, they were rinsed briefly with copious 1X TBST twice, followed by 1 hr or overnight incubation with primary antibodies. The membranes were then incubated with secondary antibodies conjugated with horseradish peroxidase (HRP) for 1 hr after removal of primary antibodies. Membranes were washed 3 x 5 min with copious 1X TBST after each antibody incubation step. Target proteins were visualized by enhanced chemiluminescence (Super Signal®, Pierce, Illinois, USA) and X-ray films (Fuji SuperRX Film, Fuji, Japan), which were developed using a Kodak X-ray film processor.

Unless otherwise stated, all steps were performed at room temperature and all incubation was done on an orbital shaker. Overnight primary antibody incubation was performed in a 4 ^{o}C cold room on a Belly Dancer® shaker (Stovall, North Carolina, USA).

3.10 iTRAQ

All steps were performed according to the manufacturer's protocol (ABI, *Applied Biosystems iTRAQ™ Reagents Chemistry Reference Guide*, 2004, http://docs.appliedbiosystems.com/pebiodocs/04351918.pdf) with minor modifications. The experiment was repeated 3 times under the same condition as stated below.

3.10.1 iTRAQ – Protein Extraction

Protein sample preparation for iTRAQ differed slightly from the above "Protein Extraction" method used. The cell samples were washed twice with ice-cold PBS and harvested with 300 μL lysis buffer (0.1 M triethylammonium bicarbonate (TEAB) pH 8.5, containing 1 % (w/v) SDS) per 10 cm culture dish. The mixtures were transferred into individual 1.5 mL microfuge tubes and boiled at 100 ^{o}C for 15 min, followed by 15 min incubation on ice, vortexing for 1 min after every 5 min. The tubes were then centrifuged at 16,000 x g for an hour at 4 ^{o}C and clarified supernatants were transferred to new microfuge tubes. A small volume from each sample was aliquot and used for protein quantification using Bio-Rad's RC DC Protein Assay Kit. Remaining sample was stored in -80 ^{o}C.

In this study, the different samples were labeled as "WT-N", "WT-H", "KO-N" and "KO-H", with "N" and "H" representing "normoxia" and "hypoxia" respectively.

3.10.2 iTRAQ – Reduction & Cysteine blocking

After protein quantification, 100μg of proteins from each sample was aliquot into fresh individual 1.5 mL microfuge tubes and the final volume was adjusted to 40 μL with the lysis buffer. Disruption of the disulphide bonds in each protein sample was carried out by adding 5 mM of tris-(2-carboxyethyl)phosphine (TCEP), a reducing agent provided by iTRAQ kit, to each sample and mixed by vortexing. Each sample mixture was then incubated at 60 ^{o}C for 1 hr. Thereafter, 10 mM methyl methanethiosulfonate (MMTS), a cysteine blocking reagent provided by iTRAQ, was

added to each tube and mixed thoroughly. This was followed by 10 min of incubation at room temperature.

3.10.3 iTRAQ – Trypsin Digestion

After reduction & cysteine blocking, the samples were diluted 20 times with 0.5 M TEAB to reduce SDS concentration to less than 0.05 %. High concentrations (> 0.1 %) of SDS would decrease or inhibit the activity of trypsin. 25 μg of porcine trypsin prepared in MilliQ (MQ) water was added to each diluted sample and vortex. The resulting mixture for each sample was incubated in a 37 ^{o}C incubator oven for 16 hr. Thereafter, the trypsin-digested samples were speed-vac to dryness and reconstituted in 25 μL dissolution buffer (containing 0.5 M TEAB) provided by the iTRAQ kit.

3.10.4 iTRAQ – Sample Labeling

All iTRAQ isobaric labels (114, 115, 116, & 117) were individually dissolved in 70 μL ethanol and the entire content of each dissolved label was mixed thoroughly by votexing with each sample as stated below.

- iTRAQ label 114 ➔ WT-N
- iTRAQ label 115 ➔ WT-H
- iTRAQ label 116 ➔ KO-N
- iTRAQ label 117 ➔ KO-H

The 4 samples were incubated at room temperature for 1 hr and they were then combined together.

3.10.5 iTRAQ – Sample Clean-up Prior to LC/MS/MS Analysis

Before performing LC/MS/MS analysis, the iTRAQ-labeled peptides were cleaned up using cation exchange chromatography with the Applied Biosystems cation-exchange cartridge system (P/N 4326747) to remove unbound iTRAQ tags and salts.

The combined iTRAQ-labeled peptides were diluted at least 10 fold with Cation Exchange Buffer (CEB)–Load (10 mM potassium phosphate (KH_2PO_4) in 25 % (v/v) acetonitrile, pH 3.0) and the pH was adjusted with phosphoric acid to 2.5~3.5. Prior to injection of the sample mixture, the SCX cartridge was conditioned with the same loading buffer. Injection of sample mixture into the SCX cartridge was done manually using a sterile 5 mL syringe (Becton Dickinson (BD), Singapore) at the rate of approximately 1 drop per second and the flow-through was collected in a fresh 15 mL Falcon® tube (Becton Dickinson, New Jersey, USA). The flow-through was re-injected into the SCX cartridge two more times and the final flow-through was collected and stored at -20 ^{o}C. An additional 1 mL of CEB–Load was injected to wash excess iTRAQ reagents, salts, and SDS from the cartridge with the flow-through collected and stored too.

Bound iTRAQ-labeled peptides were eluted by slowly injecting 500 µL of CEB–Elute (10 mM KH_2PO_4 in 25 % (v/v) acetonitrile containing 350 mM potassium chloride (KCl), pH 3.0) and the eluate was collected. Subsequently, the collected eluate was diluted 10 times with Buffer A (98 % MQ water; 2 % (v/v) acetonitrile; 0.05 % (v/v) TFA) prior to passing through a C_{18} Sep-Pak® cartridge (Waters, USA) for desalting. The cartridge was pre-activated by injecting 10 mL 100 % acetonitrile

(ACN) and pre-equilibrated with 10 mL Buffer A before injecting the diluted eluate slowly into it. The flow-through was collected and re-injected two more times and finally collected and kept at -20 ^{o}C.

The bound peptides were eluted using 5 mL elution buffer (50 % MQ water; 50 % ACN), following by another 5mL of Buffer B (20% MQ water; 80% (v/v) ACN; 0.05 % (v/v) TFA). The eluted peptides were collected in a fresh 50mL Falcon® tube (Becton Dickinson, New Jersey, USA) and mixed with 10 mL MQ water. The diluted eluate was flash-frozen with liquid nitrogen and lyophilized. Lyophilized eluate was then re-constituted in 1mL Buffer A and transferred into a fresh 1.5 mL microfuge tube. The reconstituted solution was then speed-vac to dryness and stored at -20 ^{o}C before LC/MS/MS analysis. All flow-through fractions collected were kept until MS/MS analysis verified the success loading onto SCX cartridge.

3.10.6 iTRAQ – Two-dimensional Liquid Chromatography (LC) separation & MS/MS

The dried 400 μg iTRAQ-labeled peptides were subsequently processed in the Protein and Proteomics Centre in National University of Singapore – Department of Biological Sciences (NUS-DBS).

Two-dimensional LC separation of the peptides was carried out using an UltiMate™ dual-gradient LC system (Dionex-LC Packings, California, USA). The peptides were solubilized in 30 μL Buffer A solution and 27 μL was injected into a 0.3 x 150 mm strong-cation exchange (SCX) column (FUS-15-CP, Poros 10S) (Dionex-LC Packings, California, USA). The composition of Mobile Phase A was

5mM KH_2PO_4 and 5 % (v/v) ACN (pH 3.0). Mobile Phase B was the same as Mobile Phase A with an additional 500 mM KCl added. The first flow-through (unbound peptides) was collected as the first fraction. Subsequently, 8 more fractions were separated by step gradients of Mobile Phase B (0-5, 5-10, 10-15, 15-20, 20-30, 30-40, 40-50, 50-100% B) at a flow rate of 6.0μL/min. All 9 fractions were captured alternatively onto two 0.3 x 1.0 mm PepMap™ C_{18} trap columns (3 μm, 100 Å) (Dionex-LC Packings, California, USA) and washed with 0.05 % (v/v) TFA. The captured peptides were then resolved on a reverse-phase PS-DVB capillary monolithic column (Dionex-LC Packings, California, USA) at a flow rate of 2.7 μL/min over a 20 min linear gradient from 0 to 60 % of Buffer B (20% MQ water; 80% (v/v) ACN; 0.05 % (v/v) TFA) solution, followed by a constant 2 min 90 % Buffer B solution.

The eluate was mixed with MALDI matrix (7mg/ml α-cyano-4-hydroxycinnamic acid; 130 μg/ml ammonium citrate in 75 % A(v/v) CN) at a ratio of 1:2 through a 25 nL mixing tee (Upchurch Scientific, Washington, USA) at a flow rate of 5.4 μL/min. The resulting mixture was spotted onto 192-well stainless steel MALDI target plates (Applied Biosystems, California, USA) using a offline Probot™ Microfraction Collector (Dionex-LC Packings, California, USA) at an interval of 5 sec per well.

The peptides were analyzed on a 4700 Proteomics Analyzer (Applied Biosystems, California, USA) with MALDI source and TOF/TOF™ optics. Default calibrations in MS and MS/MS were updated regularly and the deflector plates (X1, Y1, X2 and Y2) were optimized constantly for optimal sensitivity. All positive ion

MS/MS data were acquired using nitrogen with collision energy of 1 keV and a collision gas pressure of ~1 x 10^{-6} Torr. MS spectra were recorded for all 192 spots on each MALDI plate and each spectrum was generated in the mass range of 850– 3500 amu by averaging 1,000 laser shots. MS precursor ions that met the precursor selection criteria were selected for subsequent MS/MS analyses. An initial 6000 laser shots were combined to obtain precursor ions with signal to noise (s/n) greater or equal to 100. A subsequent 10,000 laser shots were acquired for precursor ions with s/n ratio between 50 and 100 inclusively.

3.10.7 iTRAQ – MS data analysis and protein identification

Peptide and protein identifications were performed by searching the MS/MS spectra against the International Protein Index (IPI) database (version 3.2.3) using a local MASCOT™ search engine (version 2.1; Matrix Science), with human chosen as the source of the proteins and the search was restricted to tryptic peptides. The following parameters were also set for the search: trypsin with maximum one missed cleavage was allowed; precursor error tolerance was set to 100 ppm and MS/MS error tolerance to 0.3 Da; iTRAQ-labeled N-termini and lysines as well as methyl methanethiosulfonate (MMTS) labeled cysteines were chosen as fixed modifications and methionine oxidation as variable modifications. The MASCOT-matched peptides included for protein identification and quantification analysis were filtered accordingly with confidence interval (C.I.) values no less than 85 % and maximum peptide rank set as 2.

3.10.8 iTRAQ – Protein Quantification and Statistical Analysis

Relative quantification of proteins was performed on the MS/MS scans. The reporter ion (m/z 114, 115, 116 and 117 – masses of tags that corresponds to the iTRAQ reagents) peak areas (RPAs) were extracted from the raw MS spectra and normalized among the samples using GPS Explorer™ software (version 3.6) (Applied Biosystems, California, USA). Individual protein pair expression ratios were computed based on the RPAs (m/z 115, 116, and 117) measurements relative to WT-N measurements (m/z 114) initially. Further expression ratios for KO-H measurements (m/z 117) relative to WT-H measurements (m/z 115) and to KO-N measurements (m/z 116) were also generated to allow greater magnitude of comparisons among the 4 samples.

With reference to previous work done earlier (DeSouza et al., 2005), many identified proteins were found with an expression ratio close to 1.0 after normalization. Therefore, protein targets exhibiting fold expression changes greater than 30% were classified as proteins showing potentially, significant altered expression. In addition, this group of selected targets must exhibit a confidence interval (C.I.) greater than or equal to 95% and were reported in at least 2 experimental replicates. Subsequently, each protein that showed significant changes was manually screened by studying their MS/MS spectra. Protein targets, satisfying the criteria, were selected for downstream verification using immunoblotting and real-time quantitative PCR (RT Q-PCR).

3.11 RNA purification

Total RNA of HCT116 WT and HCT116 p53 KO cells were extracted using TRIZOL® reagent (Invitrogen, California, USA), immediately after 18 hr of hypoxic or normoxic treatment. The procedure was carried out according to the product's instruction manual with minor modifications. Briefly, each plate (10 cm culture dish) of cells was harvested with 1 mL of TRIZOL® reagent. The harvested samples were homogenized and incubated at room temperature for 5 min before 0.2 mL of chloroform was added to each sample and shook vigorously. Next, the samples were left undisturbed at room temperature for 3 min, following by centrifugation at 11,000 x g for 15 min at 4 ^{o}C. The aqueous layer was then carefully transferred to a fresh tube and 0.5 mL isopropanol were added and mixed well to allow precipitation of RNA. The mixture was centrifuged at 11,000 x g for 10 min at 4 ^{o}C, preceding incubation at room temperature for 10 min. Supernatant was discarded and the pellet was washed with 1 mL of 75 % (v/v) ethanol by vortexing, following centrifugation at 7,000 x g for 5 min at 4 ^{o}. The resulting pellet was air-dried briefly and re-dissolved in DECP-treated sterile MilliQ-water at 60 ^{o}C prior to storage at -80 ^{o}C.

The quality and concentration of each dissolved RNA pellet were measured at wavelengths 260 nm and 280 nm. The ratio of absorbance readings at 260 nm to 280 nm indicates the quality and purity of the RNA extracted. All RNA samples were diluted with RNase-free water to a concentration of 0.6 μg/μL.

3.12 cDNA synthesis

The diluted RNA samples were used to obtain complementary DNA (cDNA) through reverse transcription using SuperScript™ First-Strand Synthesis System for

RT-PCR kit from Invitrogen (California, USA). Generation of first-strand cDNA was carried out strictly according to the kit's instruction manual. For each 20 μL reaction, 4.2 μg RNA was mixed with 1 mM dNTP mix and 1 mM Oligo(dTs). RNase-free water was used to top up the volume to 13.25 μL. The resulting mixture was incubated at 65 ^{o}C for 5 min, followed by 1 min incubation in ice. Thereafter, 4 μL of 5X RT buffer, 10 mM DTT and 0.5 μL RNAseOUT™ Recombinant RNase Inhibitor were added, mixed and incubated for 2 min at 42 ^{o}C. Fifty units (0.25 μL) of SuperScript™ II RT was then added, mixed and incubated at 42 ^{o}C for another 50 min. Reaction was then terminated at 70 ^{o}C for 15 min. All cDNAs generated were stored in -20 ^{o}C for further applications.

3.13 Quantitative Real-Time Polymerase Chain Reaction (RT-PCR)

Quantitative RT-PCR was performed according to the instruction manual from Applied Biosystems (ABI, *Applied Biosystems SYBR® Green PCR Master Mix and RT-PCR, 2002*) using ABI Prism 7000 Sequence Detection System (Applied Biosystems, California, USA) and SYBR® green dye (Applied Biosystems, Warrington, United Kingdom), as the reporter probe.

The cDNA samples were diluted 84 times with sterile MilliQ water for RT-PCR. For each RT-PCR reaction, 3 μL of pre-diluted cDNA were mixed with 400 nM of each gene specific primer pair and 10 μL of SYBR® green master mix (2X). Sterile MilliQ water was used to make up the volume to 20 μL. The RT-PCR was carried out in optical 96-well reaction plates from Applied Biosystems. Cycle threshold (Ct) value and baseline were set at 0.2 and from cycle 6 (start) to 15 (end) respectively. All primers' specificities were checked by observation of singular peaks from their

dissociation curves with no signals detected from their respective no-template controls (NTC). Results were normalized against β-actin as the internal control.

CHAPTER 4 – RESULTS

4.1 HIF-1α protein stabilizes and accumulates in cells under artificially-induced hypoxia

To confirm if our hypoxic chamber is capable of inducing low oxygen tension in cells, we used immumoblotting assays to examine the stabilization and accumulation of HIF-1α from the treated cells. Accumulation of HIF-1α protein was observed in both HCT116 p53 KO and its corresponding WT grown under hypoxic condition (1% O_2; 5% CO_2; rest N_2) as well as cells treated with $CoCl_2$ (positive control) while it was undetectable in both cells under a normoxic condition (Figure 4.1A). $CoCl_2$ has been widely used as a hypoxia mimic in both in vivo and in vitro experiments (Wang and Semenza, 1993) and it is known to exhibit hypoxia-like responses through activation of hypoxia signaling by stabilizing HIF-1α (Vengellur et al., 2003). A higher amount of HIF-1α accumulation (approximately 2 to 3 folds) was also observed in HCT116 WT samples compared to corresponding hypoxia-treated HCT116 p53 KO samples (Figure 4.1B), hinting a possible influence of p53 on the stability of HIF-1α protein. There was no significant change in the level of p53 protein (Figure 4.1C) observed when the cells were treated with hypoxia. The stabilization of HIF-1α observed in the cells indicated that our artificial hypoxic system was a success and cells were able to be cultured under low oxygen condition.

4.2 iTRAQ Data Analysis

4.2.1 Effects of Hypoxia on protein profiles in the presence/absence of p53

To examine the effects of hypoxia treatment in the presence or absence of p53 at proteome level, HCT116 cells were either treated with normoxia or hypoxia for 18

[A]

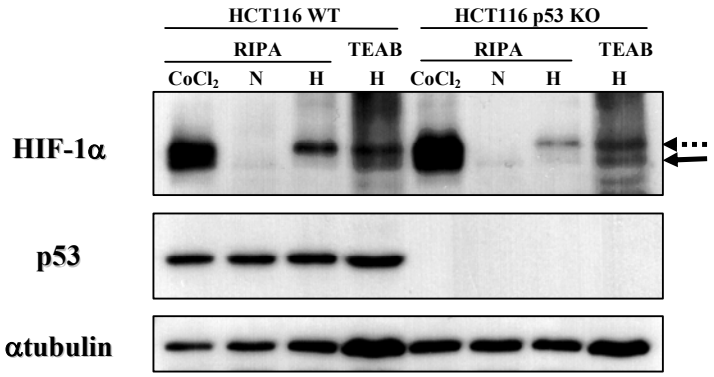

[B] **[C]**

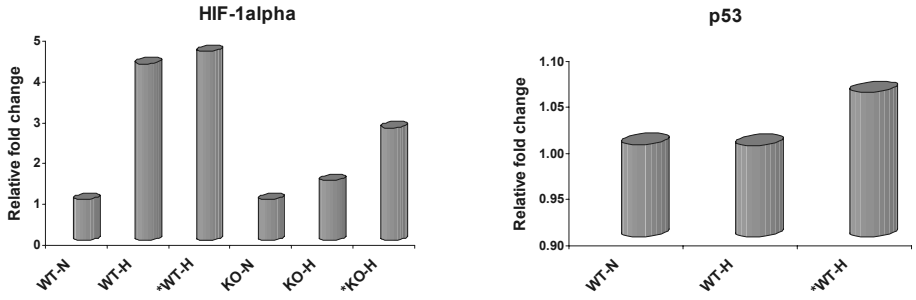

Figure 4.1: Stabilization and accumulation of HIF-1α under hypoxia. **[A]** Proteins (50μg) from each sample were separated by SDS-PAGE and the protein levels of HIF-1a and p53 were detected with respective antibodies. Accumulation of HIF-1α was observed in hypoxic samples and $CoCl_2$-treated cells (positive control). Dotted arrow indicates phosphorylated HIF-1α while solid arrow indicates non-phosphorylated HIF-1α. No significant change in p53 protein level was noted in both hypoxic sample as well as $CoCl_2$-treated cells. No p53 protein was detectable in all HCT116 p53 KO samples. A graphical representation of HIF1α **[B]** and p53 **[C]** protein levels in normal and hypoxic samples after normalization against αtubulin. Band quantitation was performed by calculating the base intensity peak area using Image J (http://rsb.info.nih.gov/ij/). All samples were compared with reference to their respective normoxic controls. ('WT-N': normoxia-treated HCT116 WT; 'WT-H': hypoxia-treated HCT116 WT; 'KO-N': normoxia-treated HCT116 p53 KO; 'KO-H': hypoxia-treated HCT116 p53 KO; asterisk (*) denotes sample harvested using triethylammonium bicarbonate (TEAB) (pH 8.5), containing 1% SDS; α–tubulin serves as a loading control.)

hrs, harvested, and labeled with specific iTRAQ isobaric tags for each sample. A multiplexed iTRAQ-based quantitation in protein profiling was performed. In addition, protein identification was done by searching the MS/MS spectra against the IPI human database using signature peptides that are generated during trypsin digestion and identified by MS/MS. The iTRAQ quantitation strategy is based on the derivation of quartet samples with isotopically distinct tags, and the relative peak intensities of the resultant isotope clusters were determined to represent changes in peptide abundance among the samples. Figure 4.2 is a representative MS/MS spectrum used for peptide ratio determination with reference to the peak intensities of signature peaks (*m/z* 114 to 117) of iTRAQ reagents.

At confidence interval (CI) greater than or equal to 95% and detected in at least two biological replicates, 217 confidently identified proteins were reported by MASCOT^{TM} (Table 4.1). After analyzing the iTRAQ expression ratios of each identified protein, we were able to recognize two groups of proteins whose expressions were significantly altered by p53 and hypoxia. The expression levels for 101 proteins (46.5%) were found altered in the absence of p53 while another 99 proteins (45.6%) exhibit changes in their protein expression levels when subjected to an 18 hrs hypoxia treatment. Several proteins were also observed to be affected by both the presence of p53 and the treatment of hypoxia. Moreover, out of the 217 proteins identified, 70 proteins (32.3%) were unaffected by both p53 and hypoxia treatment (refer to supplementary table 2 for details).

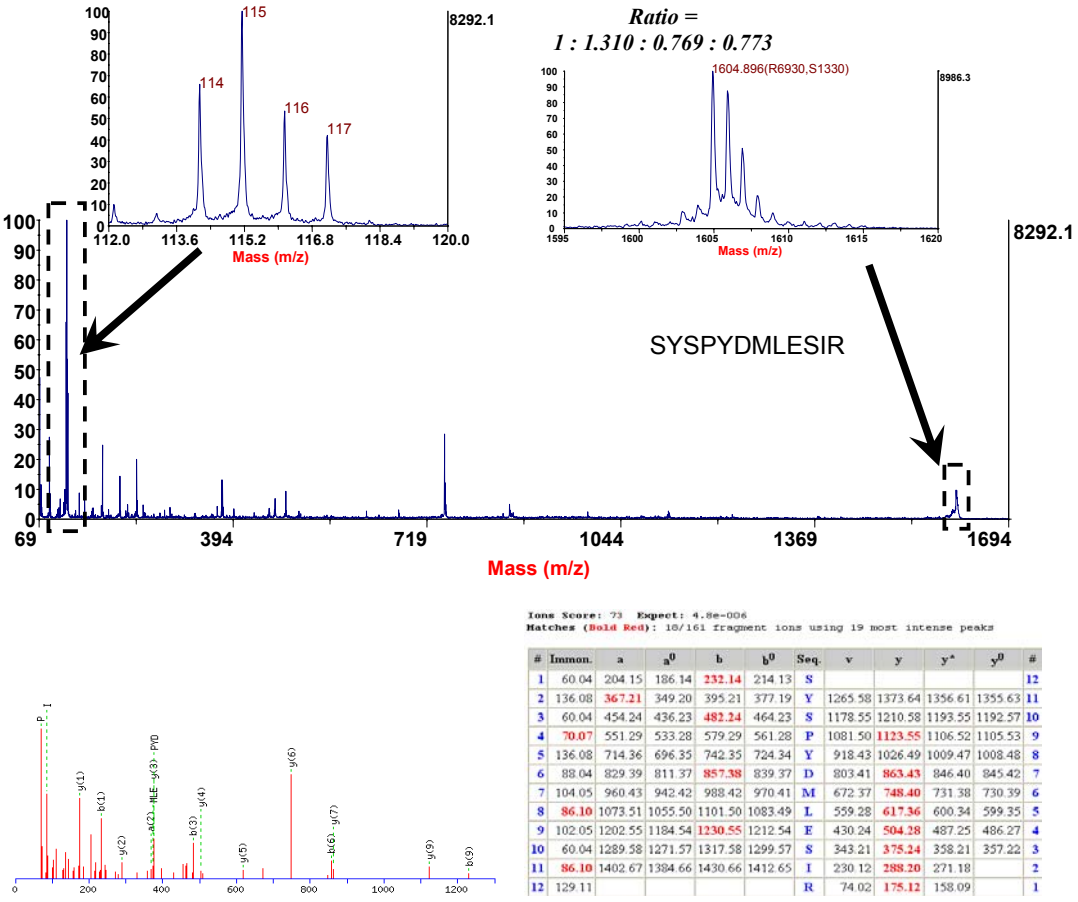

#	Immon.	a	a^0	b	b^0	Seq.	v	y	y^*	y^0	#
1	60.04	204.15	186.14	**232.14**	214.13	S					12
2	136.08	**367.21**	349.20	395.21	377.19	Y	1265.58	1373.64	1356.61	1355.63	11
3	60.04	454.24	436.23	**482.24**	464.23	S	1178.55	1210.58	1193.55	1192.57	10
4	**70.07**	551.29	533.28	579.29	561.28	P	1081.50	**1123.55**	1106.52	1105.53	9
5	136.08	714.36	696.35	742.35	724.34	Y	918.43	1026.49	1009.47	1008.48	8
6	88.04	829.39	811.37	**857.38**	839.37	D	803.41	**863.43**	846.40	845.42	7
7	104.05	960.43	942.42	988.42	970.41	M	672.37	**748.40**	731.38	730.39	6
8	**86.10**	1073.51	1055.50	1101.50	1083.49	L	559.28	**617.36**	600.34	599.35	5
9	102.05	1202.55	1184.54	**1230.55**	1212.54	E	430.24	**504.28**	487.25	486.27	4
10	60.04	1289.58	1271.57	1317.58	1299.57	S	343.21	**375.24**	358.21	357.22	3
11	**86.10**	1402.67	1384.66	1430.66	1412.65	I	230.12	**288.20**	271.18		2
12	129.11					R	74.02	**175.12**	158.09		1

Figure 4.2: A representation of a MS/MS spectrum used to determine protein abundance ratio in iTRAQ-labeled samples. The ratio of the four signature peaks (m/z 114 to 117) (see left blowup insert) reflects the relative abundance ratio of the peptides in the four samples. Signature peptides, such as the one shown "SYSPYDMLESIR, were then used for identification of proteins by searching against protein databases, e.g. international protein index (IPI) database.

Table 4.1: Number of proteins identified by LC/MS/MS through iTRAQ-based quantitation strategy.

		No. of Proteins Identified	
		In at least 2 sets	**In all 3 sets**
Proteins detected by LC/ MS/MS	**Total**	343	91
	CI ≥ 95%	217	88
	Potentially influenced by p53	101	29
	Potentially influenced by Hypoxia	99	29

Table 4.2: Number of potential protein targets influenced by p53 and/or hypoxia satisfying the given criteria. Venn diagram further illustrates the proportion of proteins that may be influenced by p53 and/or hypoxia under mentioned criteria.

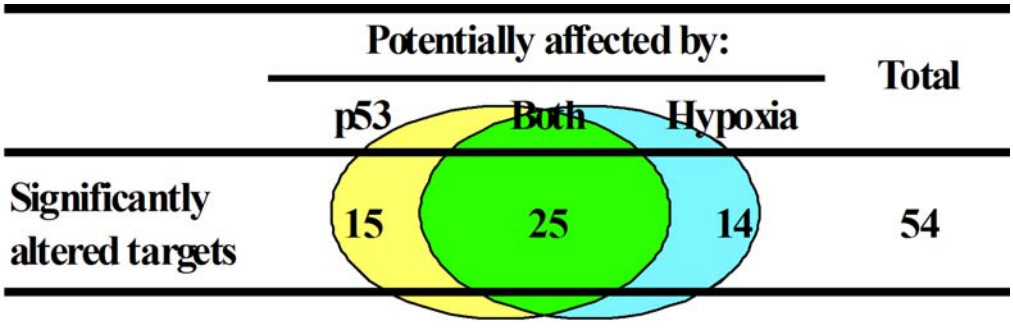

Based on 30% fold change in protein abundance, a total of 54 proteins were obtained. The expression levels of 15 proteins were found significantly changed in the absence of p53; in this group, 6 proteins were found up-regulated while 9 were down-regulated. In addition, 14 proteins were significantly altered in the case of hypoxia treatment (Table 4.2); the number of up-regulated proteins and down-regulated proteins was 5 and 9, respectively. The remaining 25 proteins appeared to be regulated, synergistically or antagonistically, in the presence of p53 and hypoxia. Our results also provided a greater confidence to our hypoxia experimental setup. For instance, there are several known hypoxia-induced proteins, such as phosphoglycerate kinase 1 (PGK1), lactate dehydrogenase A (LDHA), and fatty acid synthase (FAS), were definitely identified.

4.2.2 Gene ontology and protein-protein interaction analysis using Ingenuity Pathway Analysis (IPA) Tool

A gene ontology (GO) analysis for the two groups of targets that exhibited significant protein abundance changes in the absence of p53 or hypoxia was carried out using ingenuity pathway analysis (IPA) tool (*www.ingenuity.com*) (Figure 4.3). The top 5 biological functions and diseases identified by IPA is shown in table 4.3 and the significance value assigned to the functions is calculated using the right-tailed Fischer's Exact Test in IPA to determine the probability that the genes/proteins-of-interest participate in the biological functions. Furthermore, from the result, cellular growth and proliferation has the smallest assigned *p*-value, and is therefore the most significant biological function related to our proteins-of-interest. 25 out of 38 (~ 66%) p53-affected targets and 26 out of 35 (~ 74%) hypoxia-affected targets were classified according to their biological functions while the biological functions of the remaining

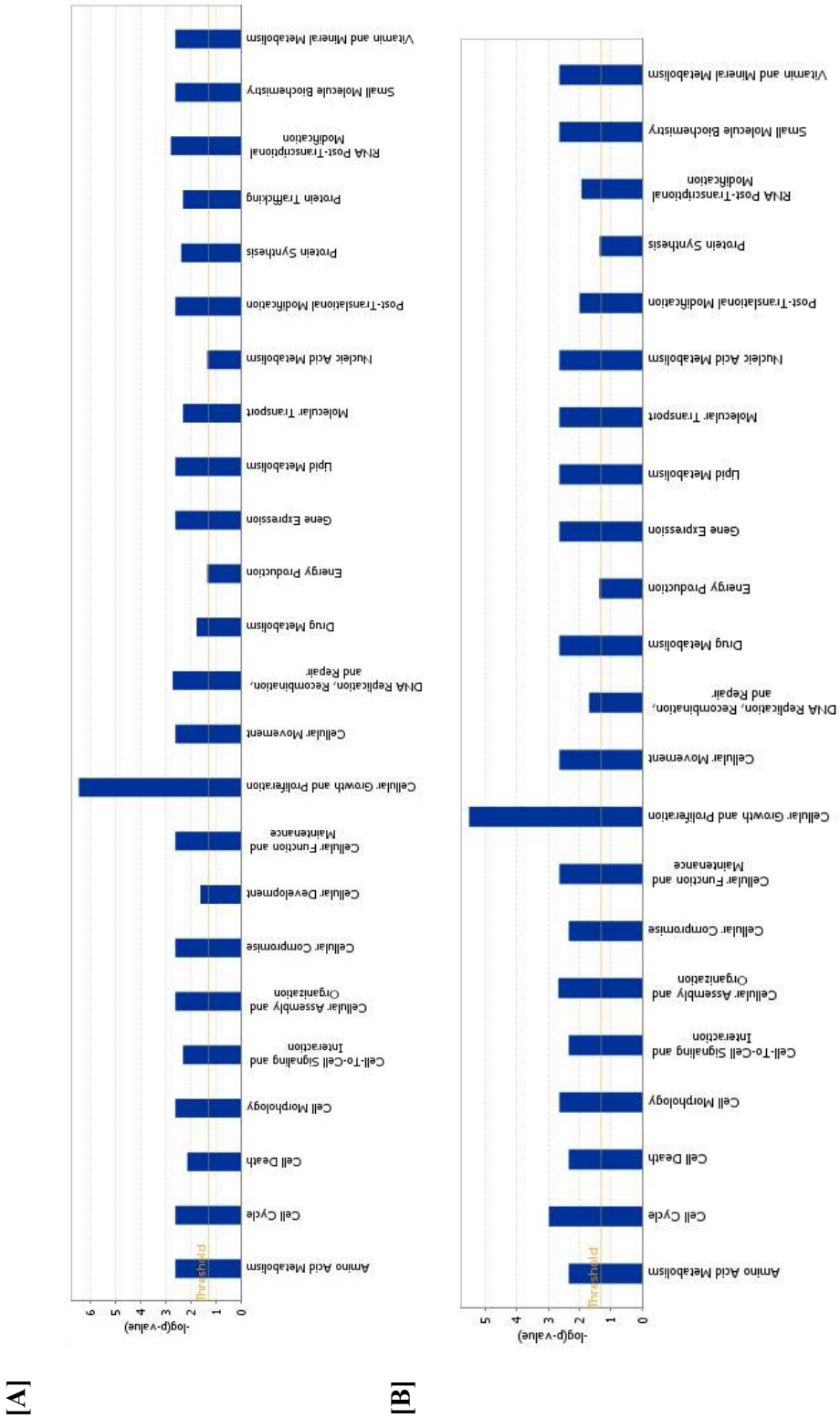
[A]
-log(p-value)
0
1
2
3
4
5
6
threshold
Amino Acid Metabolism
Cell Cycle
Cell Death
Cell Morphology
Cell-To-Cell Signaling and Interaction
Cellular Assembly and Organization
Cellular Compromise
Cellular Development
Cellular Function and Maintenance
Cellular Growth and Proliferation
Cellular Movement
DNA Replication, Recombination, and Repair
Drug Metabolism
Energy Production
Gene Expression
Lipid Metabolism
Molecular Transport
Nucleic Acid Metabolism
Post-Translational Modification
Protein Synthesis
Protein Trafficking
RNA Post-Transcriptional Modification
Small Molecule Biochemistry
Vitamin and Mineral Metabolism
[B]
-log(p-value)
0
1
2
3
4
5
threshold
Amino Acid Metabolism
Cell Cycle
Cell Death
Cell Morphology
Cell-To-Cell Signaling and Interaction
Cellular Assembly and Organization
Cellular Compromise
Cellular Function and Maintenance
Cellular Growth and Proliferation
Cellular Movement
DNA Replication, Recombination, and Repair
Drug Metabolism
Energy Production
Gene Expression
Lipid Metabolism
Molecular Transport
Nucleic Acid Metabolism
Post-Translational Modification
Protein Synthesis
RNA Post-Transcriptional Modification
Small Molecule Biochemistry
Vitamin and Mineral Metabolism

[C]

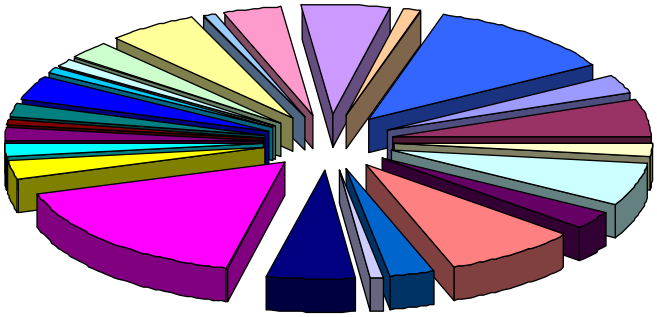

[D]

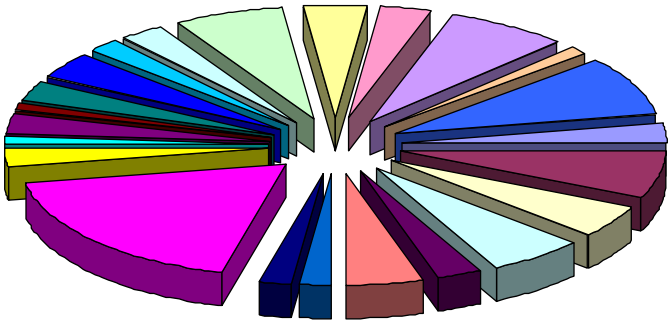

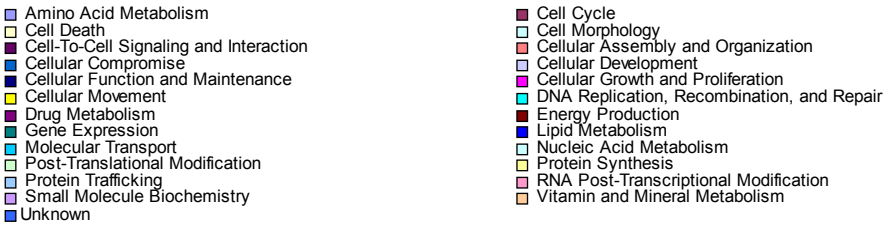

Figure 4.3: Gene ontology (GO) analysis of potential iTRAQ targets affected by p53 and hypoxia according to their biological functions using IPA tool. IPA generated histograms illustrating the classifications of targets affected by p53 [A] and hypoxia [B], according to their biological functions. In both groups, most of the targets are involved in cellular growth and proliferation. Pie charts represent iTRAQ targets affected by p53 [C] and by hypoxia [D], separated according to their biological functions proportionally.

Table 4.3: Top 5 functions and diseases of the 54 significantly affected targets by p53 and/or hypoxia identified by IPA.

Functions & Diseases	Significance	No. of associated targets	Associated targets' ID
Cellular growth & proliferation	2.17E-8 – 4.93E-2	25	ANXA2, C6ORF108, CAPN1, CCT2, CDC2, EIF3S2, FASN, LDHA, LGALS1, MAPRE1, MCM2, MCM3, NDUFA13, NOP5, PGK1, PRPF8, PSMC4, SF3B2, SLC3A2, SMC3, VIL2, RBP1, CDC123, CKS2, GPIAP1
Cancer	2.15E-3 – 4.93E-2	13	FASN, LGALS1, PTGES3, CDC2, C6ORF108, EIF3S2, LDHA, SLC3A2, SMC3, HSPA4, MCM2, CAPN1, EEF2
Cell cycle	2.15E-3 – 4.93E-2	10	FASN, LGALS1, PTGGES3, CKS2, SMC3, CDC2, MAPI, MCM2, SMC3, CDC123,
RNA post-transciptional modification	2.56E-2 – 4.1E-2	4	CDC2, NOP5, PRPF8, SF3B2
DNA regulation, recombination, and repair	3.01E-3 – 4.93E-2	3	MCM2, MCM3, FASN

number were not found by IPA. Furthermore, although the majority of the proteins were involved in cellular growth and proliferation in both p53-affected group (18 proteins; 16.7%) and hypoxia-affected group (19 proteins; 18.0%), several of these proteins were identified with more than one biological function. For example, annexin A2 (ANXA2), which is a calcium-dependent, phospholipid-binding protein, was reported in 8 of the biological functions reported by IPA and these included amino acid (aa) metabolism, lipid metabolism, cellular growth and proliferation, and cell death.

Networks of direct interactions were also generated and the top 3 networks were merged to allow identification of overlapping molecules in each network using IPA tool. By comparing the networks generated from the p53-affected group with another from the hypoxia-affected group, common proteins that were affected by p53 as well as hypoxia, either in a synergistic or antagonistic manner, can be determined easily (Figure 4.4). As an example, the top protein-protein interaction network generated by IPA tool allows examination of protein targets that were up-regulated or down-regulated under hypoxia in the presence and absence of p53 (Figure 4.5) as well as different regulation pattern of proteins observed in the absence of p53 under normoxia and hypoxia (Figure 4.6). In both figures, proteins that were commonly (blue-dotted boxes) or reversely (red-dotted boxes) regulated can be observed and the results are also tabulated in table 4.4.

4.3 Downstream validations using a subset of iTRAQ results

To further examine and provide a greater level of confidence to our observed result, a subset of the proteins exhibiting at least 30% abundance change was selected.

[A]

[B]

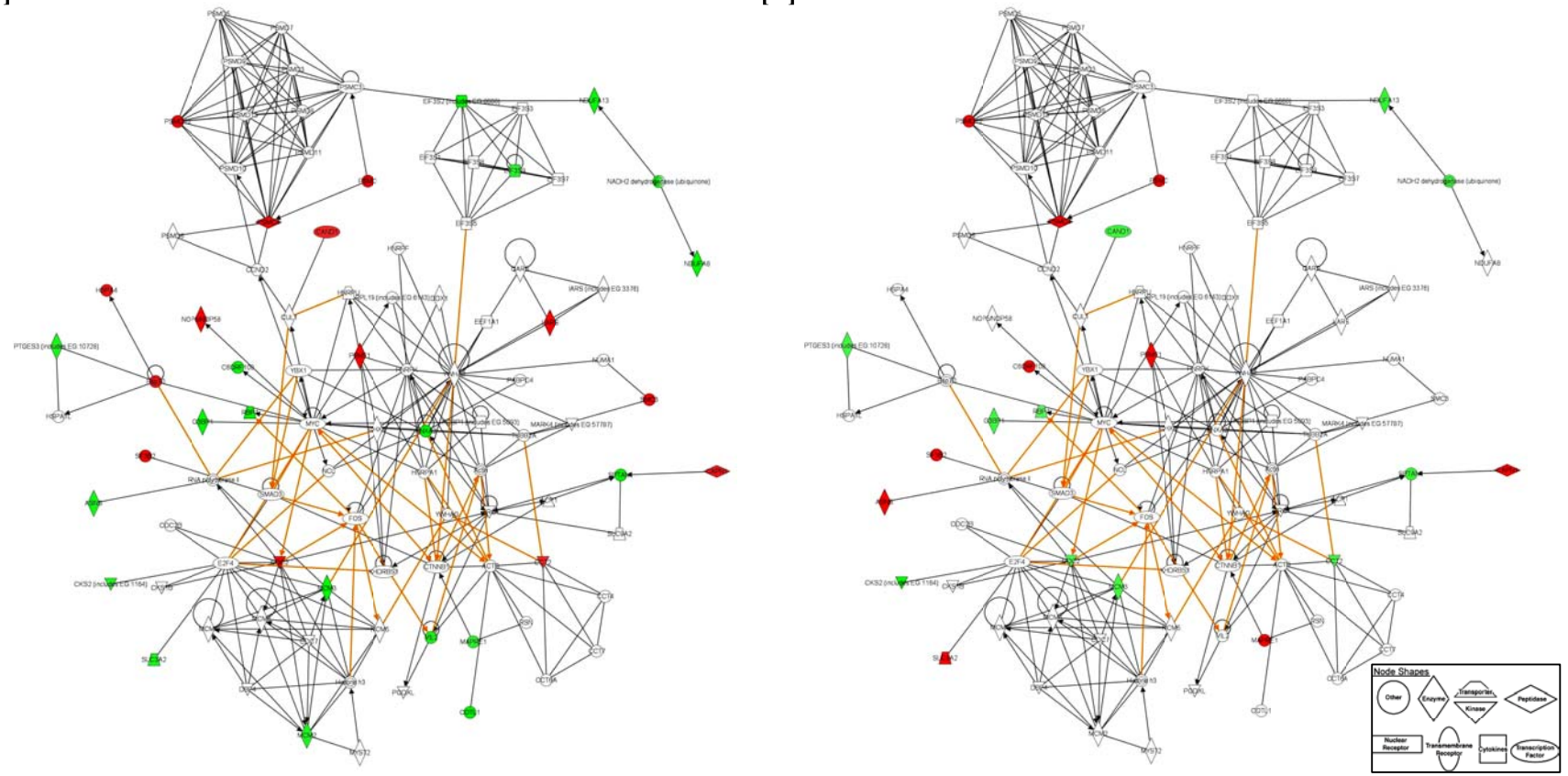

Figure 4.4: A graphical display of a merged top 3 protein-protein interaction networks generated by IPA tool from the 54 iTRAQ target proteins with at least 30% abundance change in protein expression level. This approach is used for investigating the relationship of similar proteins under two different conditions – absence of p53 **[A]** and hypoxia **[B]**. Colored boxes are iTRAQ target proteins with red indicating protein up-regulation and green indicating protein down-regulation.

[A]

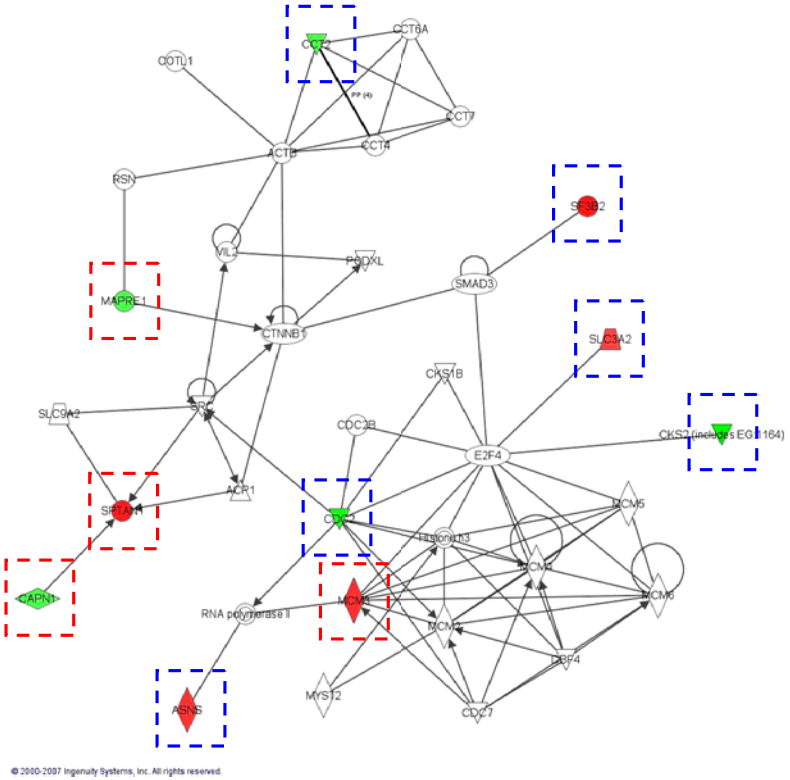

[B]

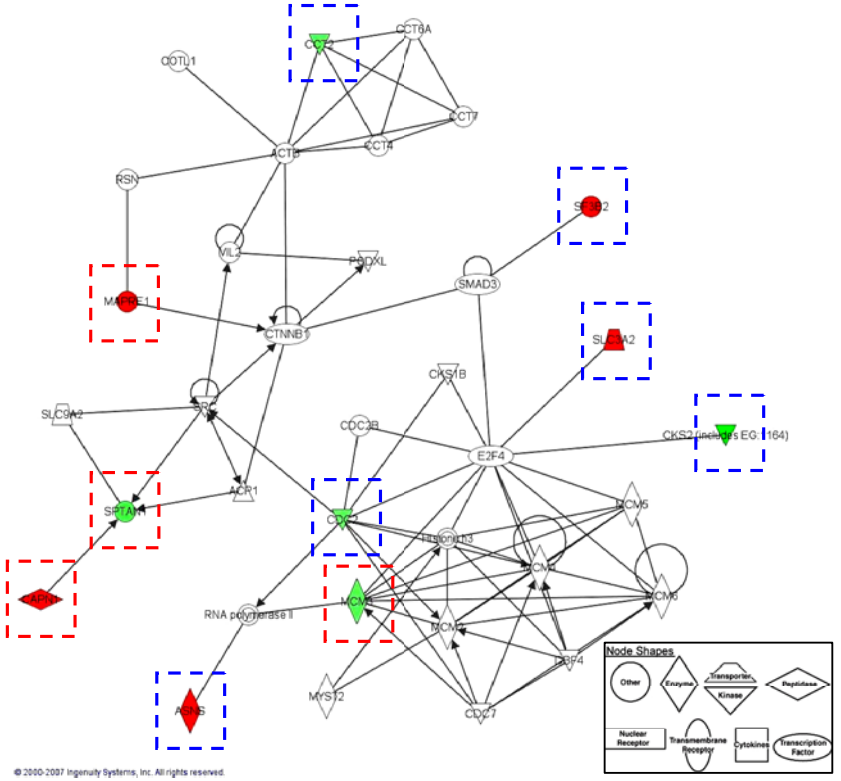

Figure 4.5: A protein expression and interaction network of proteins, involved in cellular growth, proliferation and cell cycle, under hypoxia in the presence **[A]** and absence **[B]** of p53. Proteins exhibiting similar expression trend are indicated by the blue-dotted boxes while those showing opposite trend are indicated by the red-dotted boxes. Colored boxes indicate up- (red) and down-regulation (green) of proteins detected by iTRAQ. The interaction network is generated by IPA tool.

[A]

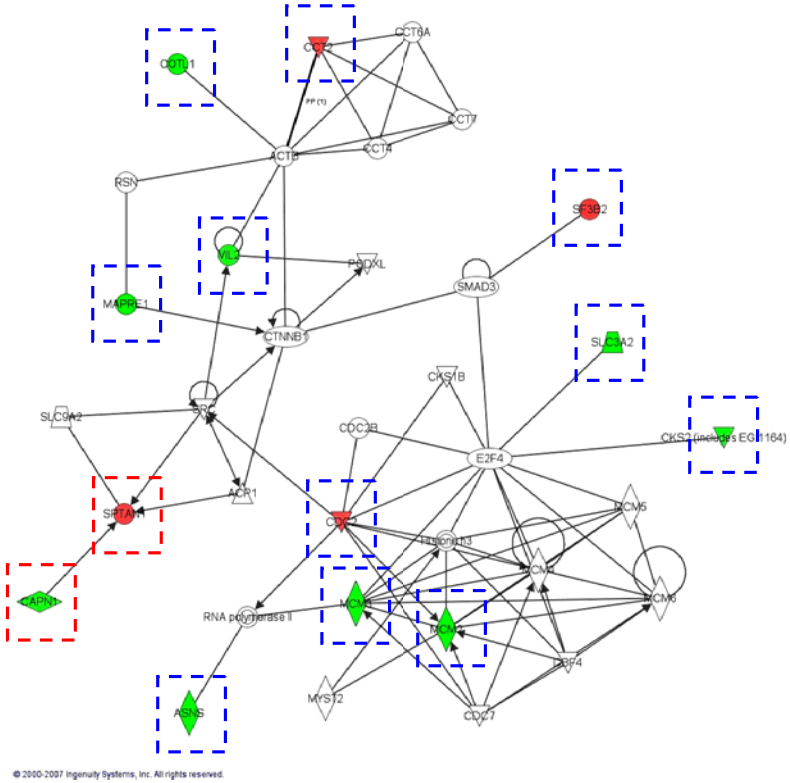

[B]

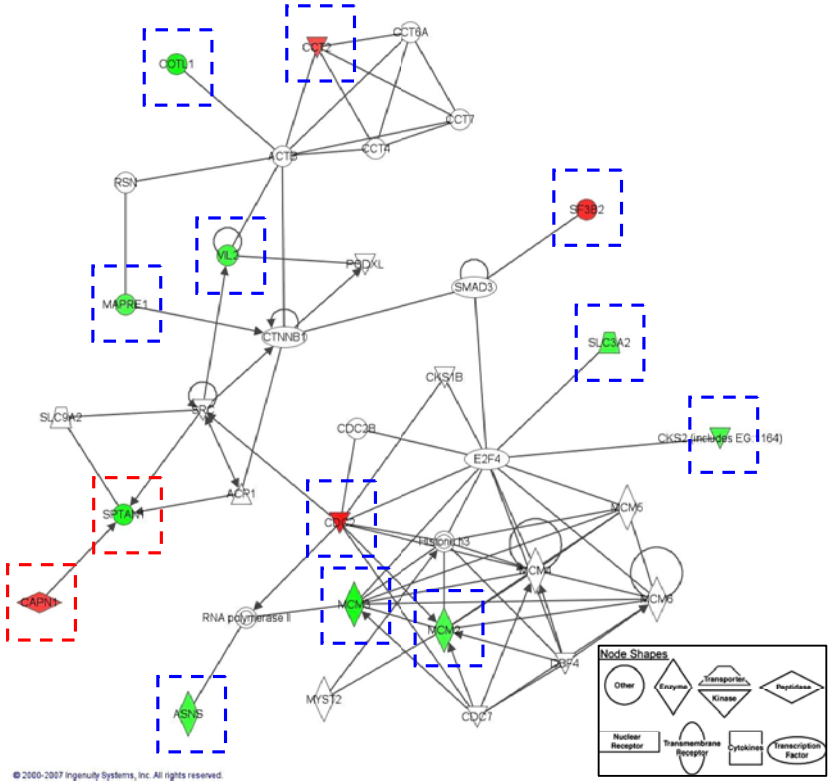

Figure 4.6: A protein expression and interaction network of proteins, involved in cellular growth, proliferation and cell cycle, in the absence of p53 under normoxia **[A]** and hypoxia **[B]**. Proteins exhibiting similar expression trend are indicated by the blue-dotted boxes while those showing opposite trend are indicated by the red-dotted boxes. Colored boxes indicate up- (red) and down-regulation (green) of proteins detected by iTRAQ. The interaction network is generated by IPA tool.

Table 4.4: Tabulation of common proteins regulated in cells under hypoxia in the presence and absence of p53 as well as in the absence of p53 under hypoxia and normoxia.

Description	iTRAQ comparison set	Down-regulated	Up-regulated	No change
Hypoxia treatment in the presence of p53	115/114	CCT6A, MAPRE1, CAPN1, CDC2, CKS2	SF3B2, SLC3A2, MCM3, SPTAN1, ASNS	COTL1, VIL2, MCM2
Hypoxia treatment in the absence of p53	117/116	CCT6A, SPTAN1, CDC2, MCM3, CKS2	SF3B2, SLC3A2, MAPRE1, CAPN1, ASNS	COTL1, VIL2, MCM2
Absence of p53 under normoxia	116/114	COTL1, VIL2, MAPRE1, CAPN1, ASNS, MCM2, MCM3, SLC3A2, CKS2	CCT2, SF3B2, SPTAN1, CDC2	--
Absence of p53 under hypoxia	117/115	COTL1, VIL2, MAPRE1, SPTAN1, ASNS, MCM2, MCM3, SLC3A2, CKS2	CCT2, SF3B2, CDC2, CAPN1	--

This subset of proteins was also selected based on the generated IPA networks which suggested possible indirect interactions between the potential novel proteins affected by p53 and/or hypoxia. Under these conditions, 20 targeted proteins (37%) were selected (Figure 4.7); these selected proteins were categorized into 3 groups, namely "affected by p53", "affected by hypoxia", and "affected by both p53 and hypoxia" (see Table 4.5). In addition, two methods of validation analysis were used: one was through detection of the mRNA levels in the cells using quantitative real-time polymerase chain reaction (RT-PCR) and the other was to determine the protein level using immunoblotting. Samples from both p53 WT and KO cells were prepared and subjected to either normoxia or hypoxia for 18 hrs prior harvesting. Furthermore, the proteins selected for downstream validations also include some known proteins affected by hypoxia (e.g. PGK1 and LDHA) and p53 (e.g. SMC3).

4.3.1 Real-Time PCR analysis

Total RNA was isolated from the cells, followed by determination of the purity and concentration for each RNA sample. Out of the 20 targets, 8 target genes exhibited similar changing trend in their mRNA level as observed in their corresponding iTRAQ result (Figure 4.8). This observation included the known hypoxia-induced genes, PGK1 and LDHA, which changed 3 to 4 folds higher than their normoxic counterparts. Other validated targets included SMC3, NSUN2, ANXA2, PCBD1, EFHD2, and G3BP1. Interestingly, the mRNA level of HIF-1α, which accumulates under hypoxia, was found significantly decreased instead. The RT-PCR result of the remaining 12 targets did not reflect the expression level or trend observed in our iTRAQ result. HIF-1α and VEGFA acts as a positive control for hypoxia while p53 was used to confirm the absence of p53 in the p53 KO cells.

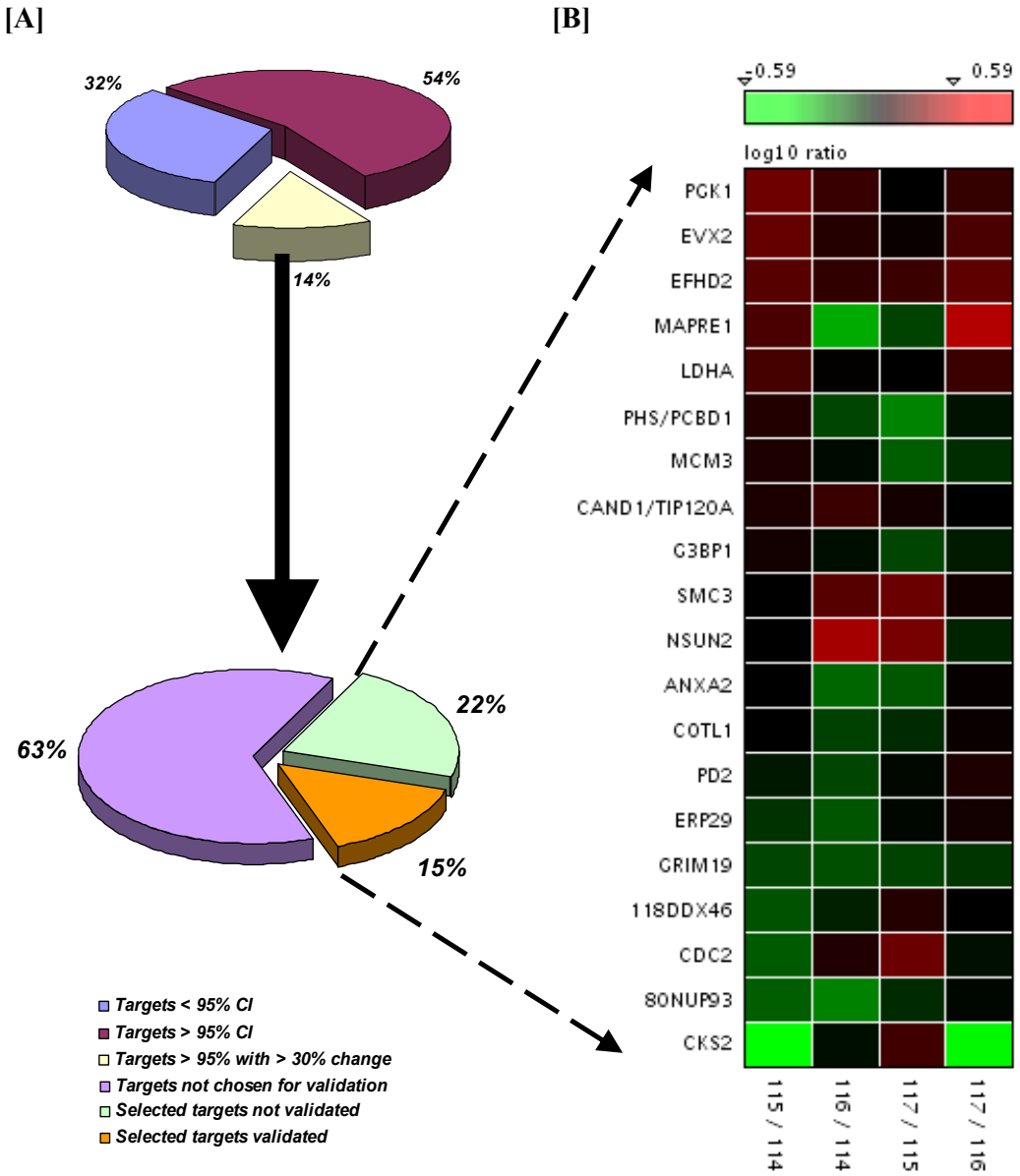
[A]
[B]
32%
54%
14%
63%
22%
15%
Targets < 95% CI
Targets > 95% CI
Targets > 95% with > 30% change
Targets not chosen for validation
Selected targets not validated
Selected targets validated
-0.59
0.59
log10 ratio
PGK1
EVX2
EFHD2
MAPRE1
LDHA
PHS/PCBD1
MCM3
CAND1/TIP120A
G3BP1
SMC3
NSUN2
ANXA2
COTL1
PD2
ERP29
GRIM19
118DDX46
CDC2
80NUP93
CKS2
115 / 114
116 / 114
117 / 115
117 / 116

[C]

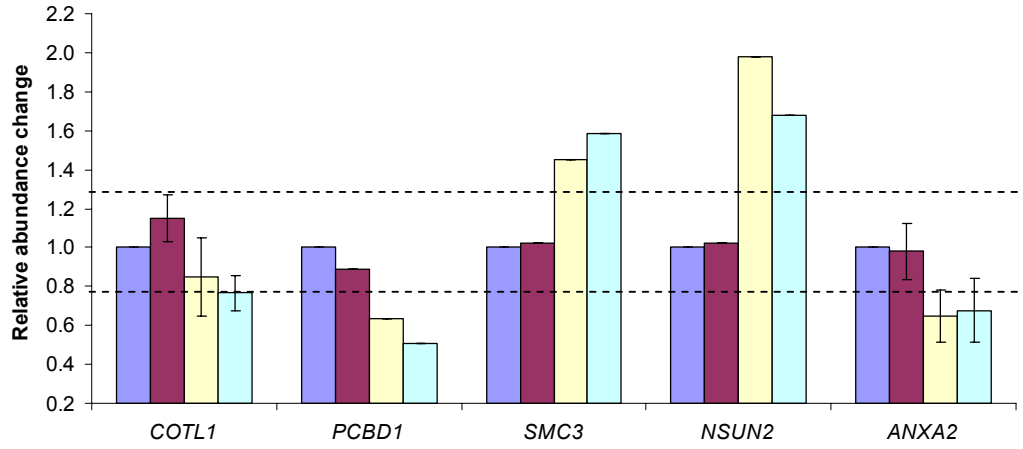
Relative abundance change
2.2
2.0
1.8
1.6
1.4
1.2
1.0
0.8
0.6
0.4
0.2
COTL1
PCBD1
SMC3
NSUN2
ANXA2

[D]

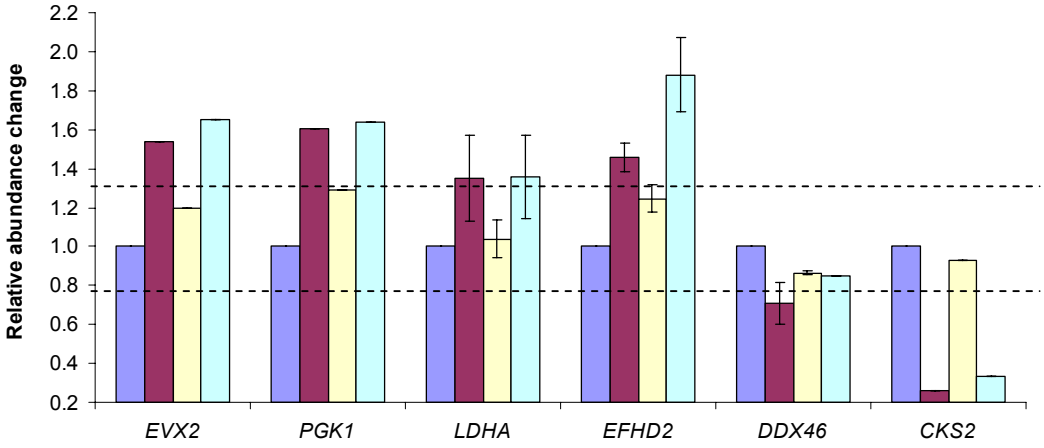
Relative abundance change
2.2
2.0
1.8
1.6
1.4
1.2
1.0
0.8
0.6
0.4
0.2
EVX2
PGK1
LDHA
EFHD2
DDX46
CKS2

[E]

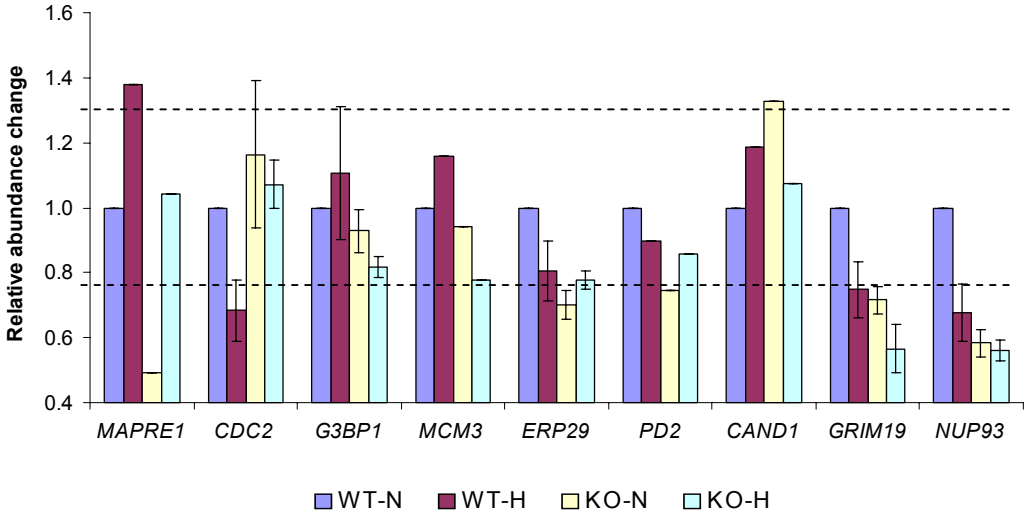
Relative abundance change
1.6
1.4
1.2
1.0
0.8
0.6
0.4
MAPRE1
CDC2
G3BP1
MCM3
ERP29
PD2
CAND1
GRIM19
NUP93
WT-N
WT-H
KO-N
KO-H

Figure 4.7: A subset of iTRAQ targets chosen for downstream validation. **[A]** Total number of targets identified using iTRAQ-based quantitation strategy and the proportion of targets chosen for verification analysis summarized in a pie-chart. **[B]** Heatmap showing the relative expression ratios for each of the 20 targets. 115/114 denotes WT-H : WT-N; 116/114 denotes KO-N : WT-N, 117/115 denotes KO-H : WT-H; 117/116 denotes KO-H : KO-N. Red and green colors indicate up- and down-regulation of the targets respectively. Histograms illustrate the relative abundance ratio of the targets chosen for p53-affected group (COTL1, PCBD1, SMC3, NSUN2 and ANXA2) **[C]**, hypoxia affected group (EVX2, PGK1, LDHA EFHD2, DDX46 and CKS2) **[D]**, and by both p53 and hypoxia (MAPRE1, CDC2, G3BP1, MCM3, ERP29, PD2 CAND1, GRIM19 and NUP93) **[E]**. All results were compared with respect to WT-N. Dotted lines across the graphs indicate the upper and lower limit of 30% fold change.

Table 4.5: List of selected targets based on iTRAQ result and selection criteria for downstream verifications. Targets are classified into 3 groups: potentially influenced by p53 (highlighted in red); potentially influenced by hypoxia (highlighted in blue); potentially influenced by both p53 and hypoxia (highlighted in yellow).

Selected Targets that satisfied the criteria						
Protein Name	Symbol	Accession Number	iTRAQ ratio 115:114	iTRAQ ratio 116:114	iTRAQ ratio 117:115	iTRAQ ratio 117:116
Coactosin-like protein	COTL1	IPI00017704	1.14791	0.85081	0.67787	0.90000
Pterin-4-alpha-carbinolamine dehydratase	PCBD1	IPI00218568	0.88842	0.63199	0.57762	0.79904
Structural maintenance of chromosome 3	SMC3	IPI00219420	1.02334	1.45287	1.57244	1.08990
NOL1/NOP2/Sun domain family 2 protein	NSUN2	IPI00306369	1.0213	1.9822	1.6543	0.8541
Annexin A2	ANXA2	IPI00455315	0.9815	0.6476	0.6904	1.0468
Homeobox even-skipped homolog protein 2	EVX2	IPI00012495	1.5355	1.1954	1.0761	1.3829
Phosphoglycerate kinase 1	PGK1	IPI00169383	1.6054	1.2898	1.0197	1.2698
Lactate dehydrogenase A	LDHA	IPI00217966	1.3507	1.0381	1.0020	1.3043
EF hand domain containing 2	EFHD2	IPI00552365	1.4554	1.2468	1.2913	1.5081
DEAD box protein 46	DDX46	IPI00657954	0.7100	0.8645	1.1932	0.9805
Cyclin-dependent kinases regulatory subunit 2	CKS2	IPI00015105	0.25874	0.92993	1.32141	0.36180
Microtubule-associated protein RP/EB family member 1	MAPRE1	IPI00017596	1.3809	0.4925	0.7528	2.1119
Cell division control protein 2	CDC2	IPI00026689	0.6836	1.1640	1.5774	0.9282
Ras-GTPase-activating protein-binding protein 1	G3BP1	IPI00012442	1.1063	0.9288	0.7442	0.8882
DNA replication licensing factor MCM3	MCM3	IPI00013214	1.15723	0.94376	0.68099	0.82171
PD2 protein	PD2	IPI00300333	0.8986	0.7453	0.9548	1.1517
Isoform 2 of Cullin-associated NEDD8-dissociated protein 1	CAND1	IPI00604431	1.18748	1.32727	0.91727	0.80758
Endoplasmic reticulum protein ERp29 precursor	ERP29	IPI00024911	0.8058	0.6998	0.9640	1.1106
Cell death-regulatory protein GRIM19	GRIM19	IPI00219685	0.7473	0.7153	0.7575	0.7917
Nucleoporin Nup93	NUP93	IPI00644506	0.6769	0.5843	0.8283	0.9600

[A]

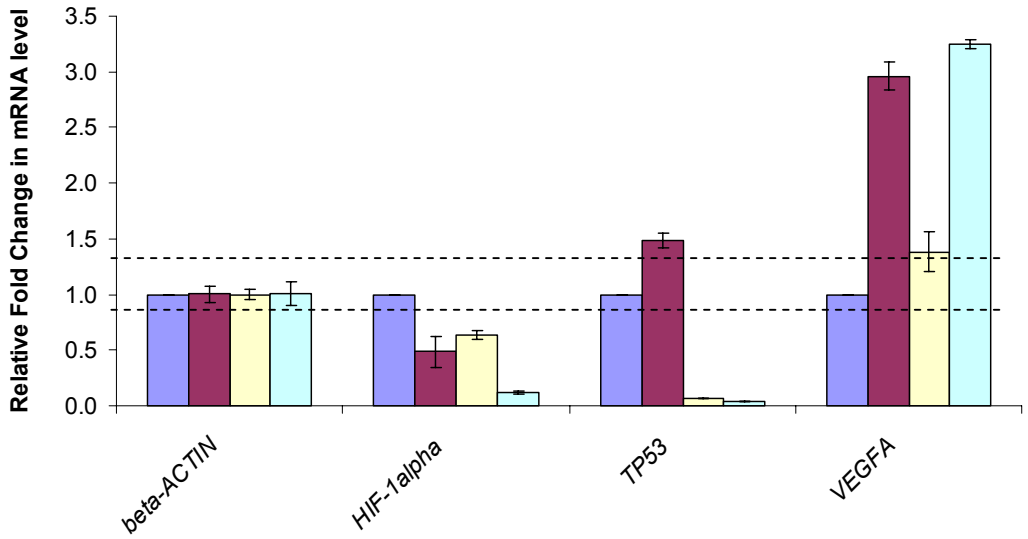
Relative Fold Change in mRNA level
3.5
3.0
2.5
2.0
1.5
1.0
0.5
0.0
beta-ACTIN
HIF-1alpha
TP53
VEGFA

[B]

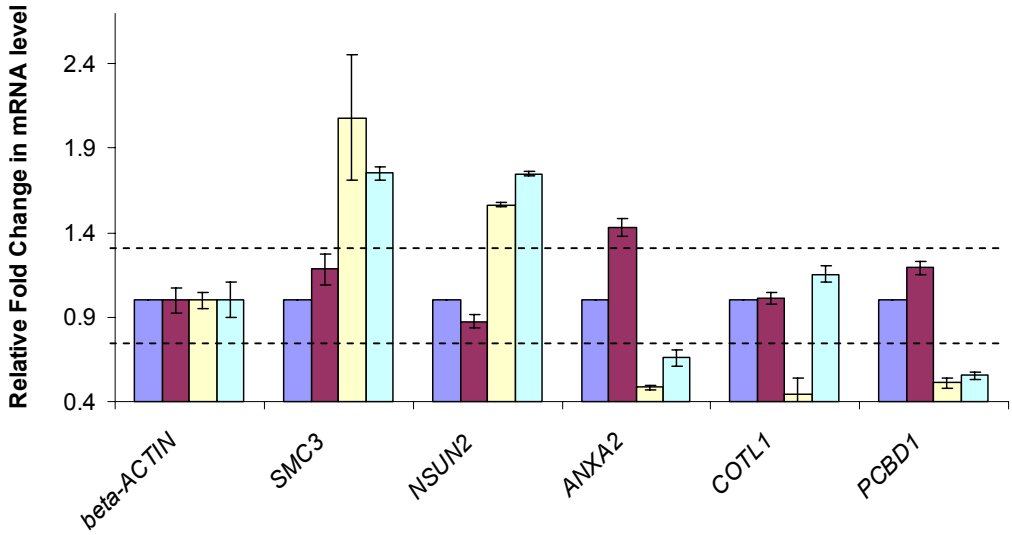
Relative Fold Change in mRNA level
2.4
1.9
1.4
0.9
0.4
beta-ACTIN
SMC3
NSUN2
ANXA2
COTL1
PCBD1

[C]

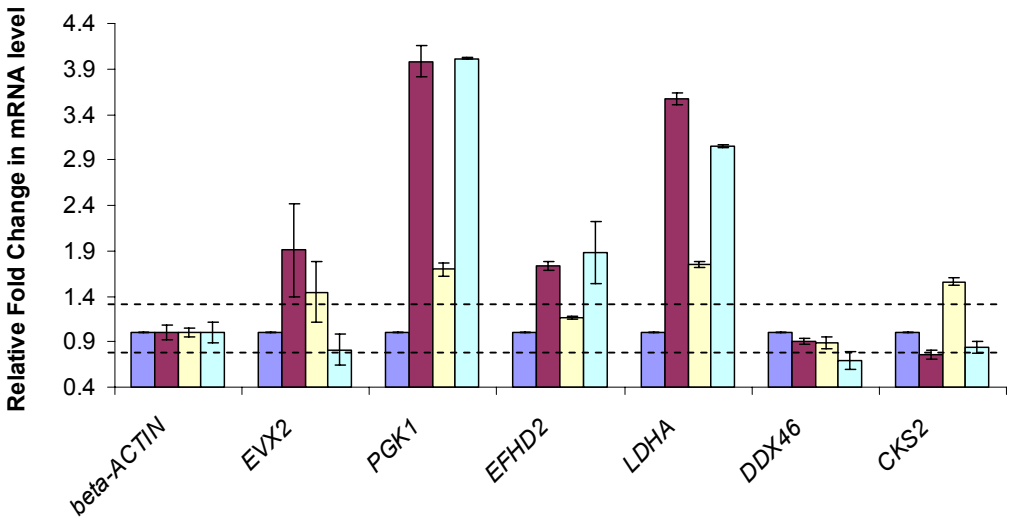

[D]

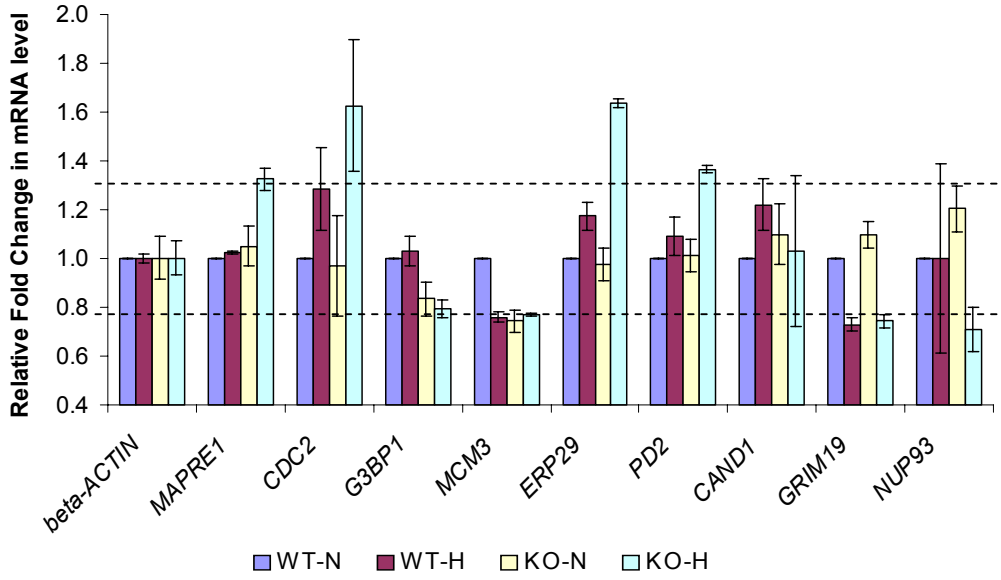

Figure 4.8: Representative graphs of real-time PCR results for targets selected from iTRAQ results. **[A]** Relative mRNA levels of HIF-1alpha, TP53, and VEGFA. **[B]** Relative mRNA levels of genes (SMC3, NSUN2, ANXA2, COTL1 and PHS) whose protein levels were significantly altered due to presence/absence of p53. **[C]** Relative mRNA levels of genes (EVX2, PGK1, EFHD2, LDHA and DDX46) with significantly altered protein levels due to hypoxic stress. **[D]** Relative mRNA levels of genes (MAPRE1, CDC2, G3BP1, MCM3, ERP29, PD2 and CAND1) exhibiting enhanced altered protein levels due to synergistic or antagonistic effects of p53 and hypoxia. All results were normalized against β-actin and compared with respect to WT-N. Dotted lines across the graphs indicate the upper and lower limit of 30% fold change.

Interestingly, mRNA level of HIF-1α was found lower in the presence of hypoxia. β-actin serves as an internal control.

4.3.2 Immunoblotting

To ensure a greater confidence in our iTRAQ results, immunoblotting was performed using total cell lysates from each sample and protein levels of PGK1, LDHA, EFHD2, CKS2, ANXA2 and PCBD1 in each sample were assayed using corresponding antibodies against each respective protein. As expected, the known hypoxia-induced proteins, PGK1 and LDHA, exhibited an increased level of expression under hypoxia (Figure 4.9). The protein expression profile of hypothesized p53-affected proteins, like ANXA2 and PCBD1, were also found significantly lowered in the absence of p53. Interestingly, the expression of CKS2 protein was found lowered under hypoxia with an opposite phenomenon observed in the absence of p53 under normoxia whereby CKS2 was found to be highly overexpressed. This was also observed in the RT-PCR but was not represented in the iTRAQ result. On the other hand, EFHD2 was only found significantly increased under hypoxia in the absence of p53 even though it was shown to be up-regulated under hypoxia in the both iTRAQ and RT-PCR results (Figure 4.7D and 4.8C, respectively).

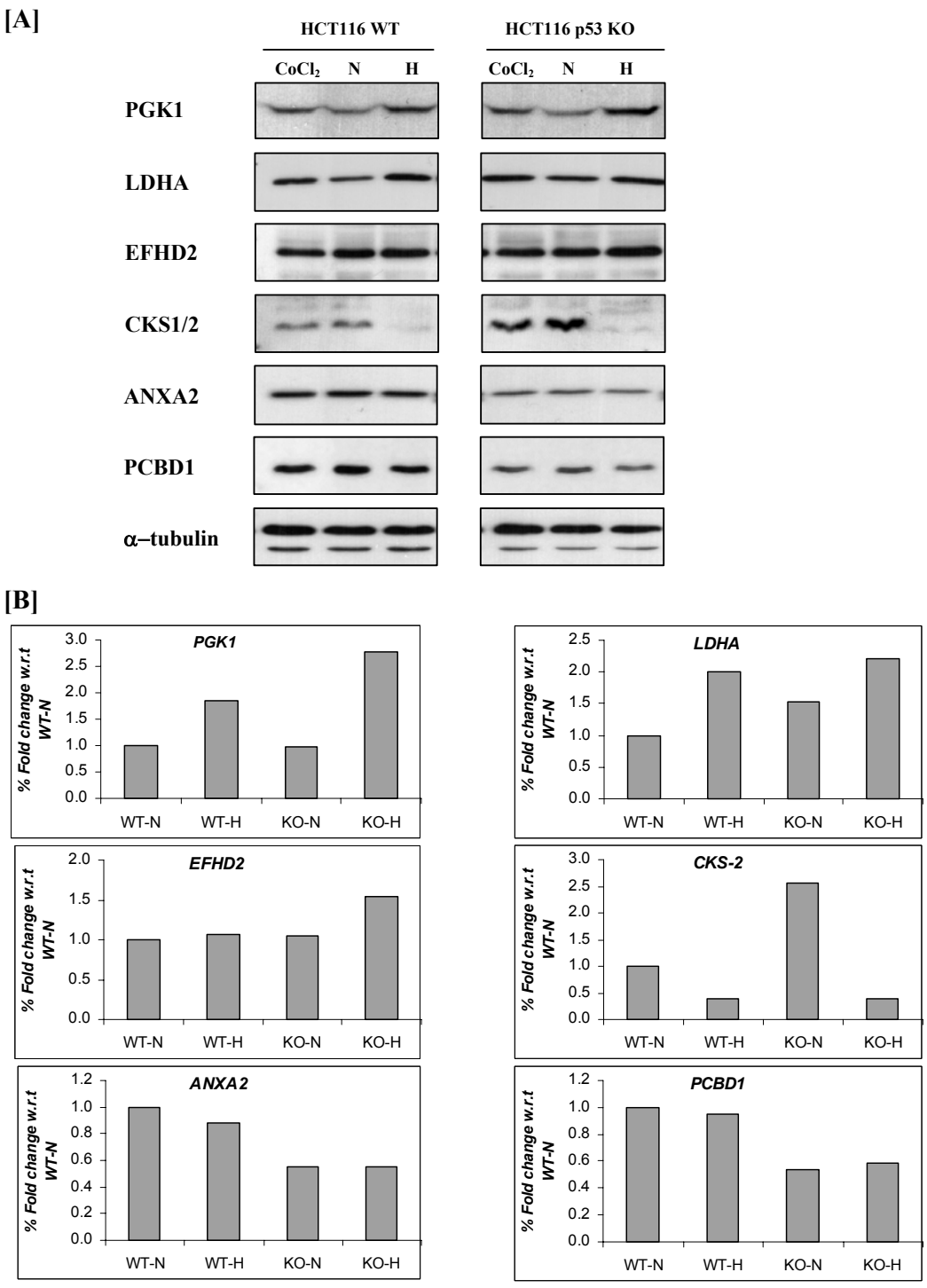

Figure 4.9: Downstream verifications of iTRAQ results by immunoblotting. **[A]** Expression levels of PGK1, LDHA, EFHD2, CKS2, ANXA2, and PCBD1 in total cell lysates were determined in both WT and p53 KO cells, subjected to 18 hrs of normoxia or hypoxia, using corresponding antibodies against each of the protein. Cells treated with $CoCl_2$ were used as a positive control. **[B]** A graphical representation of the immunoblot results. All results were initially normalized against α-tubulin and all graphs were plotted with reference to (w.r.t) WT-N. Band quantitation is performed using Image J software.

CHAPTER 5 – DISCUSSION

From the literature review (see section 1.4.5), we understand that the relationship between p53 and hypoxia in signaling transduction is controversial and therefore, this prompted us to explore plausible targets that might help to provide an explanation for the elusive relationship shared between p53 and hypoxia. In our study, we investigated the effects of hypoxia in human colon cancer cells, HCT116, in the presence and absence of p53. It has been properly demonstrated in these cells that hypoxia failed to induce apoptosis when p53 is absent (Yu et al., 2002) and only under extreme hypoxic conditions (<0.1 % O_2), p53-dependent apoptosis will occurs (Koumenis et al., 2001; Lechanteur et al., 2005). To monitor the changes of protein profiles, we adopted a well-established technique, called iTRAQ, and mass spectrometry to perform a global multiplex comparative proteomic analysis. The hypoxic condition was simulated using a CO_2 incubator that regulated the oxygen level within and thus, mimicking the low oxygen tension observed in tumors during tumorigenesis. It is important to understand that the simulation of environmental conditions using artificial setups (e.g. hypoxia) is a very difficult task to truly represent the actual situation in real biological circumstances. Development of better equipment and experimental designs has allowed closer replicates of the real situations, leading to many positive outcomes (Kubota et al., 1998; Moulder et al., 2001). Furthermore, through our approach, we are able to identify promising novel targets that are under the regulation of hypoxia/HIF-1 as well as p53. In this section, we will discuss our findings in greater details with respect to our approach and its reliability. Furthermore, a great number of background information on the selected validated targets will be discussed.

5.1 Increased accumulation of HIF-1α in HCT116 cells in the presence of p53

Under our induced hypoxia system (1% O_2, 5% CO_2, rest N_2), we reported successful stabilization and accumulation of HIF-1α in the HCT116 cells regardless of the presence of p53 with a higher accumulation observed in HCT116 p53 WT cells compared to its p53 KO counterpart. Although this observation clearly contradicted previous results from other studies which have suggested that the interaction between p53 and HIF-1α can evoke HIF-1α degradation in a pVHL-independent manner, it is also mentioned that this phenomenon will occur only at a high expression level of p53. In the presence of a low p53 expression level, interaction between p53 and HIF-1 will only attenuate HIF-1 transactivation due to competition for a common transcriptional co-activator, p300, but not its protein level (Ravi et al., 2000; Schmid et al., 2004b; Vleugel et al., 2006). However, it has also been pointed out that under hypoxic condition, p53 primarily binds to a transcriptional corepressor mSin3A instead of p300 and this may provide an explanation for the lack of p53-dependent apoptotic activity observed during hypoxia observed in some studies (Koumenis et al., 2001). Another possible reason for the lower level of HIF-1α observed in p53 KO cells may be due to the interaction of HIF-1α with HDM2 (human homolog of MDM2) which can be induced via p53-independent means (Nelson et al., 2006). Possibly similar to the case of p53 and HIF-1α competing for p300 mentioned earlier, the absence of p53 allows more HIF1α-HDM2 interactions to occur. As a result of the interaction, HIF-1α can be targeted for ubiquitylation and degradation subsequently by the p53-associated E3 ligase, MDM2/HDM2 (Ravi et al., 2000). These two possibilities may have accounted for the lower level of HIF-1α observed in HCT116 p53 KO cells treated with hypoxia. However, further investigations will be required in order to

confirm whether p53, though attenuates HIF-1 transcriptional activities, can promotes HIF-1α stability under mild hypoxia.

5.2 p53 protein does not accumulate under hypoxia

After 18 hrs of hypoxia, we observed that the expression of p53 protein remains unaffected albeit an increased mRNA level was reported in the RT-PCR analysis. Even though hypoxia-induced accumulation of p53 has been reported in many studies, this was only observed more distinctively under prolonged hypoxia or near-anoxia conditions (Schmid et al., 2004a). Such situations usually lead to the activation of p53-dependent apoptotic responses involving activation of apoptotic genes. At 1% O_2, it has been shown that p53 level remains unchanged and p53 is transcriptionally inactive (Achison and Hupp, 2003; Koumenis et al., 2001). Under normal unstressed condition, p53 interacts with its E3 ligase MDM2 and the level is kept at a low or undetectable level in normal cells. MDM2 is a known downstream transcriptional target of p53 and therefore, forms a negative feedback regulatory loop whereby in the presence of p53, MDM2 level will increase and p53 gets degraded. Interestingly, in our control HCT116 p53 WT cells, the level of p53 can be observed clearly by immunoblotting (see Figure 4.1A). A verification check with ATTC (*www.atcc.org*) indicates that HCT116 cells contain a mutation in codon 13 of the *ras* proto-oncogene and studies have shown that mutations in *ras* gene can stabilize p53 by the $p14^{ARF}$-MDM2 pathway (Honda and Yasuda, 1999; Kamijo et al., 1998). Interaction between $p14^{ARF}$ and MDM2 releases p53 from MDM2 association. This observation may explain for the noticeable expression of p53 in HCT116 cells under normoxic condition. Although p53 is stabilized in HCT116 WT cells, it does not induce apoptosis or cell cycle arrest. However, p53 is still functional and p53-

dependent apoptosis can take place when the cells are treated with cytotoxic drugs such as 5-fluorouracil (5-FU) (Yu et al., 1999; Zhang et al., 2000).

5.3 A multiplex comparative proteomic analysis using iTRAQ and mass spectrometry

The combined use of iTRAQ and LC-MS results in the discovery and identification of 54 differentially expressed proteins that are influenced by hypoxia and/or p53. Fifteen proteins were found differentially expressed only in the absence of p53 while 14 were found differentially expressed only when the cells were subjected to hypoxia. The remaining 25 appeared to be influenced by both the presence of p53 and hypoxia treatment. Downstream validation analysis has been performed for some of the targets that showed significant change in their expression levels when compared to the normal state. The targets and their validation results are discussed below. These proteins may be used for further studies as potential diagnostic biomarkers for tumor hypoxia and therapeutic targets for novel drug design.

5.3.1 Gene Ontology – potential p53 and hypoxia affected targets

A gene ontology analysis shows that majority of the targets affected by p53 (e.g. CDC2, SF3B2, ANXA2, SMC3, etc.) and hypoxia (e.g. LDHA, PGK1, CKS2, NOP5, etc.) in the study are involved in cellular growth and proliferation (see Figure 4.3). This is expected as one of the major functions of p53 is cell cycle regulation whereby cell cycle will be arrested in a p53-dependent manner in the presence of cytotoxicity (although a high level of cytotoxicity will induce apoptosis). Therefore, in the absence of p53, the p53-dependent cell cycle arrest does not occur and the absence of p53 has been shown to promote cell proliferation in mouse mammary

tumor (Guevara et al., 1999; Jones et al., 1997). Similarly, one of the key characteristic of tumor progression is cell cycle dysfunction and several studies have reported that hypoxia and accumulation of HIF-1α can promote rapid hypoxic cell proliferation in both normal and tumor cells (Humar et al., 2002; Schultz et al., 2006). Thus, the targets identified in this study might provide greater insights into the mechanism that promotes enhanced aggressive nature of hypoxic tumors carrying dysfunctional *p53* gene.

5.3.2 Downstream validations of iTRAQ results

To validate our iTRAQ results, we screened through all targets that were identified at least twice in our biological replicates at 95% confidence interval (C.I.). Thereafter, based on the set criteria (see section 3.10.8) and an extensive literature search, a total of 20 targets were chosen for RT-PCR to determine if their mRNA levels reflect the results shown by iTRAQ-based MS/MS. Several of these targets are known hypoxia- (PGK1, LDHA) or p53-related proteins (SMC3); while the others are potential novel targets that are affected by the presence of p53 and/or hypoxia. Five of the selected targets were classified as affected by p53 while 6 affected by hypoxia; the other 9 exhibits changes due to both p53 and hypoxia (Figure 4.7). Although the mRNA level may not be a true reflection of protein level, it offers two advantages as a tool for validation analysis. Firstly, it is a rapid, inexpensive and reliable technique. The primers are more inexpensive compared to antibodies which may be of doubtful quality too. Secondly and more importantly, through the analysis of mRNA level, we can determine whether the observed changes have occurred at a transcriptional or a post-transcriptional level. For example, RT-PCR results indicates that the mRNA level of *PGK1, LDHA, ANXA2, EFHD2, SMC3, G3BP1, PCBD1* and *NSUN2* exhibits

similar regulation trend as the results obtained from our iTRAQ result. This hints a possibility that the mode of regulation brought by hypoxia and/or p53 is at a transcriptional level and this hypothesis can be verified further using tools such as luciferase-promoter assays.

Interestingly, while it is shown that hypoxia leads to an accumulation of HIF-1α protein in HCT116 cells (Figure 1A), our RT-PCR results indicate that hypoxia decreases the mRNA level of *HIF-1α* with a more distinct reduction observed when p53 is absent too (Figure 4.8A). The positive up-regulation of *VEGFA, PGK1* and *LDHA* mRNA suggests that it is not due to a mix up of samples or experimental errors. Although the exact mechanism is unknown, a similar observation has been reported recently in human monocytes, THP-1 cells, whereby the HIF-1α mRNA and protein level of cells treated with either hypoxia or normoxia was determined (Frede et al., 2006). The results were similar to our study. On the other hand, previous studies have shown that hypoxia can increase the mRNA level of HIF-1α as well as stabilize HIF-1α protein (Semenza, 2000b; Yu et al., 1998) but it was also reported that HIF-1α levels can decrease in cells under prolonged exposure to hypoxia (Wiesener et al., 1998). Therefore, the decrease may indicate the existence of a feedback mechanism during hypoxic conditions to regulate HIF-1α expression and HIF-1 transcriptional activities. It is likely that this feedback mechanism is not in place during normoxic conditions as HIF-1α mRNA is found ubiquitously expressed in the cells.

Out of the 8 verified targets which showed similar trend in their mRNA expression profiles, immunoblotting assay was carried out for 6 of them, including two known HIF-1 downstream targets PGK1 and LDHA. The positive correlation

observed between the immunoblot results and the RT-PCR results of the selected targets – PGK1, LDHA, ANXA2, and PCBD1 – further affirmed the reliability of our experimental results using the iTRAQ-based quantitation approach and the potential use of this multiplex comparative proteomic strategy in identifying novel targets. Furthermore, from our study, it is highly likely that the regulation of ANXA2 and PCBD1 are related to the activity of p53 in a direct or indirect manner. Although CKS2 and EFHD2 showed slight variations between the two verification approaches, their expression levels were nonetheless significantly altered.

The remaining 12 targets were not validated by RT-PCR and were not considered for immunoblotting assay initially. However, this does not indicate that these 12 targets are not affected by hypoxia treatment and/or the presence of p53 but instead implies that they may not be affected at a transcriptional level. The implication of two factors (hypoxia and p53) in influencing the expression levels can provide a tricky situation as one factor might exert an influence at transcriptional level while the other at post-transcriptional level. Hence, it is somewhat not surprising that only close to half of our targets were validated using RT-PCR analysis.

5.3.3 Proposed targets influenced by p53

5.3.3.1 Annexin A2

Annexin A2 (ANXA2/ANX2) belongs to the Annexin family whose members are calcium-dependent phospholipid-binding proteins. Annexins are involved in the regulation of cellular growth, signal transduction pathways and possible tumorigenesis and there have been more than 160 annexins reported but only 10 of them are of human origin. These include the more well-studied annexins such as

annexin 1, 5 and 7 (ANX1, ANX5, and ANX7 respectively) and the dysregulation of annexins have been reported commonly in many human cancers. For example, ANX1 has been reported up-regulated in breast cancer (Ahn et al., 1997), pancreatic cancer (Bai et al., 2004) and hepatocellular carcinomas (Masaki et al., 1996) but down-regulated in prostate cancer (Paweletz et al., 2000). Likewise, up-regulation of ANXA2 has been found associated with a number of cancers such as colorectal and breast cancers. It has also been proposed as a possible prognostic marker for colorectal cancer (Emoto et al., 2001; Sharma et al., 2006).

In cells, ANXA2 can exist in 3 different forms, namely monomeric, heterodimeric and heterotetrameric. The most dominant form in most cells is the heterotetrameric form composed of two ANXA2 monomers and two S100A10 (p11) proteins. ANXA2 can also bind with PGK1 to form a heterodimer known as primer recognition protein (PRP), a cofactor for DNA polymerase alpha, and this heterodimeric form has been proposed to play a role in DNA synthesis and cell cycle progression (Kumble et al., 1992). Coinciding with our RT-PCR results, several studies have also shown that the mRNA level of *ANXA2* is found elevated in the presence of hypoxic stress and is HIF-1α dependent (Hu et al., 2006; Maxwell et al., 2003). However, in our proteomic result (both immunoblot and iTRAQ), the expression level of ANXA2 protein was unaffected by hypoxia treatment. This can be due to two possibilities: (1) either the mRNA is not being translated into proteins or (2) the newly translated ANXA2 monomers do not undergo post-translational modifications and therefore, are rapidly degraded under hypoxic conditions.

Annexin A2 has been associated with apoptosis induced by a widely used chemodrug in cancer therapy, 5-fluorouracil (5-FU). Upon treatment with 5-FU, an up-regulation of ANXA2 had been reported in MCF-7, a breast adenocarcinoma cell line, as well as in HCT116 cells (Kho et al., 2004; Maxwell et al., 2003). The apoptotic effect of 5-FU has also been shown to be dependent on the tumor suppressor protein p53; the absence of p53 can attenuate the genotoxic effects of 5-FU (Bunz et al., 1999). Furthermore, Maxwell et al. (2003) had also shown that the induction of ANXA2 by 5-FU was significantly reduced in the absence of p53 through cDNA microarray. Similarly, in our result, the level of ANXA2 protein was found to be down-regulated in HCT116 p53 KO. An up-regulation of ANXA2 was also observed in transient over-expression of p53 in several lung cancer cell lines; however, the exact molecular mechanism has not been reported (Huang et al., 2005). Taken together, these results suggest that ANXA2 is a potential downstream regulatory target of p53 and our result also further supports its potential use as a biomarker for determining the activity of p53-dependent responses during cancer therapy.

5.3.3.2 Pterin-4 alpha-carbinolamine dehydratase

The *PCBD1* (official gene name: pterin-4 alpha-carbinolamine dehydratase/dimerization cofactor of hepatocyte nuclear factor 1 alpha (TCF1)) gene encodes an 11 kDa bifunctional enzyme called pterin-4 alpha-carbinolamine dehydratase. This enzyme participates in the recycling of tetrahydrobiopterin (BH4) which is an essential cofactor of several metabolic functions, such as amino acid phenylalanine hydroxylation. Therefore, a decrease in PCBD1 can result in an elevated level of phenylalanine due to a deficiency of tetrahydrobiopterin (Citron et al., 1993). In addition, it can also regulate the homodimerization of the transcription

factor hepatocyte nuclear factor 1 (HNF1) by stabilizing its dimer, HNF1α and HNF1β subunits (Citron et al., 1992). The binding of PCBD1 to HNF1 also allows HNF1 to bind DNA sequences that deviate considerably from the consensus sequence; hence, modifying the DNA binding specificity of HNF1 and influencing its transcriptional activity (Rhee et al., 1997).

In colorectal cancer tissues and cell lines, PCBD1 has been found highly overexpressed but absent in their normal counterparts (Eskinazi et al., 1999). This distinct difference in its expression level in cancer and normal tissues may indicate its potential role in promoting cancer progression as a modulator of transcriptional activity. In HCT116 WT cells, strong expression of PCBD1 protein was also observed (Figure 4.9A) under both hypoxic and normoxic conditions. However, in the absence of p53, PCBD1 was found to be down-regulated by approximately 50% regardless of the conditions (hypoxia or normoxia) the cells were subjected under. Furthermore, the RT-PCR analysis of the PCBD1 mRNA level suggests that the decreased level of PCBD1 proteins is likely due to a reduced mRNA expression. Although several studies indicate that p53 is transcriptional inactive in hypoxic HCT116 cells, this is only with reference to p53 apoptotic response (Koumenis et al., 2001). Therefore, it is likely that the downstream p53 non-apoptotic target genes can still be expressed, whereby PCBD1 might be one of them (Wu et al., 2006).

Interestingly, structural studies of p53 and PCBD1 have shown that both proteins can individually form a homotetramer through a four helix bundle oligomerization interface. This four helix bundle is formed with each monomer contributing one helix to this central antiparallel helix bundle (Eskinazi et al., 1999;

Lee et al., 1994). Although the four helix bundle is a commonly observed structural motif (Harris et al., 1994), only a few proteins are known where it forms the oligomerization interface to give rise to a tetrameric form. It is possible that PCBD1 and p53 may bind to each other through this similar oligomerization interface by contributing a helix stand from each of their monomer and further stabilizes PCBD1. Indeed, a possible novel relationship may exist between PCBD1 and p53. However, more stringent studies are required in order to confirm this novel relationship between PCBD1 and p53. Proposed future studies can focus on whether PCBD1 stability is influenced by a direct interaction with p53 or it is regulated by p53 transcriptional activities.

5.3.4 Proposed targets influenced under hypoxia treatment

5.3.4.1 Cyclin-dependent kinase subunit-2

The cyclin-dependent kinase subunit-2 (CKS2), also known as CDK1/CDC28 protein kinase regulatory subunit-2, belongs to the Cks family that is composed of small proteins ranging from 9-18 kDa. CKS2 protein is approximately 9 kDa in size and has been shown highly expressed in colorectal cancer tissues (Lin et al., 2002). Two paralogs, CKS1 and CKS2, are expressed in mammalian cells and they exhibit an 81% identity in their amino acid sequence, suggesting possible overlapping of functions (Pines, 1996). Both paralogs were found with similar binding affinity for cyclin-dependent kinase 2 (CDK2) (Bourne et al., 1996). On the other hand, distinct functions have been reported for each paralog too. CKS1, but not CKS2, has been shown to participate in inducing the degradation of p27, a CDK inhibitor, by binding with E3 ligase of p27, SKP2 (Spruck et al., 2001). Furthermore, CKS2-deficient mice failed to exhibit similar phenotype that is related to p27 accumulation found in CKS1-

deficient mice; CKS2-deficient mice are found viable but sterile in both sexes due to the failure to enter anaphase during cell cycle progression (Spruck et al., 2003). Therefore, suggesting role of CKS1 and CKS2 in regulating mitotic cell cycle in distinct ways.

In our initial result (iTRAQ), a distinct negative influence on CKS2 expression in hypoxia-treated HCT116 cells independent of p53 was observed. This was further confirmed in subsequent validation results obtained from RT-PCR and immunoblot assays. Although there is no direct link between CKS2 and hypoxia or HIF-1, CKS2 has been found highly expressed in metastatic tumor tissues, promoting proliferation, oxidative phosphorylation, invasiveness, and tumor size (Li et al., 2004; Lyng et al., 2006). Since hypoxia also promotes metastasis, the decreased level of CKS2 in hypoxic HCT116 cells was puzzling. The contrasting result obtained may be due to the starting biological material used for the studies since biological tissues are known to comprise of more than one cell type, ranging from epithelial cells to vascular cells; mixture of normal and cancerous cells are also found in a biological tissue sample too. Furthermore, it was not mentioned that the cancer tissues used in the studies were hypoxic in nature. Therefore, a more thorough analysis on the effect of hypoxia on CKS2 regulation is required.

Interestingly, in the validation results, we observed an increased CKS2 level in the p53 KO cells and this suggested possible regulation of CKS2 by p53. Initially, we suspected that this phenomenon may be due to the primers and antibody used since both proteins shared high similarity in their DNA and amino acid sequences. Furthermore, according to the data sheet, the antibody against CKS2 was also used for

detecting CKS1. However, a recent article published confirmed our observation that the expression of CKS2 can be repressed by p53 at both mRNA and protein levels in a dose-dependent manner (Rother et al., 2007). This has been observed in many different cell lines, including HCT116, but the exact mechanism is still unknown. The authors suggested that this phenomenon was not due to direct or indirect binding of p53 to the *CKS2* promoter since high dosage of YA13m29, a dominant-negative mutant of NF-Y subunit NF-YA, did not affect the repression of CKS2 by p53. Chromosomal immunoprecipitation (ChIP) assay also showed that p53 itself does not bind to CK promoter. NF-Y is a transcription activator that binds to CCAAT-boxes to mediate p53-dependent repression on gene expression (Imbriano et al., 2005; Yun et al., 1999). An analysis of the status of p53 should be carried out to identify whether PTM of p53 is required to repress CKS2 since mutations of p53 are found in approximately 50% of the cancers reported which might be accountable for the high expression of CKS2 in colorectal cancers mentioned earlier. Also, the CKS2 antibody used in our study can target CKS1 and this suggests that CKS1 may be potentially repressed by p53 too.

5.3.4.2 EF-hand domain family, member D2

There is little information available on this protein EF-hand domain family, member D2 (EFHD2), also known as swiprosin-1 (SWS1), except that it may play a role in macrophage activation and function (Jin et al., 2006). The protein contains two EF-hand domains which are involved in binding intracellular calcium. Furthermore, expression of EFHD2 was found up-regulated in ovarian cancer cells treated with ciglitazone, a peroxisome proliferator–activated receptor γ (PPARγ) ligand that has been used to treat cancer through inhibition of cell growth and induction of cell death

by activating transcription factor PPARγ (Vignati et al., 2006). Although this previous study suggests a possible role in inducing cell death, the up-regulation of EFHD2 in ciglitazone-treated ovarian cancer cells may be a form of apoptotic resistance produced by the cancer cells against the anticancer drug instead. This possibility is supported by the up-regulation of EFHD2 observed in human thyroid autonomous adenomas and thyrocytes treated with thyroid-stimulating hormone (TSH), which can activate the cyclic adenosine monophosphate (cAMP) pathway (van Staveren et al., 2006; Vlaeminck-Guillem et al., 2002). Activation of TSH-cAMP pathway has been shown to promote tumorigenesis by inducing inhibitor of apoptosis protein-2 (IAP-2) and suppressing apoptosis through ERK/MAPK pathway in colon cancer cells (Nishihara et al., 2004). In our study using iTRAQ-MS/MS approach, we identified that EFHD2 protein is up-regulated in hypoxic cells regardless of p53 presence (Figure 4.7D). Furthermore, the increased expression level was validated in the RT-PCR analysis of its mRNA level (Figure 4.8C), suggesting that EFHD2 may play a potential role in promoting anti-apoptotic mechanism in the presence of mild hypoxic stresses.

5.5 General comments on application of iTRAQ and mass spectrometry to multiplex comparative proteomic studies

Interest has been growing over the past years to study cancer using proteomic approaches. Previously, 2-D GE was the most common method to perform comparative proteomic analysis between normal and cancer tissues/cells. The disadvantage of such method is that differentially expressed spots are not identified until they are excised and sent for identification using MS. Furthermore, quantitation of the differentially expressed spots is only possible using image analysis software

based on the intensity of the protein stain used which might be difficult when there is a high background staining. Accuracy of quantitation and the large error margin are also a problem. With the development of isobaric/isotopic tags such as iTRAQ, such gel-based protein analysis can be avoided and because the entire experiment sample is coupled to mass spectrometry, identification and quantitation of the protein peptides can be obtained without further downstream work. The fully-annotated protein profile will also allow ease of data analysis as well as successfulness of the experiments from analyzing the expression levels of control targets.

The use of iTRAQ labeling also allows greater magnitude of investigation since it virtually labels all the peptides at their amine group. This will allow identification of small and huge protein molecules which cannot be resolved using SDS-PAGE. Furthermore, proteins exhibiting close pH and similar molecular weight can be found hard to separate in the gel-base separation system due to the restricted pI and molecular weight ranges presented. This will not be a problem in using iTRAQ since protein identification will be based on distinct signature peptides found in highly curated databases. In our study we have shown what may be the first use of iTRAQ to perform a four-plex comparison against the different combination of hypoxia treatment and p53 presence. Although iTRAQ was originally developed as a multiplex peptide labeling system to allow simultaneous analysis of 4 different samples using tandem mass spectrometry, there had been few publications exploiting its potential. Most groups used this technique to perform replication sets instead. Identification of distinct proteins that are only affected by each condition as well as by both conditions yield positive results according to our validated data.

CHAPTER 6 – CONCLUSION AND FUTURE PERSPECTIVES

The application of proteomic approaches in the study of cancer can allow us to study and understand better the actual ongoing that is occurring within the cancer tissues at both cellular and molecular levels. Proteomics provides a truer picture in identifying targets that are involved in the process of cancer development as it allows us to study the final output than the intermediate products. Studies performed in this project aim to identify potential novel targets affected by p53 and/or hypoxia as well as identify common targets that might provide an explanation for the ever elusive relationship between p53 and hypoxia.

While the results obtained from the multiplex comparative proteomic approach we adopted provides us with exciting possibilities, they are only early indicators of potential novel targets of p53 and hypoxia/HIF-1. On the other hand, the successful validations of the selected targets though RT-PCR and immunoblot assays provided a greater confidence for our results and also illustrate the advantage of iTRAQ analysis as a multiple marker technique for initial biomarker discovery.

From our study, we propose ANXA2 and PCBD1 as potential novel targets of p53, while EFHD2 and CKS2 as novel targets regulated under hypoxia. ANXA2 and PCBD1 are both identified and validated to be down-regulated in the absence of p53, hinting a p53-dependency for the accumulation observed in WT. CKS2 is found down-regulated during hypoxia while EFHD2 is proposed to be up-regulated during hypoxia. Both have been verified using RT-PCR and immunoblotting assay. Further studies on these targets can be designed to further confirm whether this phenomenon

is at a transcriptional or post-transcriptional regulation and also determine whether the interaction is direct or indirect. Experiments, such as luciferase-promoter assays, may help to confirm whether the proposed targets are direct downstream genes regulated by p53. A detailed study will also help to identify the mechanism involved. This can be done by designing experiments involving over-expression and knockout/knockdown of the selected targets in order to determine their respective functions in the cells as well as in well-established mammalian models.

To provide further confidence on our results, a screen of the various cancer tissues using these selected targets can be done. This will allow a better insight on the expression levels of our selected targets in different types of cancer and determine if the observed trend is specific only to colorectal cancer cell lines. In addition, the screening will also allow us to determine if the targets are suitable to be used as a universal cancer biomarker or as a specific cancer biomarker. Nevertheless, the targets we have identified in this project hold potential uses in the biomedical field of cancer research.

REFERENCES

Achison, M., and Hupp, T.R. (2003). Hypoxia attenuates the p53 response to cellular damage. Oncogene *22*, 3431-3440.

Aebersold, D.M., Burri, P., Beer, K.T., Laissue, J., Djonov, V., Greiner, R.H., and Semenza, G.L. (2001). Expression of hypoxia-inducible factor-1alpha: a novel predictive and prognostic parameter in the radiotherapy of oropharyngeal cancer. Cancer Res *61*, 2911-2916.

Ahn, S.H., Sawada, H., Ro, J.Y., and Nicolson, G.L. (1997). Differential expression of annexin I in human mammary ductal epithelial cells in normal and benign and malignant breast tissues. Clin Exp Metastasis *15*, 151-156.

Albiero, A.L., and Pozzi, D.H. (1994). [Mechanisms of tumoral resistance to antineoplastic agents]. Rev Assoc Med Bras *40*, 125-128.

Alper, T., and Howard-Flanders, P. (1956). Role of oxygen in modifying the radiosensitivity of E. coli B. Nature *178*, 978-979.

An, W.G., Kanekal, M., Simon, M.C., Maltepe, E., Blagosklonny, M.V., and Neckers, L.M. (1998). Stabilization of wild-type p53 by hypoxia-inducible factor 1alpha. Nature *392*, 405-408.

Arai, N., Nomura, D., Yokota, K., Wolf, D., Brill, E., Shohat, O., and Rotter, V. (1986). Immunologically distinct p53 molecules generated by alternative splicing. Mol Cell Biol *6*, 3232-3239.

Bai, X.F., Ni, X.G., Zhao, P., Liu, S.M., Wang, H.X., Guo, B., Zhou, L.P., Liu, F., Zhang, J.S., Wang, K.*, et al.* (2004). Overexpression of annexin 1 in pancreatic cancer and its clinical significance. World J Gastroenterol *10*, 1466-1470.

Bech-Otschir, D., Kraft, R., Huang, X., Henklein, P., Kapelari, B., Pollmann, C., and Dubiel, W. (2001). COP9 signalosome-specific phosphorylation targets p53 to degradation by the ubiquitin system. Embo J *20*, 1630-1639.

Bensaad, K., and Vousden, K.H. (2005). Savior and slayer: the two faces of p53. Nat Med *11*, 1278-1279.

Berra, E., Ginouves, A., and Pouyssegur, J. (2006). The hypoxia-inducible-factor hydroxylases bring fresh air into hypoxia signalling. EMBO Rep *7*, 41-45.

Birner, P., Schindl, M., Obermair, A., Plank, C., Breitenecker, G., and Oberhuber, G. (2000). Overexpression of hypoxia-inducible factor 1alpha is a marker for an unfavorable prognosis in early-stage invasive cervical cancer. Cancer Res *60*, 4693-4696.

Bishop, J.M., and Weinberg, R.A. (1996). Molecular oncology (New York: Scientific American, Inc).

Blagosklonny, M.V., An, W.G., Romanova, L.Y., Trepel, J., Fojo, T., and Neckers, L. (1998). p53 inhibits hypoxia-inducible factor-stimulated transcription. J Biol Chem *273*, 11995-11998.

Bourne, Y., Watson, M.H., Hickey, M.J., Holmes, W., Rocque, W., Reed, S.I., and Tainer, J.A. (1996). Crystal structure and mutational analysis of the human CDK2 kinase complex with cell cycle-regulatory protein CksHs1. Cell *84*, 863-874.

Brizel, D.M., Sibley, G.S., Prosnitz, L.R., Scher, R.L., and Dewhirst, M.W. (1997). Tumor hypoxia adversely affects the prognosis of carcinoma of the head and neck. Int J Radiat Oncol Biol Phys *38*, 285-289.

Brugarolas, J., Chandrasekaran, C., Gordon, J.I., Beach, D., Jacks, T., and Hannon, G.J. (1995). Radiation-induced cell cycle arrest compromised by p21 deficiency. Nature *377*, 552-557.

Bunz, F., Hwang, P.M., Torrance, C., Waldman, T., Zhang, Y., Dillehay, L., Williams, J., Lengauer, C., Kinzler, K.W., and Vogelstein, B. (1999). Disruption of p53 in human cancer cells alters the responses to therapeutic agents. J Clin Invest *104*, 263-269.

Bykov, V.J., and Wiman, K.G. (2003). Novel cancer therapy by reactivation of the p53 apoptosis pathway. Ann Med *35*, 458-465.

Calabretta, B., Kaczmarek, L., Ming, P.M., Au, F., and Ming, S.C. (1985). Expression of c-myc and other cell cycle-dependent genes in human colon neoplasia. Cancer Res *45*, 6000-6004.

Canman, C.E., Lim, D.S., Cimprich, K.A., Taya, Y., Tamai, K., Sakaguchi, K., Appella, E., Kastan, M.B., and Siliciano, J.D. (1998). Activation of the ATM kinase by ionizing radiation and phosphorylation of p53. Science *281*, 1677-1679.

Carmeliet, P., Dor, Y., Herbert, J.M., Fukumura, D., Brusselmans, K., Dewerchin, M., Neeman, M., Bono, F., Abramovitch, R., Maxwell, P.*, et al.* (1998). Role of HIF-1alpha in hypoxia-mediated apoptosis, cell proliferation and tumour angiogenesis. Nature *394*, 485-490.

Chen, D., Li, M., Luo, J., and Gu, W. (2003). Direct interactions between HIF-1 alpha and Mdm2 modulate p53 function. J Biol Chem *278*, 13595-13598.

Chipuk, J.E., Bouchier-Hayes, L., Kuwana, T., Newmeyer, D.D., and Green, D.R. (2005). PUMA couples the nuclear and cytoplasmic proapoptotic function of p53. Science *309*, 1732-1735.

Cho, W.C. (2007). Contribution of oncoproteomics to cancer biomarker discovery. Mol Cancer *6*, 25.

Chun, Y.S., Kim, M.S., and Park, J.W. (2002). Oxygen-dependent and -independent regulation of HIF-1alpha. J Korean Med Sci *17*, 581-588.

Citron, B.A., Davis, M.D., Milstien, S., Gutierrez, J., Mendel, D.B., Crabtree, G.R., and Kaufman, S. (1992). Identity of 4a-carbinolamine dehydratase, a component of

the phenylalanine hydroxylation system, and DCoH, a transregulator of homeodomain proteins. Proc Natl Acad Sci U S A *89*, 11891-11894.

Citron, B.A., Kaufman, S., Milstien, S., Naylor, E.W., Greene, C.L., and Davis, M.D. (1993). Mutation in the 4a-carbinolamine dehydratase gene leads to mild hyperphenylalaninemia with defective cofactor metabolism. Am J Hum Genet *53*, 768-774.

Courtois, S., de Fromentel, C.C., and Hainaut, P. (2004). p53 protein variants: structural and functional similarities with p63 and p73 isoforms. Oncogene *23*, 631-638.

Courtois, S., Verhaegh, G., North, S., Luciani, M.G., Lassus, P., Hibner, U., Oren, M., and Hainaut, P. (2002). DeltaN-p53, a natural isoform of p53 lacking the first transactivation domain, counteracts growth suppression by wild-type p53. Oncogene *21*, 6722-6728.

Craig, A.L., Burch, L., Vojtesek, B., Mikutowska, J., Thompson, A., and Hupp, T.R. (1999). Novel phosphorylation sites of human tumour suppressor protein p53 at Ser20 and Thr18 that disrupt the binding of mdm2 (mouse double minute 2) protein are modified in human cancers. Biochem J *342 (Pt 1)*, 133-141.

DeSouza, L., Diehl, G., Rodrigues, M.J., Guo, J., Romaschin, A.D., Colgan, T.J., and Siu, K.W. (2005). Search for cancer markers from endometrial tissues using differentially labeled tags iTRAQ and cICAT with multidimensional liquid chromatography and tandem mass spectrometry. J Proteome Res *4*, 377-386.

Dewhirst, M.W., Ong, E.T., Rosner, G.L., Rehmus, S.W.E., Shan, S., Braun, R.D., Brizel, D.M., and Secomb, T.W. (1996). Arteriolar oxygenation in tumor and subcutaneous arterioles: effects of inspired air oxygen content. Br J Cancer *74*, 247-251.

el-Deiry, W.S. (1998). Regulation of p53 downstream genes. Semin Cancer Biol *8*, 345-357.

el-Deiry, W.S., Harper, J.W., O'Connor, P.M., Velculescu, V.E., Canman, C.E., Jackman, J., Pietenpol, J.A., Burrell, M., Hill, D.E., Wang, Y*., et al.* (1994). WAF1/CIP1 is induced in p53-mediated G1 arrest and apoptosis. Cancer Res *54*, 1169-1174.

el-Deiry, W.S., Kern, S.E., Pietenpol, J.A., Kinzler, K.W., and Vogelstein, B. (1992). Definition of a consensus binding site for p53. Nat Genet *1*, 45-49.

Ema, M., Taya, S., Yokotani, N., Sogawa, K., Matsuda, Y., and Fujii-Kuriyama, Y. (1997). A novel bHLH-PAS factor with close sequence similarity to hypoxia-inducible factor 1alpha regulates the VEGF expression and is potentially involved in lung and vascular development. Proc Natl Acad Sci U S A *94*, 4273-4278.

Emoto, K., Yamada, Y., Sawada, H., Fujimoto, H., Ueno, M., Takayama, T., Kamada, K., Naito, A., Hirao, S., and Nakajima, Y. (2001). Annexin II overexpression

correlates with stromal tenascin-C overexpression: a prognostic marker in colorectal carcinoma. Cancer *92*, 1419-1426.

Erler, J.T., Cawthorne, C.J., Williams, K.J., Koritzinsky, M., Wouters, B.G., Wilson, C., Miller, C., Demonacos, C., Stratford, I.J., and Dive, C. (2004). Hypoxia-mediated down-regulation of Bid and Bax in tumors occurs via hypoxia-inducible factor 1-dependent and -independent mechanisms and contributes to drug resistance. Mol Cell Biol *24*, 2875-2889.

Eskinazi, R., Thony, B., Svoboda, M., Robberecht, P., Dassesse, D., Heizmann, C.W., Van Laethem, J.L., and Resibois, A. (1999). Overexpression of pterin-4a-carbinolamine dehydratase/dimerization cofactor of hepatocyte nuclear factor 1 in human colon cancer. Am J Pathol *155*, 1105-1113.

Fields, S. (2001). Proteomics. Proteomics in genomeland. Science *291*, 1221-1224.

Finlay, C.A., Hinds, P.W., Tan, T.H., Eliyahu, D., Oren, M., and Levine, A.J. (1988). Activating mutations for transformation by p53 produce a gene product that forms an hsc70-p53 complex with an altered half-life. Mol Cell Biol *8*, 531-539.

Frede, S., Stockmann, C., Freitag, P., and Fandrey, J. (2006). Bacterial lipopolysaccharide induces HIF-1 activation in human monocytes via p44/42 MAPK and NF-kappaB. Biochem J *396*, 517-527.

Fuster, J.J., Sanz-Gonzalez, S.M., Moll, U.M., and Andres, V. (2007). Classic and novel roles of p53: prospects for anticancer therapy. Trends Mol Med *13*, 192-199.

Fyles, A.W., Milosevic, M., Wong, R., Kavanagh, M.C., Pintilie, M., Sun, A., Chapman, W., Levin, W., Manchul, L., Keane, T.J*., et al.* (1998). Oxygenation predicts radiation response and survival in patients with cervix cancer. Radiother Oncol *48*, 149-156.

Gartel, A.L., and Radhakrishnan, S.K. (2005). Lost in transcription: p21 repression, mechanisms, and consequences. Cancer Res *65*, 3980-3985.

Geyer, R.K., Yu, Z.K., and Maki, C.G. (2000). The MDM2 RING-finger domain is required to promote p53 nuclear export. Nat Cell Biol *2*, 569-573.

Giaccia, A.J., Simon, M.C., and Johnson, R. (2004). The biology of hypoxia: the role of oxygen sensing in development, normal function, and disease. Genes Dev *18*, 2183-2194.

Graeber, T.G., Osmanian, C., Jacks, T., Housman, D.E., Koch, C.J., Lowe, S.W., and Giaccia, A.J. (1996). Hypoxia-mediated selection of cells with diminished apoptotic potential in solid tumours. Nature *379*, 88-91.

Graeber, T.G., Peterson, J.F., Tsai, M., Monica, K., Fornace, A.J., Jr., and Giaccia, A.J. (1994). Hypoxia induces accumulation of p53 protein, but activation of a G1-phase checkpoint by low-oxygen conditions is independent of p53 status. Mol Cell Biol *14*, 6264-6277.

Gronroos, E., Terentiev, A.A., Punga, T., and Ericsson, J. (2004). YY1 inhibits the activation of the p53 tumor suppressor in response to genotoxic stress. Proc Natl Acad Sci U S A *101*, 12165-12170.

Gu, W., Shi, X.L., and Roeder, R.G. (1997). Synergistic activation of transcription by CBP and p53. Nature *387*, 819-823.

Guevara, N.V., Kim, H.S., Antonova, E.I., and Chan, L. (1999). The absence of p53 accelerates atherosclerosis by increasing cell proliferation in vivo. Nat Med *5*, 335-339.

Gygi, S.P., Rochon, Y., Franza, B.R., and Aebersold, R. (1999). Correlation between protein and mRNA abundance in yeast. Mol Cell Biol *19*, 1720-1730.

Hainaut, P., and Hollstein, M. (2000). p53 and human cancer: the first ten thousand mutations. Adv Cancer Res *77*, 81-137.

Hanahan, D., and Weinberg, R.A. (2000). The hallmarks of cancer. Cell *100*, 57-70.

Harris, N.L., Presnell, S.R., and Cohen, F.E. (1994). Four helix bundle diversity in globular proteins. J Mol Biol *236*, 1356-1368.

Harrison, L.B., Chadha, M., Hill, R.J., Hu, K., and Shasha, D. (2002). Impact of tumor hypoxia and anemia on radiation therapy outcomes. Oncologist *7*, 492-508.

Haupt, Y., Maya, R., Kazaz, A., and Oren, M. (1997). Mdm2 promotes the rapid degradation of p53. Nature *387*, 296-299.

Helmlinger, G., Yuan, F., Dellian, M., and Jain, R.K. (1997). Interstitial pH and pO2 gradients in solid tumors in vivo: high-resolution measurements reveal a lack of correlation. Nat Med *3*, 177-182.

Higashimoto, Y., Saito, S., Tong, X.H., Hong, A., Sakaguchi, K., Appella, E., and Anderson, C.W. (2000). Human p53 is phosphorylated on serines 6 and 9 in response to DNA damage-inducing agents. J Biol Chem *275*, 23199-23203.

Hockel, M., and Vaupel, P. (2001). Tumor hypoxia: definitions and current clinical, biologic, and molecular aspects. J Natl Cancer Inst *93*, 266-276.

Hogenesch, J.B., Chan, W.K., Jackiw, V.H., Brown, R.C., Gu, Y.Z., Pray-Grant, M., Perdew, G.H., and Bradfield, C.A. (1997). Characterization of a subset of the basic-helix-loop-helix-PAS superfamily that interacts with components of the dioxin signaling pathway. J Biol Chem *272*, 8581-8593.

Honda, R., Tanaka, H., and Yasuda, H. (1997). Oncoprotein MDM2 is a ubiquitin ligase E3 for tumor suppressor p53. FEBS Lett *420*, 25-27.

Honda, R., and Yasuda, H. (1999). Association of p19(ARF) with Mdm2 inhibits ubiquitin ligase activity of Mdm2 for tumor suppressor p53. Embo J *18*, 22-27.

Hu, C.J., Iyer, S., Sataur, A., Covello, K.L., Chodosh, L.A., and Simon, M.C. (2006). Differential regulation of the transcriptional activities of hypoxia-inducible factor 1 alpha (HIF-1alpha) and HIF-2alpha in stem cells. Mol Cell Biol *26*, 3514-3526.

Huang, L.E., Gu, J., Schau, M., and Bunn, H.F. (1998). Regulation of hypoxia-inducible factor 1alpha is mediated by an O2-dependent degradation domain via the ubiquitin-proteasome pathway. Proc Natl Acad Sci U S A *95*, 7987-7992.

Huang, Y., Yan, C.H., and Fu, S.B. (2005). [The cloning and expression of apoptosis associated gene ANNEXIN A2 induced by p53 gene]. Zhonghua Yi Xue Yi Chuan Xue Za Zhi *22*, 661-664.

Humar, R., Kiefer, F.N., Berns, H., Resink, T.J., and Battegay, E.J. (2002). Hypoxia enhances vascular cell proliferation and angiogenesis in vitro via rapamycin (mTOR)-dependent signaling. Faseb J *16*, 771-780.

Imbriano, C., Gurtner, A., Cocchiarella, F., Di Agostino, S., Basile, V., Gostissa, M., Dobbelstein, M., Del Sal, G., Piaggio, G., and Mantovani, R. (2005). Direct p53 transcriptional repression: in vivo analysis of CCAAT-containing G2/M promoters. Mol Cell Biol *25*, 3737-3751.

Ivan, M., Kondo, K., Yang, H., Kim, W., Valiando, J., Ohh, M., Salic, A., Asara, J.M., Lane, W.S., and Kaelin, W.G., Jr. (2001). HIFalpha targeted for VHL-mediated destruction by proline hydroxylation: implications for O2 sensing. Science *292*, 464-468.

Jang, M.S., Park, J.E., Lee, J.A., Park, S.G., Myung, P.K., Lee, D.H., Park, B.C., and Cho, S. (2005). Binding and regulation of hypoxia-inducible factor-1 by the inhibitory PAS proteins. Biochem Biophys Res Commun *337*, 209-215.

Jemal, A., Siegel, R., Ward, E., Murray, T., Xu, J., Smigal, C., and Thun, M.J. (2006). Cancer statistics, 2006. CA Cancer J Clin *56*, 106-130.

Jiang, B.H., Rue, E., Wang, G.L., Roe, R., and Semenza, G.L. (1996). Dimerization, DNA binding, and transactivation properties of hypoxia-inducible factor 1. J Biol Chem *271*, 17771-17778.

Jin, M., Diaz, P.T., Bourgeois, T., Eng, C., Marsh, C.B., and Wu, H.M. (2006). Two-dimensional gel proteome reference map of blood monocytes. Proteome Sci *4*, 16.

Jin, Y., Zeng, S.X., Dai, M.S., Yang, X.J., and Lu, H. (2002). MDM2 inhibits PCAF (p300/CREB-binding protein-associated factor)-mediated p53 acetylation. J Biol Chem *277*, 30838-30843.

Jones, J.M., Attardi, L., Godley, L.A., Laucirica, R., Medina, D., Jacks, T., Varmus, H.E., and Donehower, L.A. (1997). Absence of p53 in a mouse mammary tumor model promotes tumor cell proliferation without affecting apoptosis. Cell Growth Differ *8*, 829-838.

Kallio, P.J., Okamoto, K., O'Brien, S., Carrero, P., Makino, Y., Tanaka, H., and Poellinger, L. (1998). Signal transduction in hypoxic cells: inducible nuclear

translocation and recruitment of the CBP/p300 coactivator by the hypoxia-inducible factor-1alpha. Embo J *17*, 6573-6586.

Kallio, P.J., Wilson, W.J., O'Brien, S., Makino, Y., and Poellinger, L. (1999). Regulation of the hypoxia-inducible transcription factor 1alpha by the ubiquitin-proteasome pathway. J Biol Chem *274*, 6519-6525.

Kamijo, T., Weber, J.D., Zambetti, G., Zindy, F., Roussel, M.F., and Sherr, C.J. (1998). Functional and physical interactions of the ARF tumor suppressor with p53 and Mdm2. Proc Natl Acad Sci U S A *95*, 8292-8297.

Katschinski, D.M., Le, L., Heinrich, D., Wagner, K.F., Hofer, T., Schindler, S.G., and Wenger, R.H. (2002). Heat induction of the unphosphorylated form of hypoxia-inducible factor-1alpha is dependent on heat shock protein-90 activity. J Biol Chem *277*, 9262-9267.

Kauh, J., and Umbreit, J. (2004). Colorectal cancer prevention. Curr Probl Cancer *28*, 240-264.

Kho, P.S., Wang, Z., Zhuang, L., Li, Y., Chew, J.L., Ng, H.H., Liu, E.T., and Yu, Q. (2004). p53-regulated transcriptional program associated with genotoxic stress-induced apoptosis. J Biol Chem *279*, 21183-21192.

Kimura, H., Braun, R.D., Ong, E.T., Hsu, R., Secomb, T.W., Papahadjopoulos, D., Hong, K., and Dewhirst, M.W. (1996). Fluctuations in red cell flux in tumor microvessels can lead to transient hypoxia and reoxygenation in tumor parenchyma. Cancer Res *56*, 5522-5528.

Koch, C.J. (1982). Oxygen effects in radiobiology. Adv Exp Med Biol *157*, 123-144.

Koumenis, C., Alarcon, R., Hammond, E., Sutphin, P., Hoffman, W., Murphy, M., Derr, J., Taya, Y., Lowe, S.W., Kastan, M.*, et al.* (2001). Regulation of p53 by hypoxia: dissociation of transcriptional repression and apoptosis from p53-dependent transactivation. Mol Cell Biol *21*, 1297-1310.

Krishnamachary, B., Berg-Dixon, S., Kelly, B., Agani, F., Feldser, D., Ferreira, G., Iyer, N., LaRusch, J., Pak, B., Taghavi, P.*, et al.* (2003). Regulation of colon carcinoma cell invasion by hypoxia-inducible factor 1. Cancer Res *63*, 1138-1143.

Kubota, T., Koshizuka, K., Williamson, E.A., Asou, H., Said, J.W., Holden, S., Miyoshi, I., and Koeffler, H.P. (1998). Ligand for peroxisome proliferator-activated receptor gamma (troglitazone) has potent antitumor effect against human prostate cancer both in vitro and in vivo. Cancer Res *58*, 3344-3352.

Kumble, K.D., Iversen, P.L., and Vishwanatha, J.K. (1992). The role of primer recognition proteins in DNA replication: inhibition of cellular proliferation by antisense oligodeoxyribonucleotides. J Cell Sci *101 (Pt 1)*, 35-41.

Lamlum, H., Papadopoulou, A., Ilyas, M., Rowan, A., Gillet, C., Hanby, A., Talbot, I., Bodmer, W., and Tomlinson, I. (2000). APC mutations are sufficient for the growth of early colorectal adenomas. Proc Natl Acad Sci U S A *97*, 2225-2228.

Lando, D., Peet, D.J., Whelan, D.A., Gorman, J.J., and Whitelaw, M.L. (2002). Asparagine hydroxylation of the HIF transactivation domain a hypoxic switch. Science *295*, 858-861.

Lane, D.P. (1992). Cancer. p53, guardian of the genome. Nature *358*, 15-16.

Lechanteur, C., Jacobs, N., Greimers, R., Benoit, V., Deregowski, V., Chariot, A., Merville, M.P., and Bours, V. (2005). Low daunomycin concentrations protect colorectal cancer cells from hypoxia-induced apoptosis. Oncogene *24*, 1788-1793.

Lee, W., Harvey, T.S., Yin, Y., Yau, P., Litchfield, D., and Arrowsmith, C.H. (1994). Solution structure of the tetrameric minimum transforming domain of p53. Nat Struct Biol *1*, 877-890.

Leu, J.I., Dumont, P., Hafey, M., Murphy, M.E., and George, D.L. (2004). Mitochondrial p53 activates Bak and causes disruption of a Bak-Mcl1 complex. Nat Cell Biol *6*, 443-450.

Levine, A.J. (1997). p53, the cellular gatekeeper for growth and division. Cell *88*, 323-331.

Lewis, J., Laforest, R., Buettner, T., Song, S., Fujibayashi, Y., Connett, J., and Welch, M. (2001). Copper-64-diacetyl-bis(N4-methylthiosemicarbazone): An agent for radiotherapy. Proc Natl Acad Sci U S A *98*, 1206-1211.

Li, M., Lin, Y.M., Hasegawa, S., Shimokawa, T., Murata, K., Kameyama, M., Ishikawa, O., Katagiri, T., Tsunoda, T., Nakamura, Y*., et al.* (2004). Genes associated with liver metastasis of colon cancer, identified by genome-wide cDNA microarray. Int J Oncol *24*, 305-312.

Liang, X.Q., Cao, E.H., Zhang, Y., and Qin, J.F. (2004). A P53 target gene, PIG11, contributes to chemosensitivity of cells to arsenic trioxide. FEBS Lett *569*, 94-98.

Lin, Y.M., Furukawa, Y., Tsunoda, T., Yue, C.T., Yang, K.C., and Nakamura, Y. (2002). Molecular diagnosis of colorectal tumors by expression profiles of 50 genes expressed differentially in adenomas and carcinomas. Oncogene *21*, 4120-4128.

Lu, H., and Levine, A.J. (1995). Human TAFII31 protein is a transcriptional coactivator of the p53 protein. Proc Natl Acad Sci U S A *92*, 5154-5158.

Lumachi, F., Brandes, A.A., Ermani, M., Bruno, G., and Boccagni, P. (2000). Sensitivity of serum tumor markers CEA and CA 15-3 in breast cancer recurrences and correlation with different prognostic factors. Anticancer Res *20*, 4751-4755.

Lyng, H., Brovig, R.S., Svendsrud, D.H., Holm, R., Kaalhus, O., Knutstad, K., Oksefjell, H., Sundfor, K., Kristensen, G.B., and Stokke, T. (2006). Gene expressions and copy numbers associated with metastatic phenotypes of uterine cervical cancer. BMC Genomics *7*, 268.

Marine, J.C., Francoz, S., Maetens, M., Wahl, G., Toledo, F., and Lozano, G. (2006). Keeping p53 in check: essential and synergistic functions of Mdm2 and Mdm4. Cell Death Differ *13*, 927-934.

Masaki, T., Tokuda, M., Ohnishi, M., Watanabe, S., Fujimura, T., Miyamoto, K., Itano, T., Matsui, H., Arima, K., Shirai, M.*, et al.* (1996). Enhanced expression of the protein kinase substrate annexin in human hepatocellular carcinoma. Hepatology *24*, 72-81.

Maurya, P., Meleady, P., Dowling, P., and Clynes, M. (2007). Proteomic approaches for serum biomarker discovery in cancer. Anticancer Res *27*, 1247-1255.

Maxwell, P.H., Wiesener, M.S., Chang, G.W., Clifford, S.C., Vaux, E.C., Cockman, M.E., Wykoff, C.C., Pugh, C.W., Maher, E.R., and Ratcliffe, P.J. (1999). The tumour suppressor protein VHL targets hypoxia-inducible factors for oxygen-dependent proteolysis. Nature *399*, 271-275.

Maxwell, P.J., Longley, D.B., Latif, T., Boyer, J., Allen, W., Lynch, M., McDermott, U., Harkin, D.P., Allegra, C.J., and Johnston, P.G. (2003). Identification of 5-fluorouracil-inducible target genes using cDNA microarray profiling. Cancer Res *63*, 4602-4606.

Melville, A., Sheldon, T.A., Gray, R., and Sowden, A. (1998). Management of colorectal cancer. Qual Health Care *7*, 103-108.

Michael, D., and Oren, M. (2003). The p53-Mdm2 module and the ubiquitin system. Semin Cancer Biol *13*, 49-58.

Mihara, M., Erster, S., Zaika, A., Petrenko, O., Chittenden, T., Pancoska, P., and Moll, U.M. (2003). p53 has a direct apoptogenic role at the mitochondria. Mol Cell *11*, 577-590.

Miyoshi, Y., Ando, H., Nagase, H., Nishisho, I., Horii, A., Miki, Y., Mori, T., Utsunomiya, J., Baba, S., Petersen, G.*, et al.* (1992). Germ-line mutations of the APC gene in 53 familial adenomatous polyposis patients. Proc Natl Acad Sci U S A *89*, 4452-4456.

Momand, J., Wu, H.H., and Dasgupta, G. (2000). MDM2--master regulator of the p53 tumor suppressor protein. Gene *242*, 15-29.

Moulder, S.L., Yakes, F.M., Muthuswamy, S.K., Bianco, R., Simpson, J.F., and Arteaga, C.L. (2001). Epidermal growth factor receptor (HER1) tyrosine kinase inhibitor ZD1839 (Iressa) inhibits HER2/neu (erbB2)-overexpressing breast cancer cells in vitro and in vivo. Cancer Res *61*, 8887-8895.

Movsas, B., Chapman, J.D., Hanlon, A.L., Horwitz, E.M., Greenberg, R.E., Stobbe, C., Hanks, G.E., and Pollack, A. (2002). Hypoxic prostate/muscle pO2 ratio predicts for biochemical failure in patients with prostate cancer: preliminary findings. Urology *60*, 634-639.

Nakayama, K., Frew, I.J., Hagensen, M., Skals, M., Habelhah, H., Bhoumik, A., Kadoya, T., Erdjument-Bromage, H., Tempst, P., Frappell, P.B.*, et al.* (2004). Siah2 regulates stability of prolyl-hydroxylases, controls HIF1alpha abundance, and modulates physiological responses to hypoxia. Cell *117*, 941-952.

Nelson, D.M., Bhaskaran, V., Foster, W.R., and Lehman-McKeeman, L.D. (2006). p53-independent induction of rat hepatic Mdm2 following administration of phenobarbital and pregnenolone 16alpha-carbonitrile. Toxicol Sci *94*, 272-280.

Neufeld, K.L., Zhang, F., Cullen, B.R., and White, R.L. (2000). APC-mediated downregulation of beta-catenin activity involves nuclear sequestration and nuclear export. EMBO Rep *1*, 519-523.

Nishihara, H., Hwang, M., Kizaka-Kondoh, S., Eckmann, L., and Insel, P.A. (2004). Cyclic AMP promotes cAMP-responsive element-binding protein-dependent induction of cellular inhibitor of apoptosis protein-2 and suppresses apoptosis of colon cancer cells through ERK1/2 and p38 MAPK. J Biol Chem *279*, 26176-26183.

Obata, A., Kasamatsu, S., Lewis, J.S., Furukawa, T., Takamatsu, S., Toyohara, J., Asai, T., Welch, M.J., Adams, S.G., Saji, H*., et al.* (2005). Basic characterization of 64Cu-ATSM as a radiotherapy agent. Nucl Med Biol *32*, 21-28.

Padhani, A.R., Krohn, K.A., Lewis, J.S., and Alber, M. (2007). Imaging oxygenation of human tumours. Eur Radiol *17*, 861-872.

Pan, Y., Mansfield, K.D., Bertozzi, C.C., Rudenko, V., Chan, D.A., Giaccia, A.J., and Simon, M.C. (2007). Multiple factors affecting cellular redox status and energy metabolism modulate hypoxia-inducible factor prolyl hydroxylase activity in vivo and in vitro. Mol Cell Biol *27*, 912-925.

Pan, Y., Oprysko, P.R., Asham, A.M., Koch, C.J., and Simon, M.C. (2004). p53 cannot be induced by hypoxia alone but responds to the hypoxic microenvironment. Oncogene *23*, 4975-4983.

Parker, C., Milosevic, M., Toi, A., Sweet, J., Panzarella, T., Bristow, R., Catton, C., Catton, P., Crook, J., Gospodarowicz, M*., et al.* (2004). Polarographic electrode study of tumor oxygenation in clinically localized prostate cancer. Int J Radiat Oncol Biol Phys *58*, 750-757.

Paweletz, C.P., Ornstein, D.K., Roth, M.J., Bichsel, V.E., Gillespie, J.W., Calvert, V.S., Vocke, C.D., Hewitt, S.M., Duray, P.H., Herring, J*., et al.* (2000). Loss of annexin 1 correlates with early onset of tumorigenesis in esophageal and prostate carcinoma. Cancer Res *60*, 6293-6297.

Pines, J. (1996). Cell cycle: reaching for a role for the Cks proteins. Curr Biol *6*, 1399-1402.

Pomerantz, J., Schreiber-Agus, N., Liegeois, N.J., Silverman, A., Alland, L., Chin, L., Potes, J., Chen, K., Orlow, I., Lee, H.W*., et al.* (1998). The Ink4a tumor suppressor gene product, p19Arf, interacts with MDM2 and neutralizes MDM2's inhibition of p53. Cell *92*, 713-723.

Pouyssegur, J., Dayan, F., and Mazure, N.M. (2006). Hypoxia signalling in cancer and approaches to enforce tumour regression. Nature *441*, 437-443.

Prives, C. (1998). Signaling to p53: breaking the MDM2-p53 circuit. Cell *95*, 5-8.

Prives, C., and Hall, P.A. (1999). The p53 pathway. J Pathol *187*, 112-126.

Pugh, C.W., O'Rourke, J.F., Nagao, M., Gleadle, J.M., and Ratcliffe, P.J. (1997). Activation of hypoxia-inducible factor-1; definition of regulatory domains within the alpha subunit. J Biol Chem *272*, 11205-11214.

Ravi, R., Mookerjee, B., Bhujwalla, Z.M., Sutter, C.H., Artemov, D., Zeng, Q., Dillehay, L.E., Madan, A., Semenza, G.L., and Bedi, A. (2000). Regulation of tumor angiogenesis by p53-induced degradation of hypoxia-inducible factor 1alpha. Genes Dev *14*, 34-44.

Rechsteiner, M., and Rogers, S.W. (1996). PEST sequences and regulation by proteolysis. Trends Biochem Sci *21*, 267-271.

Renan, M.J. (1993). How many mutations are required for tumorigenesis? Implications from human cancer data. Mol Carcinog *7*, 139-146.

Rhee, K.H., Stier, G., Becker, P.B., Suck, D., and Sandaltzopoulos, R. (1997). The bifunctional protein DCoH modulates interactions of the homeodomain transcription factor HNF1 with nucleic acids. J Mol Biol *265*, 20-29.

Rother, K., Dengl, M., Lorenz, J., Tschop, K., Kirschner, R., Mossner, J., and Engeland, K. (2007). Gene expression of cyclin-dependent kinase subunit Cks2 is repressed by the tumor suppressor p53 but not by the related proteins p63 or p73. FEBS Lett *581*, 1166-1172.

Sablina, A.A., Budanov, A.V., Ilyinskaya, G.V., Agapova, L.S., Kravchenko, J.E., and Chumakov, P.M. (2005). The antioxidant function of the p53 tumor suppressor. Nat Med *11*, 1306-1313.

Saito, S., Goodarzi, A.A., Higashimoto, Y., Noda, Y., Lees-Miller, S.P., Appella, E., and Anderson, C.W. (2002). ATM mediates phosphorylation at multiple p53 sites, including Ser(46), in response to ionizing radiation. J Biol Chem *277*, 12491-12494.

Sakaguchi, K., Herrera, J.E., Saito, S., Miki, T., Bustin, M., Vassilev, A., Anderson, C.W., and Appella, E. (1998). DNA damage activates p53 through a phosphorylation-acetylation cascade. Genes Dev *12*, 2831-2841.

Sakaguchi, K., Saito, S., Higashimoto, Y., Roy, S., Anderson, C.W., and Appella, E. (2000). Damage-mediated phosphorylation of human p53 threonine 18 through a cascade mediated by a casein 1-like kinase. Effect on Mdm2 binding. J Biol Chem *275*, 9278-9283.

Salceda, S., and Caro, J. (1997). Hypoxia-inducible factor 1alpha (HIF-1alpha) protein is rapidly degraded by the ubiquitin-proteasome system under normoxic conditions. Its stabilization by hypoxia depends on redox-induced changes. J Biol Chem *272*, 22642-22647.

Sanchez-Puig, N., Veprintsev, D.B., and Fersht, A.R. (2005). Binding of natively unfolded HIF-1alpha ODD domain to p53. Mol Cell *17*, 11-21.

Schmid, T., Zhou, J., and Brune, B. (2004a). HIF-1 and p53: communication of transcription factors under hypoxia. J Cell Mol Med *8*, 423-431.

Schmid, T., Zhou, J., Kohl, R., and Brune, B. (2004b). p300 relieves p53-evoked transcriptional repression of hypoxia-inducible factor-1 (HIF-1). Biochem J *380*, 289-295.

Schultz, K., Fanburg, B.L., and Beasley, D. (2006). Hypoxia and hypoxia-inducible factor-1alpha promote growth factor-induced proliferation of human vascular smooth muscle cells. Am J Physiol Heart Circ Physiol *290*, H2528-2534.

Secomb, T.W., Hsu, R., Dewhirst, M.W., Klitzman, B., and Gross, J.F. (1993). Analysis of oxygen transport to tumor tissue by microvascular networks. Int J Radiat Oncol Biol Phys *25*, 481-489.

Secomb, T.W., Hsu, R., Ong, E.T., Gross, J.F., and Dewhirst, M.W. (1995). Analysis of the effects of oxygen supply and demand on hypoxic fraction in tumors. Acta Oncol *34*, 313-316.

Semenza, G.L. (1999). Regulation of mammalian O2 homeostasis by hypoxia-inducible factor 1. Annu Rev Cell Dev Biol *15*, 551-578.

Semenza, G.L. (2000a). HIF-1: mediator of physiological and pathophysiological responses to hypoxia. J Appl Physiol *88*, 1474-1480.

Semenza, G.L. (2000b). Hypoxia, clonal selection, and the role of HIF-1 in tumor progression. Crit Rev Biochem Mol Biol *35*, 71-103.

Semenza, G.L. (2003). Targeting HIF-1 for cancer therapy. Nat Rev Cancer *3*, 721-732.

Semenza, G.L., Jiang, B.H., Leung, S.W., Passantino, R., Concordet, J.P., Maire, P., and Giallongo, A. (1996). Hypoxia response elements in the aldolase A, enolase 1, and lactate dehydrogenase A gene promoters contain essential binding sites for hypoxia-inducible factor 1. J Biol Chem *271*, 32529-32537.

Semenza, G.L., and Wang, G.L. (1992). A nuclear factor induced by hypoxia via de novo protein synthesis binds to the human erythropoietin gene enhancer at a site required for transcriptional activation. Mol Cell Biol *12*, 5447-5454.

Seow, A., Koh, W.P., Chia, K.S., Shi, L.M., Lee, H.P., and Shanmugaratnam, K. (2004). Trends in cancer incidence in Singapore 1968 - 2002. Singapore Cancer Registry Report *6*.

Sharma, M.R., Koltowski, L., Ownbey, R.T., Tuszynski, G.P., and Sharma, M.C. (2006). Angiogenesis-associated protein annexin II in breast cancer: selective expression in invasive breast cancer and contribution to tumor invasion and progression. Exp Mol Pathol *81*, 146-156.

Shimizu, S., Eguchi, Y., Kosaka, H., Kamiike, W., Matsuda, H., and Tsujimoto, Y. (1995). Prevention of hypoxia-induced cell death by Bcl-2 and Bcl-xL. Nature *374*, 811-813.

Siliciano, J.D., Canman, C.E., Taya, Y., Sakaguchi, K., Appella, E., and Kastan, M.B. (1997). DNA damage induces phosphorylation of the amino terminus of p53. Genes Dev *11*, 3471-3481.

Spruck, C., Strohmaier, H., Watson, M., Smith, A.P., Ryan, A., Krek, T.W., and Reed, S.I. (2001). A CDK-independent function of mammalian Cks1: targeting of SCF(Skp2) to the CDK inhibitor p27Kip1. Mol Cell *7*, 639-650.

Spruck, C.H., de Miguel, M.P., Smith, A.P., Ryan, A., Stein, P., Schultz, R.M., Lincoln, A.J., Donovan, P.J., and Reed, S.I. (2003). Requirement of Cks2 for the first metaphase/anaphase transition of mammalian meiosis. Science *300*, 647-650.

Sundfor, K., Lyng, H., Trope, C.G., and Rofstad, E.K. (2000). Treatment outcome in advanced squamous cell carcinoma of the uterine cervix: relationships to pretreatment tumor oxygenation and vascularization. Radiother Oncol *54*, 101-107.

Talks, K.L., Turley, H., Gatter, K.C., Maxwell, P.H., Pugh, C.W., Ratcliffe, P.J., and Harris, A.L. (2000). The expression and distribution of the hypoxia-inducible factors HIF-1alpha and HIF-2alpha in normal human tissues, cancers, and tumor-associated macrophages. Am J Pathol *157*, 411-421.

Tannu, N.S., and Hemby, S.E. (2006). Methods for proteomics in neuroscience. Prog Brain Res *158*, 41-82.

Teicher, B.A. (1994). Hypoxia and drug resistance. Cancer Metastasis Rev *13*, 139-168.

Teicher, B.A. (1995). Physiologic mechanisms of therapeutic resistance. Blood flow and hypoxia. Hematol Oncol Clin North Am *9*, 475-506.

Unger, T., Juven-Gershon, T., Moallem, E., Berger, M., Vogt Sionov, R., Lozano, G., Oren, M., and Haupt, Y. (1999). Critical role for Ser20 of human p53 in the negative regulation of p53 by Mdm2. Embo J *18*, 1805-1814.

van Staveren, W.C., Solis, D.W., Delys, L., Venet, D., Cappello, M., Andry, G., Dumont, J.E., Libert, F., Detours, V., and Maenhaut, C. (2006). Gene expression in human thyrocytes and autonomous adenomas reveals suppression of negative feedbacks in tumorigenesis. Proc Natl Acad Sci U S A *103*, 413-418.

Vaupel, P. (2004). The role of hypoxia-induced factors in tumor progression. Oncologist *9 Suppl 5*, 10-17.

Vaupel, P., Briest, S., and Hockel, M. (2002). Hypoxia in breast cancer: pathogenesis, characterization and biological/therapeutic implications. Wien Med Wochenschr *152*, 334-342.

Vaupel, P., and Harrison, L. (2004). Tumor hypoxia: causative factors, compensatory mechanisms, and cellular response. Oncologist *9 Suppl 5*, 4-9.

Vaupel, P., Kelleher, D.K., and Hockel, M. (2001). Oxygen status of malignant tumors: pathogenesis of hypoxia and significance for tumor therapy. Semin Oncol *28*, 29-35.

Vengellur, A., Woods, B.G., Ryan, H.E., Johnson, R.S., and LaPres, J.J. (2003). Gene expression profiling of the hypoxia signaling pathway in hypoxia-inducible factor 1alpha null mouse embryonic fibroblasts. Gene Expr *11*, 181-197.

Vignati, S., Albertini, V., Rinaldi, A., Kwee, I., Riva, C., Oldrini, R., Capella, C., Bertoni, F., Carbone, G.M., and Catapano, C.V. (2006). Cellular and molecular consequences of peroxisome proliferator-activated receptor-gamma activation in ovarian cancer cells. Neoplasia *8*, 851-861.

Villunger, A., Michalak, E.M., Coultas, L., Mullauer, F., Bock, G., Ausserlechner, M.J., Adams, J.M., and Strasser, A. (2003). p53- and drug-induced apoptotic responses mediated by BH3-only proteins puma and noxa. Science *302*, 1036-1038.

Vlaeminck-Guillem, V., Ho, S.C., Rodien, P., Vassart, G., and Costagliola, S. (2002). Activation of the cAMP pathway by the TSH receptor involves switching of the ectodomain from a tethered inverse agonist to an agonist. Mol Endocrinol *16*, 736-746.

Vlatkovic, N., Guerrera, S., Li, Y., Linn, S., Haines, D.S., and Boyd, M.T. (2000). MDM2 interacts with the C-terminus of the catalytic subunit of DNA polymerase epsilon. Nucleic Acids Res *28*, 3581-3586.

Vleugel, M.M., Shvarts, D., van der Wall, E., and van Diest, P.J. (2006). p300 and p53 levels determine activation of HIF-1 downstream targets in invasive breast cancer. Hum Pathol *37*, 1085-1092.

Vogelstein, B., Lane, D., and Levine, A.J. (2000). Surfing the p53 network. Nature *408*, 307-310.

Volm, M., and Koomagi, R. (2000). Hypoxia-inducible factor (HIF-1) and its relationship to apoptosis and proliferation in lung cancer. Anticancer Res *20*, 1527-1533.

Vousden, K.H. (2000). p53: death star. Cell *103*, 691-694.

Vousden, K.H., and Lane, D.P. (2007). p53 in health and disease. Nat Rev Mol Cell Biol *8*, 275-283.

Wachsberger, P., Burd, R., and Dicker, A.P. (2003). Tumor response to ionizing radiation combined with antiangiogenesis or vascular targeting agents: exploring mechanisms of interaction. Clin Cancer Res *9*, 1957-1971.

Wang, G.L., Jiang, B.H., Rue, E.A., and Semenza, G.L. (1995a). Hypoxia-inducible factor 1 is a basic-helix-loop-helix-PAS heterodimer regulated by cellular O2 tension. Proc Natl Acad Sci U S A *92*, 5510-5514.

Wang, G.L., Jiang, B.H., and Semenza, G.L. (1995b). Effect of protein kinase and phosphatase inhibitors on expression of hypoxia-inducible factor 1. Biochem Biophys Res Commun *216*, 669-675.

Wang, G.L., and Semenza, G.L. (1993). Desferrioxamine induces erythropoietin gene expression and hypoxia-inducible factor 1 DNA-binding activity: implications for models of hypoxia signal transduction. Blood *82*, 3610-3615.

Wang, G.L., and Semenza, G.L. (1995). Purification and characterization of hypoxia-inducible factor 1. J Biol Chem *270*, 1230-1237.

Wenger, R.H. (2002). Cellular adaptation to hypoxia: O2-sensing protein hydroxylases, hypoxia-inducible transcription factors, and O2-regulated gene expression. Faseb J *16*, 1151-1162.

Wenger, R.H., Camenisch, G., Desbaillets, I., Chilov, D., and Gassmann, M. (1998). Up-regulation of hypoxia-inducible factor-1alpha is not sufficient for hypoxic/anoxic p53 induction. Cancer Res *58*, 5678-5680.

Wiesener, M.S., Jurgensen, J.S., Rosenberger, C., Scholze, C.K., Horstrup, J.H., Warnecke, C., Mandriota, S., Bechmann, I., Frei, U.A., Pugh, C.W.*, et al.* (2003). Widespread hypoxia-inducible expression of HIF-2alpha in distinct cell populations of different organs. Faseb J *17*, 271-273.

Wiesener, M.S., Turley, H., Allen, W.E., Willam, C., Eckardt, K.U., Talks, K.L., Wood, S.M., Gatter, K.C., Harris, A.L., Pugh, C.W.*, et al.* (1998). Induction of endothelial PAS domain protein-1 by hypoxia: characterization and comparison with hypoxia-inducible factor-1alpha. Blood *92*, 2260-2268.

Wu, W.W., Wang, G., Baek, S.J., and Shen, R.F. (2006). Comparative study of three proteomic quantitative methods, DIGE, cICAT, and iTRAQ, using 2D gel- or LC-MALDI TOF/TOF. J Proteome Res *5*, 651-658.

Wykoff, C.C., Pugh, C.W., Maxwell, P.H., Harris, A.L., and Ratcliffe, P.J. (2000). Identification of novel hypoxia dependent and independent target genes of the von Hippel-Lindau (VHL) tumour suppressor by mRNA differential expression profiling. Oncogene *19*, 6297-6305.

Yamaguchi, A., Tamatani, M., Matsuzaki, H., Namikawa, K., Kiyama, H., Vitek, M.P., Mitsuda, N., and Tohyama, M. (2001). Akt activation protects hippocampal neurons from apoptosis by inhibiting transcriptional activity of p53. J Biol Chem *276*, 5256-5264.

Yang, W.H., Kim, J.E., Nam, H.W., Ju, J.W., Kim, H.S., Kim, Y.S., and Cho, J.W. (2006). Modification of p53 with O-linked N-acetylglucosamine regulates p53 activity and stability. Nat Cell Biol *8*, 1074-1083.

Yao, K.S., Clayton, M., and O'Dwyer, P.J. (1995). Apoptosis in human adenocarcinoma HT29 cells induced by exposure to hypoxia. J Natl Cancer Inst *87*, 117-122.

Yu, A.Y., Frid, M.G., Shimoda, L.A., Wiener, C.M., Stenmark, K., and Semenza, G.L. (1998). Temporal, spatial, and oxygen-regulated expression of hypoxia-inducible factor-1 in the lung. Am J Physiol *275*, L818-826.

Yu, J., Wang, Z., Kinzler, K.W., Vogelstein, B., and Zhang, L. (2003). PUMA mediates the apoptotic response to p53 in colorectal cancer cells. Proc Natl Acad Sci U S A *100*, 1931-1936.

Yu, J., Zhang, L., Hwang, P.M., Rago, C., Kinzler, K.W., and Vogelstein, B. (1999). Identification and classification of p53-regulated genes. Proc Natl Acad Sci U S A *96*, 14517-14522.

Yu, J.L., Coomber, B.L., and Kerbel, R.S. (2002). A paradigm for therapy-induced microenvironmental changes in solid tumors leading to drug resistance. Differentiation *70*, 599-609.

Yun, J., Chae, H.D., Choy, H.E., Chung, J., Yoo, H.S., Han, M.H., and Shin, D.Y. (1999). p53 negatively regulates cdc2 transcription via the CCAAT-binding NF-Y transcription factor. J Biol Chem *274*, 29677-29682.

Zagorska, A., and Dulak, J. (2004). HIF-1: the knowns and unknowns of hypoxia sensing. Acta Biochim Pol *51*, 563-585.

Zhang, H., Hannon, G.J., Casso, D., and Beach, D. (1994). p21 is a component of active cell cycle kinases. Cold Spring Harb Symp Quant Biol *59*, 21-29.

Zhang, L., Yu, J., Park, B.H., Kinzler, K.W., and Vogelstein, B. (2000). Role of BAX in the apoptotic response to anticancer agents. Science *290*, 989-992.

Zhu, Y., Mao, X.O., Sun, Y., Xia, Z., and Greenberg, D.A. (2002). p38 Mitogen-activated protein kinase mediates hypoxic regulation of Mdm2 and p53 in neurons. J Biol Chem *277*, 22909-22914.

APPENDICES

[A]

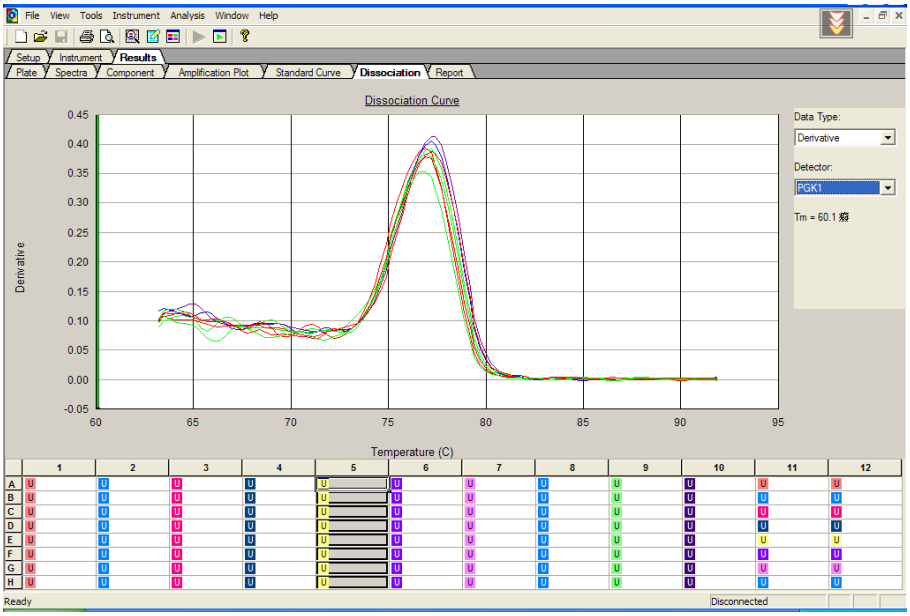

[B]

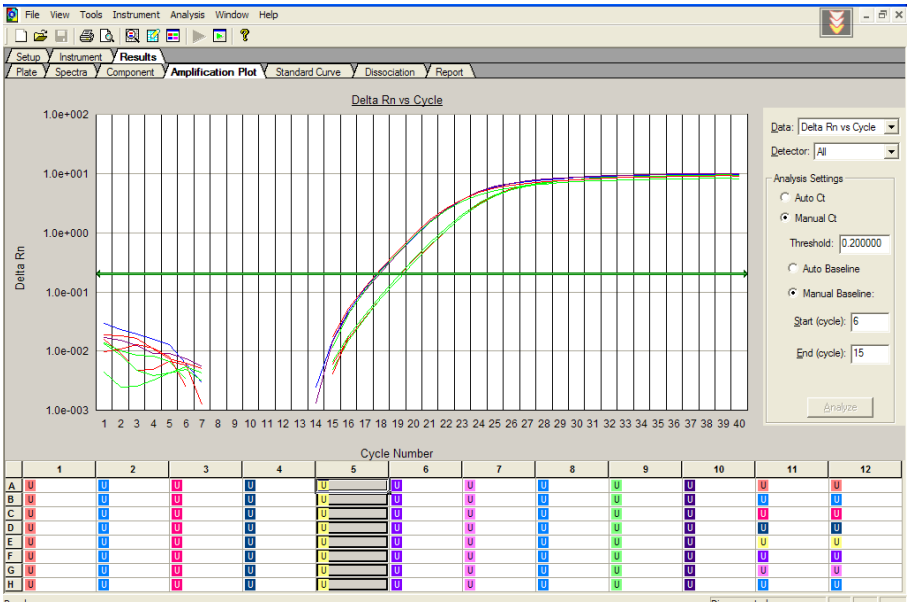

Supplementary figure 1: Dissociation curve and amplification plot of PGK1 primer set. [A] A single peak observed in the primer pair dissociation curve indicates specificity of primers used as well as absence of amplification of primer pairs due to primer dimerization. [B] Amplification curves of the gene-of-interest in each sample performed in duplicates. The different rates (curves) observed indicates the different cycle threshold values obtained in each sample.

Supplementary table 1: List of primers used for RT-PCR. All primers are arranged in the order of 5' to 3'

COTL1	
Forward Primer	GCAGGGAGCGGAGTACCA
Reverse Primer	GCAAACAACCGGACGTCATC
PHS/PCBD1	
Forward Primer	GGGCCTTTGGGTTCATGAC
Reverse Primer	GGATGGTGGTCCAGTTTCTCA
SMC3	
Forward Primer	CGAGACTCGTGCCAAACTTG
Reverse Primer	TGTCTGGATTTTTCTCCACTAGTCTCT
NSUN2	
Forward Primer	TCGTCAAGAAGCTGTTAGCATGA
Reverse Primer	TGATGAGGCCGCACGTT
ANXA2	
Forward Primer	GCCTATTGAAGACACCTGCTCAGT
Reverse Primer	CAGCCCCTTCATGGAAGCT
EVX2	
Forward Primer	CGCCGCTCAGCTTAAGGA
Reverse Primer	CAGCCGAGCCGCTCTCT
PGK1	
Forward Primer	CCGAGCCAGCCAAAATAGAA
Reverse Primer	CATAGACATCCCCTAGCTTGGAA
LDHA	
Forward Primer	TGGCCTGTGCCATCAGTATC
Reverse Primer	CGATGACATCAACAAGAGCAAGT
EFHD2	
Forward Primer	GGCGGGACGGCTTCA
Reverse Primer	CCCCAAGTTTCTCCATCATGA
DDX46	
Forward Primer	CCCACGCCCATCCAAA
Reverse Primer	CCAATCAAATCTCGTCCAGACA
CKS2	
Forward Primer	TGGCCCACAAGCAGATCTACT
Reverse Primer	CATGCCGGTACTCGTAGTGTTC
MAPRE1	
Forward Primer	GGCTGCCAGA CAAGGTCAA
Reverse Primer	TTTATTCAGAGCTGGAGCAACAAG
CDC2	
Forward Primer	CCTCAAAATCTCTTGATTGATGACA
Reverse Primer	GCTCTGGCAAGGCCAAAAT

G3BP1	
Forward Primer	TTCGCCATGTTGATGCTCAT
Reverse Primer	CCCCATCACCTGGACTACCA
MCM3	
Forward Primer	CCCCGCGGACTCTTACCT
Reverse Primer	GACAATGCCCTCCACACAGA
PD2	
Forward Primer	CGCATCGACCCCAATGTT
Reverse Primer	GCCTGAATCTCCTCTTCCAAAA
CAND1	
Forward Primer	GCTTCCAGTGGCTCTGCATT
Reverse Primer	ATTGCACTTGTAAGACGTCCAGTAA
ERP29	
Forward Primer	CCCTACGGTGAGAAGCAGGAT
Reverse Primer	ATCGCTGGAAGCCGAGTTTT
NUP93	
Forward Primer	AGGACAATGCCCTGCTGTCT
Reverse Primer	CCATGCCGAAGGTCCTCTT
GRIM19	
Forward Primer	CATAGGGATTGGAACCCTGATC
Reverse Primer	CGCTCACGGTTCCACTTCAT
HIF-1α	
Forward Primer	AGCCGAGGAAGAACTATGAACATAA
Reverse Primer	GTGGCCTGTGCAGTGCAA
p53	
Forward Primer	TCTGTCCCTTCCCAGAAAACC
Reverse Primer	CAAGAAGCCCAGACGGAAAC
VEGFA	
Forward Primer	AACCATGAACTTTCTGCTGTCTTG
Reverse Primer	TGGTGGAGGTAGAGCAGCAA
β-ACTIN	
Forward Primer	CTGGCACCCAGCACAATG
Reverse Primer	GCCGATCCACACGGAGTACT

Supplementary table 2: Tabulation of the 54 targets selected from iTRAQ analysis.

Protein Name	Accession Number	Peptide Count	Avg iTRAQ ratio * (115/114)	Avg iTRAQ ratio * (116/114)	Avg iTRAQ ratio * (117/115)	Avg iTRAQ ratio * (117/116)	Avg iTRAQ ratio * (117/114)	iTRAQ Standard Deviation * (115/114)
Eukaryotic translation initiation factor 3 subunit 2	IPI00012795	1	9.422E-01	7.122E-01	5.976E-01	7.780E-01	5.545E-01	4.689E-02
Coactosin-like protein	IPI00017704	2	1.148E+00	8.508E-01	6.779E-01	9.000E-01	7.663E-01	1.210E-01
Leucyl-tRNA synthetase, cytoplasmic	IPI00103994	4	9.773E-01	1.541E+00	1.307E+00	8.295E-01	1.279E+00	2.659E-01
Pterin-4-alpha-carbinolamine dehydratase	IPI00218568	1	8.884E-01	6.320E-01	5.776E-01	7.990E-01	5.054E-01	0.000E+00
NADH dehydrogenase [ubiquinone] 1 alpha subcomplex subunit 8	IPI00219034	2	1.008E+00	8.610E-01	7.314E-01	8.582E-01	7.331E-01	1.402E-01
Structural maintenance of chromosome 3	IPI00219420	1	1.023E+00	1.453E+00	1.572E+00	1.090E+00	1.585E+00	0.000E+00
NOL1/NOP2/Sun domain family 2 protein	IPI00306369	1	1.021E+00	1.982E+00	1.654E+00	8.541E-01	1.679E+00	0.000E+00
Annexin A2	IPI00455315	4	9.815E-01	6.476E-01	6.904E-01	1.047E+00	6.782E-01	1.449E-01
Isoform 2 of Eukaryotic translation initiation factor 3 subunit 9	IPI00719752	2	8.477E-01	6.249E-01	7.496E-01	1.017E+00	6.360E-01	1.083E-01
12 kDa protein	IPI00797738	2	9.163E-01	6.949E-01	6.752E-01	8.920E-01	6.149E-01	4.561E-02
Heat shock 70 kDa protein 4	IPI00002966	1	9.018E-01	1.419E+00	1.314E+00	8.358E-01	1.186E+00	1.186E+00
Nucleolar protein NOP5	IPI00006379	1	6.355E-01	1.333E+00	1.325E+00	6.321E-01	8.428E-01	4.889E-03
Protein S100-A14	IPI00010214	1	8.820E-01	1.361E+00	1.653E+00	1.072E+00	1.460E+00	0.000E+00
DNA replication licensing factor MCM2	IPI00184330	1	9.543E-01	7.553E-01	7.463E-01	9.433E-01	7.128E-01	9.509E-02
Ezrin	IPI00746388	7	1.178E+00	8.787E-01	7.223E-01	9.525E-01	8.376E-01	1.300E-01
Homeobox even-skipped homolog protein 2	IPI00012495	1	1.536E+00	1.195E+00	1.076E+00	1.383E+00	1.654E+00	0.000E+00
membrane component chromosome 11 surface marker 1 isoform 1	IPI00150961	1	8.274E-01	1.041E+00	8.603E-01	6.843E-01	7.124E-01	0.000E+00
Phosphoglycerate kinase 1	IPI00169383	1	1.605E+00	1.290E+00	1.020E+00	1.270E+00	1.638E+00	0.000E+00
Elongation factor 2	IPI00186290	11	7.420E-01	9.452E-01	1.194E+00	9.390E-01	8.805E-01	2.136E-01
lactate dehydrogenase A	IPI00217966	3	1.351E+00	1.038E+00	1.002E+00	1.304E+00	1.355E+00	2.208E-01
EF hand domain containing 2	IPI00552365	1	1.455E+00	1.247E+00	1.291E+00	1.508E+00	1.881E+00	7.451E-02
fatty acid synthase	IPI00645907	2	7.280E-01	1.131E+00	1.150E+00	7.416E-01	8.322E-01	4.706E-03
118 kDa protein	IPI00657954	1	7.100E-01	8.645E-01	1.193E+00	9.805E-01	8.479E-01	1.053E-01
43 kDa protein	IPI00789029	1	7.213E-01	9.803E-01	1.002E+00	7.256E-01	7.118E-01	3.909E-01

Galectin-1	IPI00219219	1	1.479E+00	1.265E+00	1.133E+00	1.325E+00	1.677E+00	0.000E+00
L-aminoadipate-semialdehyde dehydrogenase-phosphopantetheinyl transferase	IPI00250297	1	7.646E-01	1.121E+00	9.508E-01	6.380E-01	7.159E-01	0.000E+00
41 kDa protein	IPI00514175	1	7.565E-01	9.217E-01	9.757E-01	7.881E-01	7.270E-01	0.000E+00
Rab geranylgeranyltransferase, beta subunit	IPI00514956	1	7.046E-01	1.055E+00	1.105E+00	7.382E-01	7.790E-01	2.450E-02
Microtubule-associated protein RP/EB family member 1	IPI00017596	1	1.381E+00	4.925E-01	7.528E-01	2.112E+00	1.041E+00	0.000E+00
HRMT1L2 protein	IPI00215734	1	5.958E-01	8.983E-01	1.504E+00	9.998E-01	8.910E-01	0.000E+00
Isoform 2 of 26S protease regulatory subunit 6B	IPI00216770	1	8.308E-01	7.217E-01	1.352E+00	1.532E+00	1.106E+00	0.000E+00
cell death-regulatory protein GRIM19	IPI00219685	1	7.473E-01	7.153E-01	7.575E-01	7.917E-01	5.665E-01	8.454E-02
Lactoylglutathione lyase	IPI00220766	1	8.741E-01	1.398E+00	1.032E+00	6.347E-01	8.881E-01	0.000E+00
80 kDa protein	IPI00644506	1	6.769E-01	5.843E-01	8.283E-01	9.600E-01	5.612E-01	9.027E-02
19 kDa protein	IPI00789101	3	1.305E+00	1.304E+00	9.531E-01	9.544E-01	1.245E+00	6.565E-02
Cyclin-dependent kinases regulatory subunit 2	IPI00015105	1	2.587E-01	9.299E-01	1.321E+00	3.618E-01	3.367E-01	0.000E+00
Hypothetical protein DKFZp686L20222	IPI00026689	2	6.836E-01	1.164E+00	1.577E+00	9.282E-01	1.072E+00	9.422E-02
Hypothetical protein DKFZp781L0540	IPI00477803	1	1.024E+00	1.008E+00	1.317E+00	1.337E+00	1.349E+00	0.000E+00
Asparagine synthetase	IPI00554777	3	8.745E-01	5.499E-01	8.173E-01	1.301E+00	7.154E-01	4.105E-02
Ras-GTPase-activating protein-binding protein 1	IPI00012442	2	1.106E+00	9.288E-01	7.442E-01	8.882E-01	8.184E-01	2.037E-01
DNA replication licensing factor MCM3	IPI00013214	1	1.157E+00	9.438E-01	6.810E-01	8.217E-01	7.761E-01	0.000E+00
Endoplasmic reticulum protein ERp29 precursor	IPI00024911	1	8.058E-01	6.998E-01	9.640E-01	1.111E+00	7.775E-01	9.250E-02
26S proteasome non-ATPase regulatory subunit 12	IPI00185374	1	9.816E-01	1.145E+00	1.310E+00	1.105E+00	1.266E+00	3.216E-02
Retinol-binding protein I, cellular	IPI00219718	1	1.109E+00	9.305E-01	6.193E-01	7.263E-01	6.763E-01	0.000E+00
PD2 protein	IPI00300333	1	8.986E-01	7.453E-01	9.548E-01	1.152E+00	8.587E-01	0.000E+00
GTP:AMP phosphotransferase	IPI00478236	1	1.019E+00	1.125E+00	1.396E+00	1.244E+00	9.553E-01	0.000E+00
285 kDa protein	IPI00478292	1	1.132E+00	1.090E+00	6.927E-01	7.196E-01	7.845E-01	7.164E-02